General Anaesthetic Modulation of Memory-Related Gene Expression in the Cerebral Cortex

A thesis

submitted in partial fulfilment

of the requirements for the degree of

Master of Science (Research)

in **Biological Sciences**

at

The University of Waikato

by

Laura Maree Bell

THE UNIVERSITY OF
WAIKATO
Te Whare Wānanga o Waikato

2015

Abstract

General anaesthetics have been widely used in a clinical setting, having remained one of the most important drugs in medicine for their role in enabling major surgical procedures to be carried out. One of the fundamental outcomes of an anaesthetic is amnesia, as this prevents patient recall of events surrounding surgery. The hippocampal region of the mammalian brain has been investigated for its role in memory formation, however the cerebral cortex also has recognised importance in memory consolidation and storage processes. General anaesthetics cause widespread neurochemical changes in the brain and the disruption to memory consolidation processes is likely to involve alteration to the expression patterns of memory-related genes. The aim of this research was to investigate the cerebrocortical gene expression pattern of five memory-related genes, *Arc, Bdnf, CaMKIIα, Gjd2* and *Grin1* during exposure to anaesthesia induced by sevoflurane, isoflurane and propofol. Real-time quantitative PCR (qPCR) was used to analyse expression of the individual mRNA transcripts and REST© software was used to carry out statistical analysis of the mRNA expression of each gene of interest.

Our research demonstrated that *Bdnf* was significantly down-regulated by sevoflurane at t=2 hours and t=4 hours and propofol at t=2 hours ($p<0.05$). Up-regulation of *Arc* after a four exposure to propofol was also observed but no change in *Arc* was found at the other time points. There was no change in the expression of *CaMKIIα, Gjd2* or *Grin1* during sevoflurane- or propofol- induced anaesthesia. We recommend analysis of other *Bdnf* transcript variants in the

mouse brain during anaesthesia, as well as levels of the BDNF protein to further validate these results.

Acknowledgements

Firstly, I would like to thank my supervisors Dr Linda Peters and Dr Logan Voss for their on-going support and encouragement throughout this project. They have taught me a range of valuable skills of which I am very grateful for. I would also like to thank the other staff members of our lab including Dr Steve Bird, Dr Ray Cursons, Dr Gregory Jacobsen, Olivia Patty, Sari Karppen and Keiran Oxton for their help and patience in teaching me various laboratory techniques.

The Summer Research Scholarship that I received from the Waikato Clinical School in 2013 helped to launch this project and provided an opportunity for me to learn basic molecular techniques and research my literature review. Furthermore, the travel grants I received both from the School of Science at the University of Waikato and the Department of Psychology at the University of Otago made it possible for me to attend the Australasian Winter Conference on Brain Research, which was an extremely valuable experience.

Finally, I would like to give thanks to my fellow MSc students, Sarah, Grant, Nick, Callie and Kirsty, who all made the tough days easier with their understanding and willingness to take long breaks from our work. A very special thank you is also owed to Alastair Clark. Without your constant patience and support I would never have made it this far. Thank you for putting up with me and my crazy ambitions. Thank you Mum and Dad for your words of wisdom and your on-going emotional (and financial) support. You have always encouraged me to believe in myself and I know that you will both be so proud of this achievement. I love you both very much and I dedicate this work to you.

Ethics Statement

Animal ethics approval for this research was received from the University of Waikato (UoW) Animal Ethics Committee in November 2013 (Protocol number: 905, Appendix 1). All provisions outlined in the approval were adhered to. Training was received for the humane euthanisation of mice, according to the Standard Operating Procedure number 9 (SOP 9, UoW, Appendix 2). Wild type C57:BL6/129SV mice were dissected in the animal house at UoW and further processed in the Molecular Genetics laboratory (C.2.03, UoW). In total, twelve 8-week-old adult mice (male and female) and six 18-month-old elderly mice (male and female) were used for this research.

Table of Contents

List of Figures

List of Tables and Equations

List of Abbreviations

α	Alpha
Δ	Change in
ΔΔC_T	Delta delta C_T (equation)
µL	Microlitre
µM	Micromole
aa	Amino acid
Actβ	Beta-actin, mouse gene name
AMPA	α-Amino-3-hydroxy-5-methyl-4-isoxazolepropionic acid, protein name
AMPAR	α-Amino-3-hydroxy-5-methyl-4-isoxazolepropionic acid receptor, protein name
Arc	Activity-regulated cytoskeletal-associated protein, mouse gene name
ARC	Activity-regulated cytoskeletal-associated protein, protein name
Arg3.1	Activity-regulated cytoskeletal-associated protein, alternate gene name
β2m	Beta-2 microglobulin, mouse gene name
Bdnf	Brain-derived neurotrophic factor, mouse gene name
BDNF	Brain-derived neurotrophic factor, protein name
BLAST	Basic Local Alignment Search Tool
bp	Base pair

Ca^{2+}	Calcium ions
Ca^{2+}/CaM	Calcium/calmodulin
CaM	Calmodulin
CaMKIIα	Calcium/calmodulin-dependent protein kinase alpha subunit, mouse gene name
CaMKIIα	Calcium/calmodulin-dependent protein kinase alpha subunit, protein name
cDNA	Complementary DNA
CE	Capillary Electrophoresis
CMR	Cerebral Metabolic Rate
CNS	Central Nervous System
CP	Crossing point
C_T	Cycle threshold
Cx36	Connexin 36, protein name
De-I	Deionized
DEPC	Diethylpyrocarbonate
DNA	Dioxyribose Nucleic Acid
E	Efficiency
ED_{50}	Effective Dose
EDTA	Ethylenediaminetetraacetic Acid
EEO	Electroendoosmosis
EtBr	Ethidium Bromide
G	Gravity

g	Gram
GABRA5	γ-aminobutyric acid, protein name
Gapdh	Glyceraldehyde 3-phosphate dehydrogenase, mouse gene name
gDNA	Genomic DNA
Gjd2	Gap junction delta 2, mouse gene name
GOI	Gene Of Interest
GluN2B	Glutamate NMDA receptor subunit epsilon-2, protein name
Grin1	Glutamate NMDA receptor subunit zeta-1, mouse gene name
GRIN1	Glutamate NMDA receptor subunit zeta-1, protein name
HPRT1	Hypoxanthine-guanine phosphoribosyltransferase, mouse gene name
IDT	Integrated DNA Technologies
IEG	Intermediate Early Gene
IP	Intraperitoneal
JCAHO	Joint Commission on Accreditation of Healthcare Organisations
kB	Kilobases
kBp	Kilobase pairs
KO	Knockout
LB+	Lysogeny Broth with antibiotic (ampicillin)
LB	Lysogeny Broth

LTD	Long-Term Depression
LTP	Long-Term Potentiation
MAC	Minimum Alveolar Concentration
mg	Milligram
Mg	Magnesium
mL	Millilitre
mM	Millimole
MOPS	3-(N-morpholino)propanesulfonic acid
mRNA	Messenger RNA
mQ$H_2$0	Milli-Q $H_2$0
NCBI	National Centre for Biotechnology Information
ng	Nanogram
nM	Nanomole
NMD	Nonsense-Mediated Decay
NMDA	N-methyl-D-aspartate, protein name
NMDAR	N-methyl-D-aspartate receptor, protein name
NTC	No Template Control
OD	Optical Density
ORF	Open Reading Frame
PET	Positron Emission Tomography
PCR	Polymerase Chain Reaction
POCD	Post-Operative Cognitive Decline

PSD	Postsynaptic Density
qPCR	Real-time quantitative Polymerase Chain Reaction
QC	Quality Control
QT	Q-wave T-wave
R	Relative expression ratio
REST®	Relative Expression Software Tool
Rf	Reference gene
RNA	Ribonucleic acid
rRNA	Ribosomal RNA
RNases	Ribonuclease
RT	Room Temperature
-RT	No Reverse Transcription
SOP	Standard Operating Procedure
SNP	Single Nucleotide Polymorphism
t	Time
$\mathbf{T}_m$	Melting temperature
TA	Thymine Adenine
TE	Tris-EDTA buffer
U	Unit
UCSC	University of California, Santa Cruz
UoW	University of Waikato
UTR	Untranslated Region

Chapter One

Literature Review and Introduction

Anaesthetic agents include a wide variety of molecules that act on channels and receptors in the central nervous system (CNS) to induce anaesthesia [1]. At medically relevant concentrations, general anaesthetics depress neuronal activity in the brain resulting in the clinically desirable outcomes of analgesia, unconsciousness, numbed autonomic reflexes and amnesia [2]. Inhalation anaesthetics such as ether and nitrous oxide were first used in the mid-1800s and remained the standard for anaesthetic agents for many decades [3]. These molecules were relatively slow acting and caused a range of adverse effects including severe vomiting and nausea[3]. Non-flammable fluorinated hydrocarbon compounds such as isoflurane and sevoflurane were developed in the mid-1900s for use as volatile liquid anaesthetics and demonstrated less severe post-operative side effects [3]. The overall safety of anaesthetic agents has long been endorsed by valuable clinical outcomes [4]. Although anaesthetics are commonly used in medicine, their molecular substrates are still a matter of debate and the molecular mechanism underlying their amnesic effects is largely unknown [2,3]. There is currently no way of clinically monitoring the effect of anaesthetic drugs on memory. Therefore, the only way to ensure no memory is formed during surgical procedures is to keep the patient deeply anaesthetised [3]. However, prolonged exposure to high levels of anaesthetics is a major factor in anaesthetic neurotoxicity, which can cause deficits in synaptic density in the brain [4]. Anaesthetic exposure can also lead to altered gene expression of hundreds of genes and can enhance or reduce memory by influencing any of the encoding, consolidation or retention phases of memory processing [5,6]. Some of the molecular changes induced by anaesthesia may lead to

adverse effects that persist beyond the anaesthetic period, such as confusion and memory loss [6]. Studies investigating the effects of general anaesthetics on memory impairment have focused on physiological changes such as blood flow, brain electrical activity and energy metabolism, with little investigation into the effects on cells and tissues at the gene expression level [7]. General anaesthetics may have a powerful effect on the proteins that control genomic changes, which would result in altered gene expression [6]. Microarray studies have demonstrated that 1.5% of 10,000 genes analysed from whole brain tissue in the *Rattus* (rat) genome were affected by inhalation anaesthesia, the majority of which were down-regulated [8].

Amnesia is an essential outcome of anaesthesia as it prevents a patients' recall of the events surrounding surgery. Only low doses of anaesthetic (0.7% isoflurane or 1% sevoflurane) are required to suppress working memory, however the immobilizing dose of anaesthetic has been shown to vary by as much as 24% [1,9]. It is widely understood that newly acquired memories remain susceptible to disruption for a period of time after the learning event has occurred [10]. Memories that have been transferred to long-term storage prior to the administration of general anaesthetics are not generally affected [11]. The long-term memory of events that occur during low-dose anaesthetic exposure are often unable to be recalled, which may be due to the memory of the event not being transferred to long-term memory storage [11]. Additionally, while long-term memory processes have been previously associated with the hippocampus, neural substrates of specific memory functions have become increasingly identified within prefrontal cortical areas [12].

The use of general anaesthetics in medicine has provided a range of advantages for physicians when managing disease through surgery [13]. However, where hypoxia and organ failure were once the most concerning complications of surgery, intraoperative awareness has also become an identified risk [13]. Intraoperative awareness describes the unexpected memory recall of some or all of the events surrounding surgical procedures [13]. Present data suggests that intraoperative awareness occurs in 0.1 - 0.2% of patients, correlating to nearly 20,000 patients annually in the USA alone [13]. In 2004, the Joint Commission on Accreditation of Healthcare Organisations (JCAHO) suggested that anaesthetists should identify patients at greater risk of awareness prior to surgery to minimise adverse outcomes [13]. However, there still remains no method for identifying at risk patients and doctors have remained unsuccessful in preventing episodes of intraoperative awareness [13].

The overall risk of anaesthesia has progressively decreased since its introduction to medical use. Nevertheless, a lack of understanding of the molecular mechanisms of anaesthetics limits optimal use of these drugs and hinders efforts to produce safer anaesthetics [9]. The causes of intraoperative awareness are unknown and may be due to a range of factors, including individual variability in the expression of target receptors in the brain [9]. Preclinical studies using mice indicated that resistance to memory-blocking properties of the anaesthetic etomidate resulted from a genetic deficiency in α5-containing γ-aminobutyric acid (GABRA5) receptors [9]. Etomidate was found to impair memory and learning processes in the wild-type mice where there was no change in the genetically modified mice that lacked the altered GABRA5 receptors [9]. The human *GABRA5* gene contains many polymorphisms but the functional implications of these

polymorphisms are unknown and may be linked to anaesthetic resistance [9]. Genetic variability between individuals may be an important factor in regards to incidents of intraoperative awareness.

General anaesthesia can affect protein expression after the period of intended use, suggesting that post-operative memory impairment can also become prolonged [14]. Some effects following anaesthesia, such as vasodilation, can be clinically useful, however other adverse effects such as nausea, post-operative cognitive dysfunction (POCD) and long QT syndrome, (a prolonged Q-wave T-wave) have also been observed [6]. POCD is recognised as a relatively common post-operative complication, though the extent to which general anaesthetics contribute to this condition is unknown [14]. The degree of anaesthetic exposure is a recognised factor in determining anaesthetic neurotoxicity, which both younger and elderly patients are at risk of developing [4]. Studies using rodents have shown that anaesthetic exposure during stages of brain development can lead to a persistent decline in the number of synapses in the brain [4]. In similar studies, isoflurane administered to both young and adult rats demonstrated impaired memory in young rats with increasing deficits with age [4].

Therefore, this study investigated anaesthetic effects at the genetic level, focussing on genes involved in the long-term consolidation of memories that could be targets for anaesthetic drugs. These genes included *Arc*, *Bdnf, CaMKIIα, Gjd2* and *Grin1*. Specifically, the cerebral cortex of *Mus musculus* (mouse) brain tissue was analysed.

1.1 Neural Communication and Memory Consolidation in the Adult Mammalian Brain

Neurons in the adult mammalian brain form excitatory synapses that provide sites for information processing and storage throughout the brain [15,16]. Communication between neurons differs to that of other adult cells in that they possess the capacity for long-range signalling using chemical messengers called neurotransmitters [17]. Binding of neurotransmitters to specific cell surface receptors initiates signal transduction in neurons by converting chemical stimulation into electrical signals. Under conditions of repetitive neuronal firing, long-lasting cellular modifications may result, forming the basis of synaptic strengthening and memory consolidation [16,17].

Memory can be described in the most simple terms as conscious or unconscious, and short or long term [3]. Short term memory lasts only a few seconds but can be maintained by constant rehearsal [3]. In order to recall information beyond just a few seconds, consolidation from short-term to long-term memory must occur [3]. Memory consolidation describes a process whereby the transmission and storage of a memory trace occurs in response to the strengthening and restructuring of synapses in the brain [17]. Many molecular processes occur following the acquisition of a new memory and cellular response to changes in synaptic transmission include the activation of second messenger systems that reorganise synaptic networks [3,17]. The concept of memory consolidation is based around the theory that memory formation occurs in a series of different stages that produce a permanent memory trace as the stability and strength of the synapses increases (Figure 1) [17]. Enduring memory traces rely on *de novo* messenger RNA (mRNA) transcription and protein synthesis that result from specific signalling between the

synapse and nucleus [17,18] This signalling system provides a mechanism for permanent changes in synaptic strength, allowing the memory of specific events to be transferred into long-term storage [18].

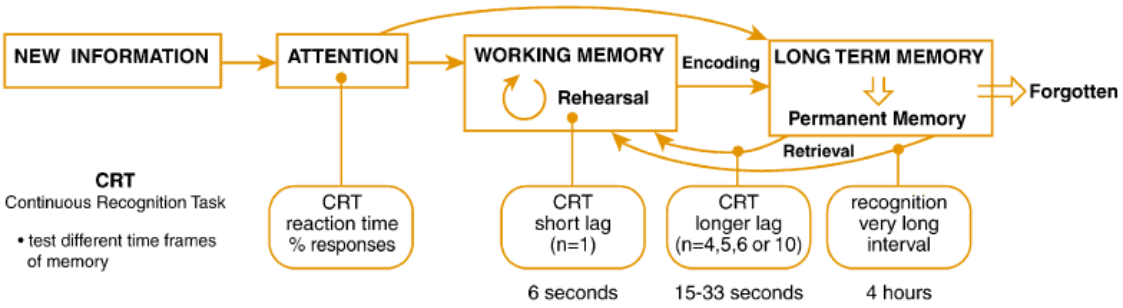

Figure 5: Long Term Memory Formation [19]. When new information is present, it is attended to and becomes resident in working memory. If nothing else happens it is forgotten, however if it is rehearsed and no new information comes in, it can stay in working memory. The only other way for information to be remembered is to be transferred into long-term storage, where it becomes a permanent memory.

Disruption to memory formation processes is an area of interest to neuroscience. Of all memory types, "conscious" or episodic memory is affected the most by general anaesthetics [3]. It has been suggested that amnesic drugs such as propofol do not prevent the acquisition of memories, but instead block the consolidation of those memories into long-term storage [3]. Memories acquired during a propofol dosage of 0.9 μg/mL are quickly forgotten, with the majority within the first 30 minutes [3]. This demonstrates an increased rate of memory loss following anaesthetic exposure, however the reason this occurs is still unknown [3]. Recent studies have indicated that general anaesthetic-induced memory impairment lasted at least two days in adult rats and up to two weeks in aged rats, with more pronounced effects at higher drug concentrations [7]. This indicated that the period of altered molecular events caused by anaesthesia also exists beyond the duration of drug exposure and initial recovery period.

1.2 Synaptic Plasticity and Long-Term Potentiation as Proposed Mechanisms for Memory Consolidation

Changes to activity-dependent gene expression is thought to underlie higher-order cognitive functions such as learning and memory [20]. Accurate learning and memory functions involve long-lasting structural modifications to synapses and increased synaptic transmission [5]. The strengthening of synapses in the brain is referred to as synaptic plasticity. It is a time-dependent process that is vital for the information processing that underlies memory function [11,21]. *In vitro* studies of synaptic plasticity have demonstrated the requirement of *de novo* protein synthesis in the long-term modification of synapses (Figure 2) [22]. General anaesthetics have demonstrated the ability to have both presynaptic and postsynaptic effects on the release and function of neurotransmitters in the brain, therefore affecting the synaptic transmission between neurons [23].

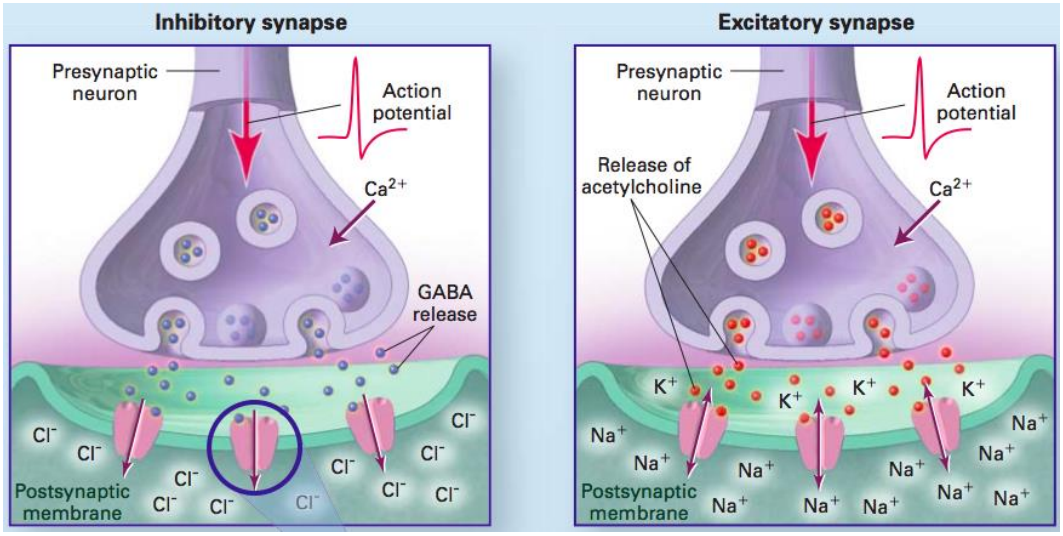

Figure 6: Inhibitory and Excitatory Synapses [23]. General anaesthetics can both activate inhibitory synapses and depress excitatory synapses. This action forms the basis of the current theory of anaesthetic action on specific molecular targets.

Understanding the neural activity that underlies synaptic plasticity is a fundamental objective of clinical neuroscience [15,21]. Long-term potentiation (LTP)

has been proposed as a mechanism for consolidation of long-term memory [15,24]. LTP and long-term depression (LTD) allow the development of enduring synaptic changes [15,24]. There are a wide variety of potential targets in the brain for drug-induced amnesia, including direct action on mechanisms such as LTP [3]. LTP is induced by increases in intracellular calcium ions in the postsynaptic terminal [15]. Glutamate opening of N-methyl-D-aspartate receptor (NMDAR) channels mediates entry of calcium into the cell as well as depolarization secondary to the activation of α-Amino-3-hydroxy-5-methyl-4-isoxazolepropionic acid receptor (AMPAR) channels in the postsynaptic terminal [6]. The newly imported calcium ions initiate a cascade of signalling events within the neuron that induce gene transcription and translation [6]. LTP has been widely researched in the hippocampus, where its induction follows NMDAR activation, causing increases in intracellular calcium levels [21]. LTP can be genetically and pharmacologically disrupted, which may be causally related to memory disruption post-anaesthesia [2]. As described earlier, general anaesthetics can modify the neurotransmitter systems central to synaptic plasticity, which results in a reduction in LTP [11]. Uncovering the neural effects of general anaesthetics *in vivo* has however, proven difficult [23].

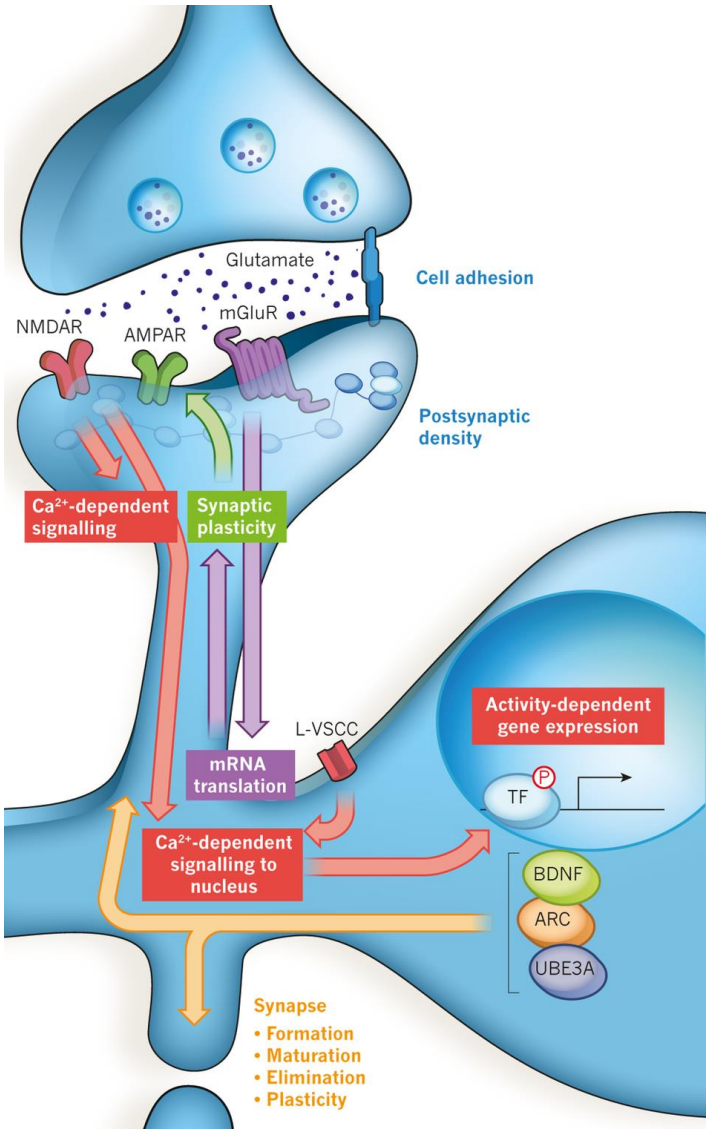

Figure 7: Signalling Events During Synaptic Activation [25]. Activity-dependent synaptic function in neurons is dependent on calcium signalling initiated by the binding of glutamate to NMDA receptors. The calcium signalling triggers activity-dependent gene expression in the nucleus and local mRNA translation.

1.3 The Cerebral Cortex and Long-Term Memory Consolidation

A study conducted over 50 years ago demonstrated a clear link between protein synthesis and long-term memory function in the cerebral cortex [22]. The cerebral cortex is the outermost layer of the brain (Figure 4) and plays a role in many higher-order cognitive functions [1]. The cortex and hippocampus are regions of the brain that have a well established role in all three phases of memory function; encoding, storage and retrieval [26]. Although much memory-related research has

focussed on the hippocampus, recent research has demonstrated that while the hippocampus is required for organising spatial information, the cerebral cortex is crucial for memory acquisition and storage [27]. The hippocampus has been developed into a major model system to study memory function however, the neural substrates of specific memory functions have been identified within prefrontal cortical regions [12]. Furthermore, Fidalgo et al. (2012) demonstrated that although isoflurane was able to impair neocortex-dependent memory in the mouse, it did not impair hippocampus-dependent memory.

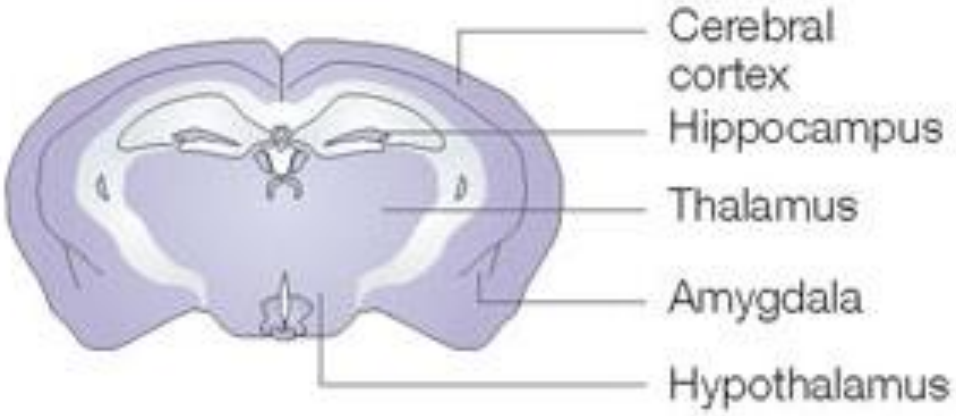

Figure 8: Memory-Related Regions of the Mouse Brain [28]. Depicted are the regions of the cerebral cortex, hippocampus, thalamus, amygdala and hypothalamus.

In the mammalian brain, the cortex is believed to store remote memories but little is understood regarding the sites and cellular circuits that underlie this process [29]. Active neurons in the cortex form organised clusters that are continuously re-shaped by learning, forming a neural network that is strengthened during memory consolidation [27]. Excitatory cortical neurons use dendrites to receive input from both distal and local neurons [27]. These functional excitatory interactions require the recruitment of NMDAR and form a cellular representation of memory [27]. Large-scale changes in neuronal activity, as well as activation of intermediate early genes (IEGs), strengthen existing synaptic connections whilst also producing new ones [27].

The prefrontal and superior and posterior parietal cortices are areas that have been linked to cognitive functions such as memory and perception, displaying depression during anaesthesia [1]. The frontoparietal cortex has also been previously identified as a region strongly suppressed by anaesthetics [1]. In one study, unconscious patients were found to have impaired cerebral metabolism for glucose in prefrontal and parietotemporal cortex regions [1]. Alkire et al. (2008) described a common circuit to anaesthesia and unconsciousness that includes the medial parietal cortex and posterior cingulate cortex, as well as lateral frontoparietal association areas and the thalamus. Similarly, a breakdown of this network during anaesthesia has been observed in other studies [1].

Decreased cortical activity is an important consequence of administered anaesthetics; as the firing patterns in cortical neurons decreases, a loss of feedback in the cortex occurs, resulting in the integration of less informative information and therefore disruption to memory processing [30,31]. At a clinically relevant concentration (1.4%), volatile isoflurane can reduce cortical metabolism by up to 50% [30]. Altered cortical activity during anaesthesia has been previously observed both *in vitro* and *in vivo* [30]. Brain regions involved in memory blockade have also been studied using imaging techniques. Functional MRI studies in humans demonstrated that sevoflurane at 0.25 MAC over 25 minutes was able to depress memory-related regions including the visual cortex, thalamus and hippocampus [11]. Other cortical areas, such as the primary visual cortex, are also sensitive to memory-blocking concentrations of anaesthetic [11].

1.4 General Anaesthetic Agents

Modern anaesthetic agents such as isoflurane and sevoflurane (Figure 5) provide rapid induction, faster recovery times and less severe post-operative side effects [32]. Adverse effects of anaesthesia can include nausea, vomiting, autonomic instability and delirium [23]. These adverse reactions may be the result of low target specificity of the anaesthetic drug [23]. However, as a range of autonomic brain functions are still active during anaesthesia, the suppression of neural activity is at least partly specific [1]. The clinical effects of anaesthetic agents are likely due to specific action on a limited number of molecular targets in the CNS [23]. Identifying these molecular targets is an area of current research and the differential sensitivity to anaesthetics that individual patients present indicates that anaesthetic effects may have a genetic basis [23]. The use of anaesthetics has enabled the rapid development of many medical procedures, from major surgeries to non-invasive diagnostic therapies [23]. Therefore, minimising side effects and improving the overall safety of general anaesthetics is very important in a clinical setting.

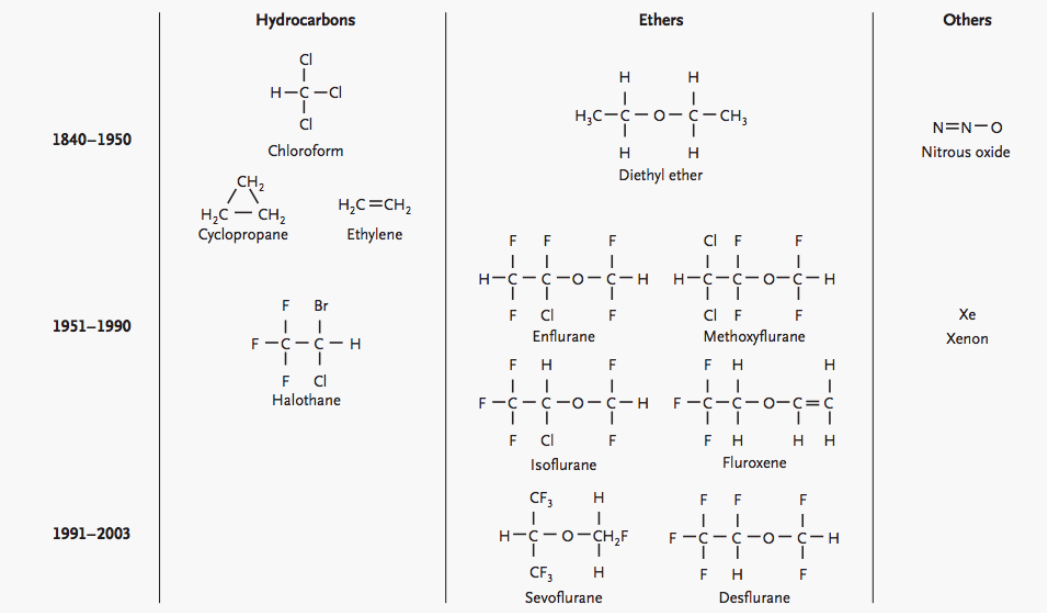

Figure 9: Different Classes of Inhalation Anaesthetics [23]. Hydrocarbons and ethers were introduced as anaesthetic agents in the mid-eighteenth century however, these agents proved to be either highly toxic or explosive. Halogenated ethers such as isoflurane, were first used in 1972 and further improved inhalation agents such as sevoflurane and desflurane, were introduced in the 1990s and remain the common choice for general anaesthetic.

The notion of anaesthetics targeting specific molecules differs from the classic view that all general anaesthetics act in a non-specific manner [23]. Early theories of anaesthetic mechanisms included non-specific action on the hydrophobic lipid components of cells by increasing lipid fluidity, triggering lipid phase transitions and altering lipid bilayer permeability [23,33]. This theory was based on observations that the potency of anaesthetics increased in direct proportion to its oil/water partition coefficient [33]. However, further research indicated that only slight perturbations in lipids occurred in response to general anaesthetics and the theory was largely abandoned [23]. In the mammalian brain, general anaesthetics produce depressed blood flow and glucose metabolism whilst also causing selective depression of specific cortical regions [23]. Therefore, global depression in the brain may be a result of altered ion channel activity [34]. Ion channels such as $GABA_A$, NMDA and AMPA receptors have displayed sensitivity to inhaled anaesthetics in previous studies [23]. These receptors can alter postsynaptic excitability by

influencing the presynaptic release of neurotransmitters to enhance inhibitory postsynaptic channel activity whilst also inhibiting excitatory activity [23]. Therefore, it is now widely assumed that general anaesthetics act on specific molecular targets to produce clinical effects such as amnesia. The potency of memory-blocking properties also differs between anaesthetics, which has been demonstrated using Pavlovian conditioning techniques [11]. During these behavioural assays, 0.3% sevoflurane was able to impair memory in mice where more than twice the dose (ED_{50}=0.47 MC) was required for isoflurane to produce the same result [11].

1.4.1 Sevoflurane

Sevoflurane (1,1,1,3,3,3-hexafluoro-2-(fluoromethoxy)propane) is a commonly utilised inhalation anaesthetic that has demonstrated a dose-dependent influence over memory in humans and rodents alike (Figure 6) [7]. High doses of 2% sevoflurane can induce large reductions in frontal cerebral blood flow [1]. Administration of sevoflurane also appears to have the ability to impair both the acquisition and consolidation phases of memory [5]. Limited processing and memory of auditory information has been demonstrated in studies using sevoflurane-induced anaesthesia [1]. Sub-anaesthetic doses of sevoflurane (0.3%) have also demonstrated impaired memory retention [5].

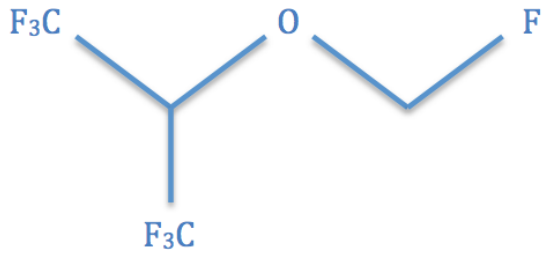

Figure 10: Skeletal Model of the Sevoflurane Molecule. Sevoflurane (1,1,1,3,3,3-hexafluoro-2-(fluoromethoxy)propane) is used in medicine as a volatile liquid anaesthetic for inhalation anaesthesia.

Studies conducted on whole rat brain tissue have demonstrated that sevoflurane administration can initiate changes at the gene expression level [8]. These studies have observed altered gene expression patterns that did not recover to control levels until at least 24 hours after anaesthesia, demonstrating long-lasting effects that persisted after awakening [8]. Genome-wide studies have also indicated down-regulation of over 350 genes in the hippocampus of rats following exposure to sevoflurane [7]. These genes were involved in cellular metabolism, development, structural processes, signal transduction and communication [7].

1.4.2 Isoflurane

Isoflurane (2-chloro-2-(difluoromethoxy)-1,1,1-trifluoro-ethane) is a halogenated ether that is used in medicine as a volatile liquid anaesthetic (Figure 7) [32]. Isoflurane-induced anaesthesia has been reported to increase beta amyloid deposition in human and rat cell cultures, indicating its potential for adverse effects on cognitive function [14]. *In vitro* studies have shown that both isoflurane and propofol can cause significant reductions in synaptic density [4]. Studies using mice have demonstrated that isoflurane-induced anaesthesia can impair neocortex-dependent memory [14]. Isoflurane has also been shown to impair LTP in the hippocampus in a dose-dependent manner [14]. Depression of action potential firing by isoflurane is almost identical *in vitro* and *in vivo*, indicating depression of rodent cortical activity in response to isoflurane-induced anaesthesia [30]. Exposure to inhaled isoflurane has also demonstrated prolonged changes to genomic networks in neurons [6]. Reduction in expression of AMPA channels and calmodulin with increased expression of voltage-gated calcium channels can be observed during brief exposures to isoflurane [6].

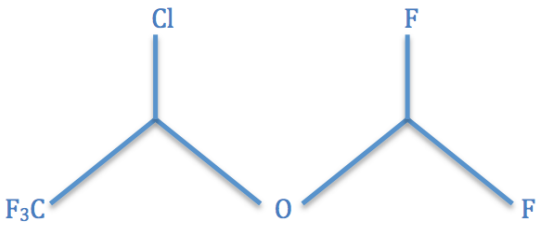

Figure 11: Skeletal Model of the Isoflurane Compound. Isoflurane (2-chloro-2-(difluoromethoxy)-1,1,1-trifluoro-ethane) is used in medicine as a volatile liquid anaesthetic for inhalation anaesthesia.

1.4.3 Propofol

Propofol (2,6-diisopropylphenol) is applied intravenously, providing clinically significant levels of amnesia as well as rapid recovery times (Figure 8) [35,36]. It was introduced in the 1970s, providing the advantages of short induction times (30 to 50 seconds) and rapid awakening (4 to 6 minutes) [37]. Propofol also induces deeper sedation than other anaesthetics, making it an attractive agent to use for longer surgical procedures [36]. Positron emission tomography (PET) studies have showed that propofol anaesthesia reduced the cerebral metabolic rate (CMR) by up to 70%, displaying more heterogeneous effects than CMR reduced by isoflurane [1]. Other studies have also reported impaired LTP in the hippocampus during propofol-induced anaesthesia [5]. Propofol displays selective disruption to long-term episodic memory and inhibition of calcium/calmodulin-dependent protein kinase α (*CaMKIIα)*, brain-derived neurotrophic factor (*Bdnf)* and activity-regulated cytoskeletal-associated (*Arc)* protein expression *in vivo* [38]. The intravenous anaesthetic propofol is also known to cause adverse effects such as nausea and hallucination, which may be a result of its narrow therapeutic window [35,36].

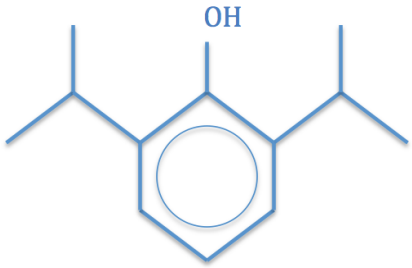

Figure 12: Skeletal Model of the Propofol Molecule. Propofol (2,6-diisopropylphenol) is used in medicine as an intravenous anaesthetic agent.

1.5 Genes of Interest

The expression of protein-coding genes occurs in a series of highly coordinated reactions that are under strict regulatory control [39]. Messenger RNA (mRNA) is an essential intermediate between translation of DNA sequence into functional proteins [40]. The transcription of DNA sequence into mRNA is the first step in protein synthesis and changes in this process can lead to phenotypic and morphological changes in the cell, as well as alterations to the way in which cells respond to environmental stimuli [41].

The translation of mRNA into functional proteins is a process that is essential to all cells, including neurons [22]. However, protein-based approaches are generally less sensitive and have lower throughput than RNA-based methods [22,41]. Polymerase chain reaction (PCR) and quantitative real-time PCR (qPCR) are common methods used to measure gene expression changes at the DNA transcription level and can provide information on changes in mRNA abundance in the cell, reflecting actual changes in gene expression [41]. Studies have shown that targeted disruption of protein-coding gene expression can interfere with long-term synaptic transmission, a mechanism vital to memory function [22]. As a single gene can influence multiple processes and many cognitive processes are

intercorrelated, it is likely that memory impairment caused by general anaesthetics involves a complex molecular network and altered expression of many genes [7]. Therefore, five genes were selected for qPCR analysis in this research.

The concept of pharmacogenomics was proposed in the 1960s and describes a genetically-influenced response to drugs [37]. Pharmacogenomics has been the object of much medical research and may provide a basis for personalised anaesthesiology in the future [37]. If specific genetic pathways altered by general anaesthetic agents can be identified, it may be possible to therapeutically reduce undesirable cellular responses and produce safer anaesthetics. By using information on human genetic variability, individualised use of anaesthetics may also become possible, which would enable optimised use of anaesthetics based on individual drug response [37].

Our research aimed to investigate altered mRNA expression of five memory-related genes within the cerebral cortex during periods of anaesthesia in pursuit of identifying molecular substrates of anaesthetic agents. Each gene was chosen on the basis of its described role in various aspects of the memory consolidation processes. The genes of interest (GOI) analysed in this study are discussed below in further detail.

1.5.1 Activity-Regulated Cytoskeletal-Associated Protein (*Arc*)

The *Arc* gene, sometimes known as *Arg3.1*, is an IEG that has been previously implicated in memory consolidation for its role in altering synaptic strength [31]. IEGs are rapidly induced in response to neuronal activity and can directly affect neuronal function, having been correlated with frequency spiking in

electrophysiological recordings [5,29]. Neuronal activity triggers rapid activation of approximately fifty IEGs in the brain [42]. The expression of IEGs is tightly linked to patterns of synaptic activity, making IEGs interesting candidates in the initiation of synaptic plasticity that underlies long-term memory storage and retrieval [17]. *Arc* transcription can be increased several-fold in cortical neurons, making it one of the most dynamically regulated IEGs [43]. The *Arc* gene also lacks homology with any other gene and does not belong to any major gene family, indicating a highly specific function [17]. Although expression occurs in the nucleus, *Arc* mRNA rapidly accumulates at sites of synaptic activity (Figure 9) and is produced following induction of LTP [15].

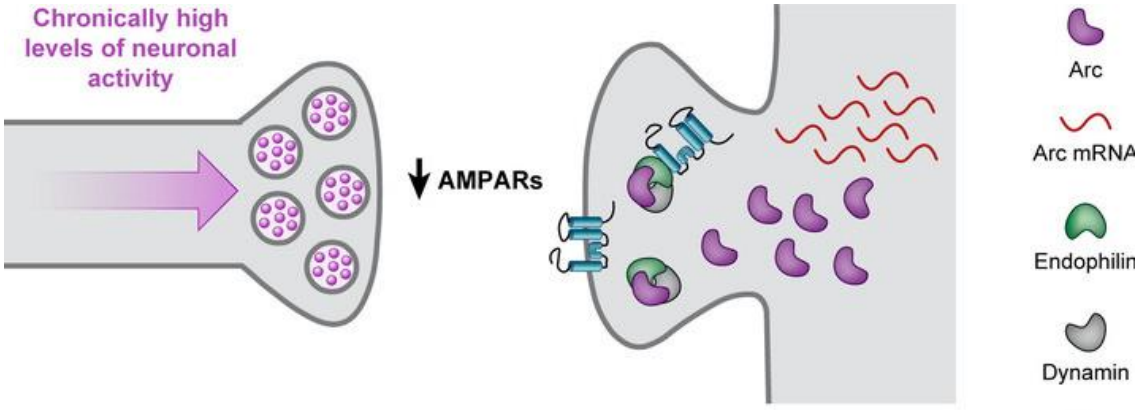

Figure 13: *Arc* Localisation to Active Synapses [44]. During periods of high neuronal activity, *Arc* mRNA and translated protein localise to dendritic sites.

The *Arc* gene (Figure 10) is located on chromosome 15 in mice and contains three exons separated by two introns. It is transcribed in the antisense direction to produce two mRNA variants that are 3056 and 3059 bp long, respectively [45]. *De novo Arc* synthesis is targeted by proteasomal degradation, displaying rapid translation-dependent degradation [45]. The 3' untranslated region (UTR) of *Arc* is a natural target for nonsense-mediated decay (NMD), resulting in destabilization of the mRNA after only a few rounds of translation [45]. *Arc* expression has been associated with information processing, resulting in enduring changes to the

synaptic plasticity of neurons [18]. It is controlled by strict regulatory mechanisms and disruption to these systems, which may occur during anaesthetic exposure, can lead to abnormal synaptic plasticity and impaired memory function [46].

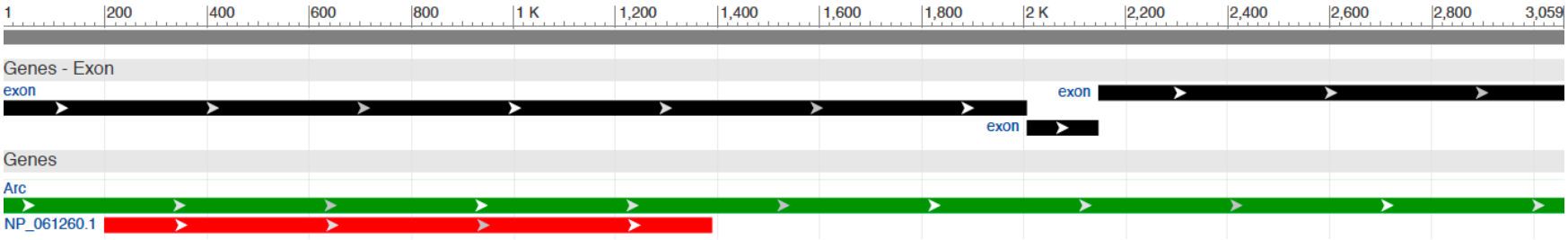

Figure 14: *Mus musculus Arc* Gene Structure [46]. The *Arc* gene is located on chromosome 8 in humans and chromosome 15 in mice. mRNA Transcript variant 1 of the mouse *Arc* gene is located on chromosome 15:74669081-74672570, and is 3056 bp long (green bar). The position of the three exons are indicated by the black bars. The open reading frame (ORF) is located within exon one and spans 1,191 bp, as depicted by the red bar. In the mouse, the translated *Arc* gene is predicted to express a protein consisting of 396 amino acids (aa) and weighing 55kDa.

Activation of NMDAR and the subsequent rise in intracellular calcium is also vital to *Arc* transcription [15]. *Arc* mRNA is expressed at high levels in the cortex in response to synaptic activation, which is vital to LTP and the consolidation of long-term memory [17,47]. The *Arc* mRNA transcripts are enriched in dendritic spines and are induced in a CAMKIIα- and NMDAR- dependant manner in the neocortex [17,47]. Following induction of LTP, *Arc* mRNA is transcribed and transported to dendrites where it is targeted to active synapses [18]. The *Arc* protein interacts with CAMKIIα and plays a selective role in the induction and maintenance of LTP and long-term memory function [43,46]. *Arc* knockout (KO) mice have demonstrated altered LTP and LTD as well as the inability to produce stable synaptic transmission, resulting in long-term memory impairment [17]. In addition, disruption to *Arc* expression has led to impairment in synaptic efficiency and memory consolidation in previous studies [43,46]. Inhibition of *Arc* synthesis with antisense oligonucleotides was shown to cause deficits in memory consolidation [48]. Other gene expression studies have also shown *Arc* was amongst the IEGs identified as being altered in response to inhalation anaesthesia, demonstrating suppression of *Arc* expression during sevoflurane-induced anaesthesia [8]. Both *Arc* mRNA and protein levels display up-regulation during periods of heightened synaptic activity, therefore we expect to see down-regulation in response to a period of anaesthesia as a result of decreased brain activity [49].

1.5.2 Brain-Derived Neurotrophic Factor (*Bdnf*)

The *Bdnf* gene is a member of the nerve growth factor superfamily, functioning to influence differentiation and survival of neurons in the mammalian brain [49]. Both the biosynthesis and secretion of neurotrophins is dependent on neuronal activity

and BDNF, specifically, has been implicated in both short- and long- term synaptic changes [49,50]. It has been previously suggested that neurotrophic factors, especially BDNF, play an important role in the reduction of synaptic density in response to both isoflurane and propofol [4]. Research has demonstrated that BDNF induces translation of dendritically-localised mRNAs, such as *Arc*, to support activity-dependent changes to synaptic efficiency [49]. BDNF has revealed a key role in regulating activity-induced LTP and various other cognitive functions including short- and long- term plasticity of glutamatergic synapses [49,51]. Lasting effects on synaptic efficiency may therefore involve BDNF regulation of local protein synthesis at postsynaptic sites [49]. When exogenous BDNF was applied to hippocampal and cortical tissue, it induced rapid and long-lasting enhancement of synaptic transmission resulting in increased glutamate release and heightened probability that NMDAR channels would be open [49]. Transcriptional activation of *Bdnf* is also required for maintenance of LTP and may be necessary for memory consolidation and recall [52]. *In vivo* rat studies have shown that BDNF alone can activate LTP, which requires transcription of plasticity-related genes including IEGs such as the previously implicated *Arc* gene [52].

Bdnf transcripts in the mouse brain consist of a protein-coding exon spliced to one of nine non-coding exons and different transcript variants are specific to different regions of the brain (Figure 11) [53]. The *Bdnf* gene contains at least nine upstream promoters, some of which are more sensitive to neuronal activity than others [20]. It is transcribed in the sense direction to produce a heterogeneous population of *Bdnf* mRNAs [54].

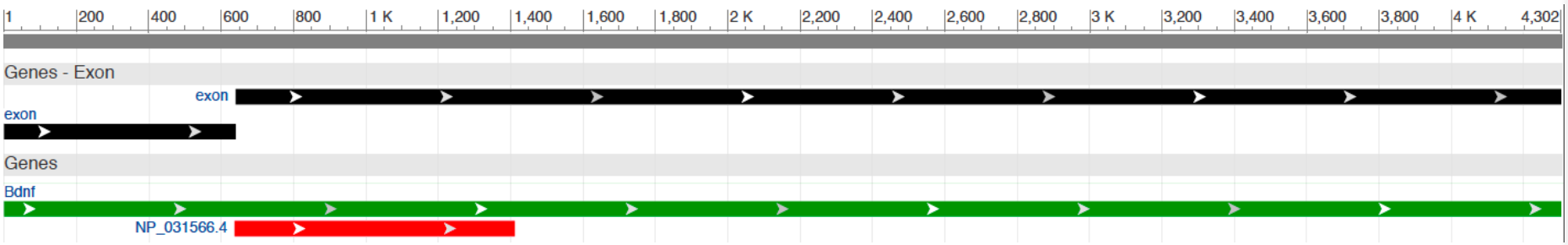

Figure 15: *Mus musculus Bdnf* Gene Structure [46]. The *Bdnf* gene is located on human chromosome 11 and chromosome 2 in the mouse. Mouse *Bdnf* mRNA transcript variant 1 is located at chromosome 2:109674700-109727043 in mice and contains two exons (black), with the ORF found in the protein-coding exon two The ORF of transcript variant 1 (red) spans 774 bp, producing a protein of 257 aa. All nine transcript variants of mouse *Bdnf* differ in the first exon present and expressed differentially throughout the body.

Neurotrophin-induced expression of plasticity-related genes may indicate a mechanism for the maintenance of synaptic activity and could potentially be modified by general anaesthetics [52]. A number of studies have investigated *Bdnf*-induced protein changes, however, the molecular genetics of BDNF-induced synaptic plasticity are unknown [49,52]. Reduced BDNF levels after administration of the intravenous anaesthetic propofol have been previously observed in the hippocampus [38]. Also of relevance, *Arc* and *CaMKIIα* mRNAs are both sensitive to BDNF regulation [49].

1.5.3 Calcium/Calmodulin-Dependent Protein Kinase α (*CaMKIIα*)

The *CaMKIIα* gene encodes the vital alpha (α) isoform of the CaMKII protein, which plays an important role in the post-induction phase of LTP [55]. The open reading frame (ORF) of *CaMKIIα* consists of 18 exons that span over 50 kilobase pairs (kbp) on chromosome 18 in the mouse (Figure 12) [16]. *CaMKIIα* mRNA is located in dendritic spines in the cerebral cortex, in similar subcellular distribution as *Arc* mRNA [16]. *CaMKIIα* mRNA accumulation in the dendrites of hippocampal and cortical neurons is regulated by its 3' UTR [56]. Although proteins are known to interact with the promoter region of *CaMKIIα,* properties of these proteins have not been characterised and transcriptional regulatory mechanisms of *CaMKIIα* gene expression is not known [16]. CaMKIIα is present in high concentrations in the brain and makes up a significant portion of the protein found in postsynaptic density (PSD) [16].

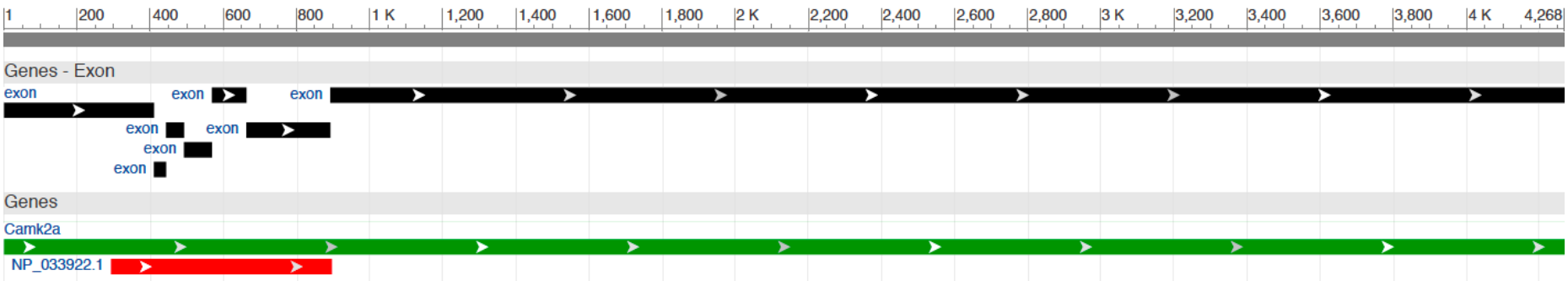

Figure 16: *Mus musculus CaMKIIα* Gene Structure [46]. The *CaMKIIα* gene is located on human chromosome 5 and chromosome 18 in the mouse. In mice, *CamKII* α transcript variant 1 is located at chromosome 18:60963554-60988152 and is produced by alternate splicing to contain seven exons (black) spanning 4268 bp. The ORF of transcript variant 1 (red) spans 603 bp, producing a 200 aa protein.

Neuronal CaMKIIα is known to regulate several important functions including neurotransmitter synthesis and release, modulation of ion channel activity, cell morphology, synaptic plasticity, memory processing and gene expression [16]. CaMKIIα regulation of other proteins involves phosphorylation and previous studies have indicated that inhibition of *CaMKIIα* can have a very strong amnesic effect [55]. Mice lacking the α isoform of CaMKII also demonstrate defective LTP [16]. Some data suggests that *CaMKIIα* expression can be increased with BDNF treatment [49]. The concentration of CaMKIIα in neurons varies with age, demonstrating markedly increased expression in activated synapses [16]. Furthermore, previous research has demonstrated Ca^{2+}/CaMKIIα signalling is inhibited by the intravenous anaesthetic propofol [38].

CaMKII is highly abundant in the brain and has been previously implicated in LTP [57]. LTP has been proposed as a molecular mechanism of memory formation and is a central process in the regulation of glutamatergic synapses, requiring calcium/calmodulin (Ca^{2+}/CaM) activation of CaMKII (Figure 13) [58]. During the induction phase of LTP, Ca^{2+} enters the neuron via NMDAR and binds to calmodulin (CaM), causing an increase in intracellular Ca^{2+} levels and activation of CaMKII [57,58]. Increases in intracellular calcium concentration can influence a range of biochemical processes in the brain, including synaptic plasticity [42]. Elevation of intracellular calcium ions acts as a secondary messenger system to activate expression of genes related to LTP maintenance [42]. Following induction, LTP is maintained by an increase in the CaMKII/NMDAR complex that persists for the duration of LTP [57]. *In vitro* studies have shown that mutations near the CaMKII phosphorylation site blocked LTP [57]. Other experiments have also used mice with mutated glutamate NMDAR subunit epsilon-2 (GluN2B) to interfere

with the CaMKII/NMDA complex and found a 50% reduction in LTP as well as significantly reduced spatial memory [57]. Calcium-sensitive genes may therefore be important substrates of general anaesthetics [42].

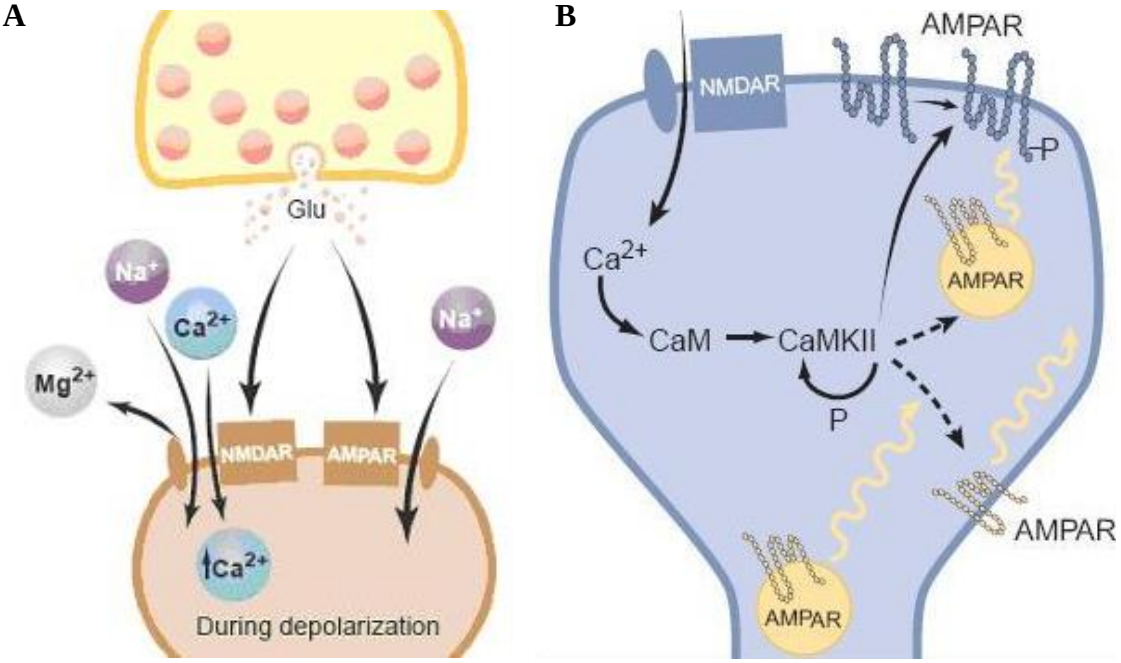

Figure 17: Activation of CaMKII during LTP [59]. A) During depolarization, glutamate binding to NMDAR causes an increase in intracellular calcium. B) Intracellular calcium binds to CaM to activate CaMKII, which influences the localisation of AMPAR to the synaptic plasma membrane.

1.5.4 Gap Junction Delta-2 Protein (*Gjd2*)

Gap junctions form specialised electrical synapses between adjacent cells that allow direct transfer of ions, metabolites and secondary messengers (Figure 14) [60,61]. Connexin proteins form the gap junctions that provide electrical coupling between neurons in the brain [60]. Electrical cell coupling is dependent on cell-type specific expression patterns of each connexin molecule [60]. Neuronal glial cells in particular contain a large repertoire of connexins that is not seen in any other cell type [61]. Connexin molecules play an important role in synchronizing synaptic activity and long-range signalling between neurons [62]. Twenty connexin proteins have been identified in the mouse and 21 in humans, each forming a

multimeric assembly of proteins that form a transmembrane domain [62]. Several pathological conditions have been identified as a result of altered connexin expression [60].

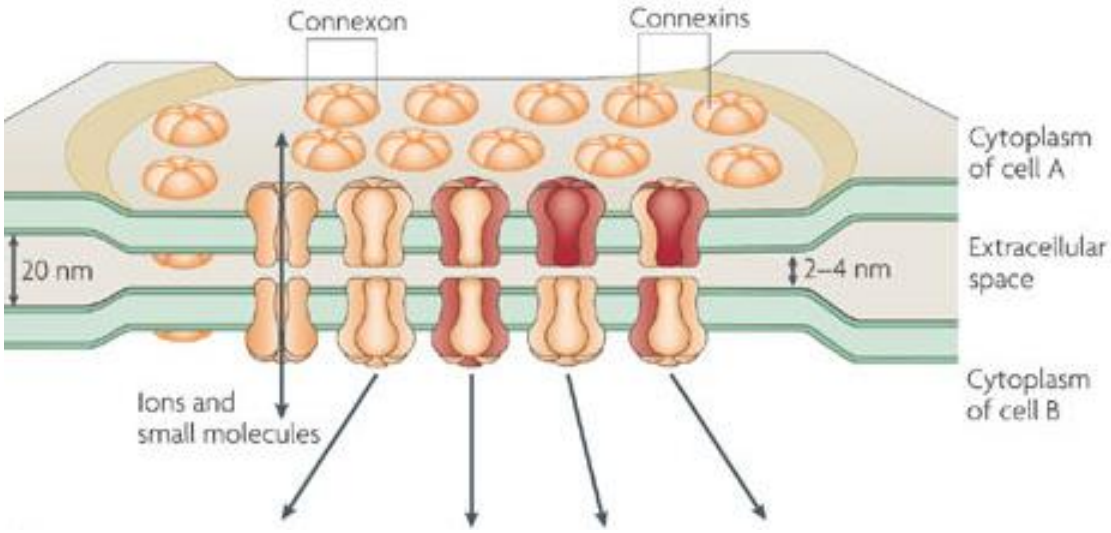

Figure 18: Gap Junctions Between Neighbouring Neurons [63]. Connexin proteins form gap junctions between adjacent neurons in the brain for the transfer of ions and other small molecules.

The *Gdj2* gene is located on mouse chromosome 2 and encodes connexin36 (Cx36); a connexin protein that is specific to neuronal cells in human and mice [62]. The coding region of *Gjd2* is positioned on two exons that are interrupted by a 1.14 kB intron, differing from other connexin proteins that have only one coding exon (Figure 15) [60,62]. Comparison between coding regions of *Gjd2* homologs indicate that there are highly conserved regions of this gene [62].

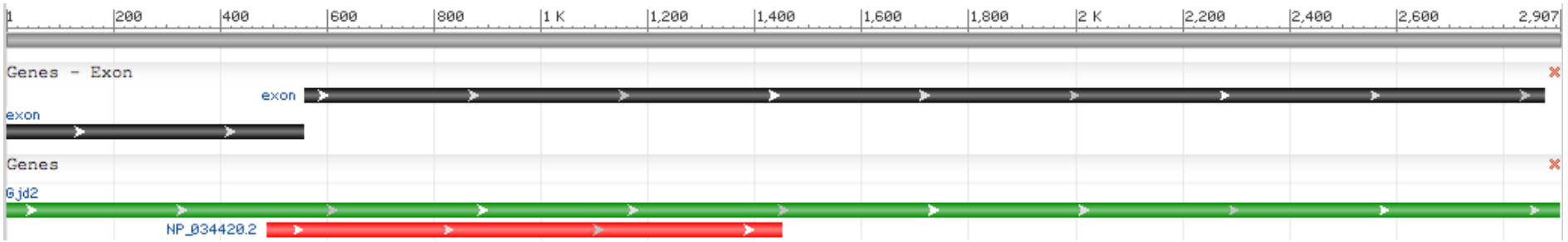

Figure 19: *Mus musculus Gjd2* Gene Structure [46]. The *Gjd2* gene is located on chromosome 2:114009601-114013619 in the mouse and on human chromosome 15. Mouse *Gjd2* mRNA is made up of two exons (black), with the ORF (red) beginning in exon one and ending part way through exon two. The ORF spans 966 bp and produces a protein 321 aa in length.

Cx36 demonstrates a broad distribution pattern in electrical networks in the adult rodent brain, especially in interneurons of the cerebral cortex [61]. *Gjd2* KOs display reduced interneuronal synchronization in the cortex and impaired cerebellar learning, as well as down-regulation of LTP in the hippocampus [64].

1.5.5 Glutamate NMDA Receptor Subunit Zeta-1 (*Grin1*)

Glutamate is the major excitatory neurotransmitter in the mammalian brain, binding to two main types of surface receptors; NMDAR and AMPAR [65]. NMDAR are located at postsynaptic sites of excitatory synapses and are made up of two GluN1 subunits and two of either GluN2 or GluN3 subunits [26]. The *Grin1* gene encodes the essential GluN1 subunit of NDMARs and undergoes alternative splicing to produce eight transcript variants (Figure 16) [66]. All eight transcript variants have heterogeneous expression patterns in the brain, displaying an age-dependent decline in the number of receptors throughout the brain [26]. The age-related decline of *Grin1* protein and mRNA variants has also been observed in the cortex of the brain [26].

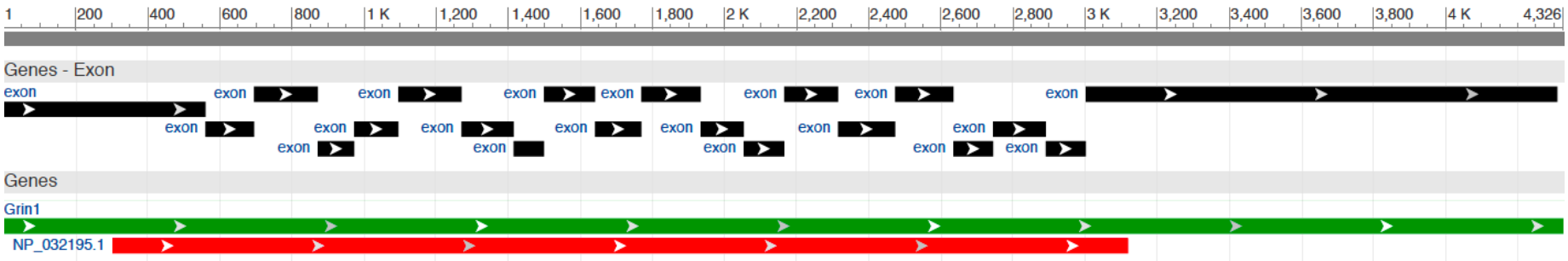

Figure 20: *Mus musculus Grin1* Gene Structure [46]. The *Grin1* gene is located on human chromosome 9 and chromosome 2 in mice. There are eight splice variants of *Grin1* mRNA in the mouse, all of which are expressed in the brain. Transcript variant 1 is located at chromosome 2:25291177-25319187 and contains twenty exons (black). The ORF (red) spans 2,817 bp, producing a protein 938 aa in length.

NMDAR mediate Ca^{2+} flux into neurons, which is essential to synaptic plasticity and synapse development (Figure 17) [67]. Due to high Ca^{2+} permeability, NMDAR cause large fluxes in intracellular Ca^{2+} levels, however the mechanisms that control NMDAR activation are largely unknown [67]. NMDA receptor antagonists have been shown to impair memory function and block LTP initiation [26]. A virus-based genetic approach to selectively knockout *Grin1* from the cortex of mice demonstrated strong evidence that LTP was then unable to be initiated *in vivo* [27]. This study also discovered that synaptic plasticity in the cortex of these mice was impaired during associative learning tasks [27]. Other studies have showed that *Grin1* deletion reduced acquisition of spatial and temporal memories [27]. As high frequency stimulation is required to activate NMDA receptors, reduced neural activity during anaesthesia may result in down-regulation of the *Grin1* gene. Furthermore, brief exposure to the anaesthetic isoflurane had previously demonstrated a reduction in the expression of *Grin1* [6].

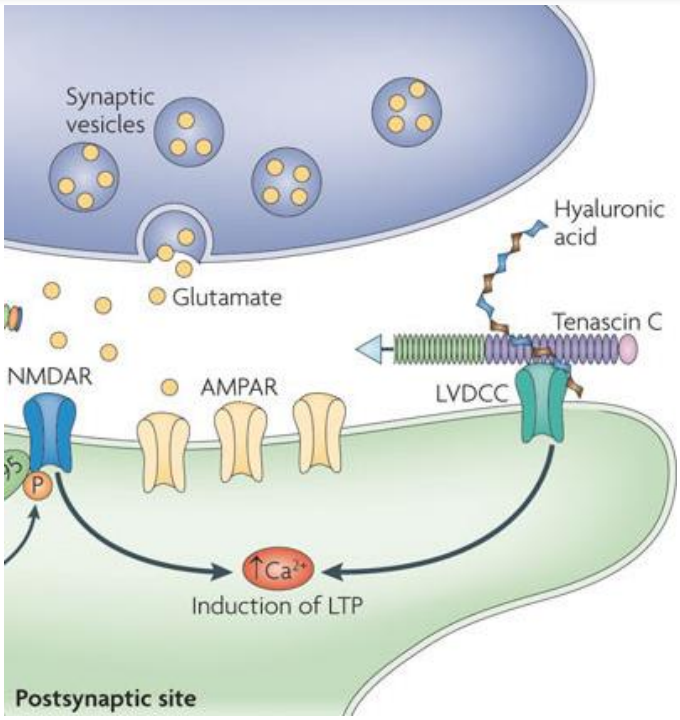

Figure 21: LTP Induction During Synaptic Plasticity [68]. Glutamate binding to NMDAR causes an influx of calcium ions into the postsynaptic cell. Calcium flux through NMDAR on the postsynaptic cell induces LTP.

1.6 Bioinformatic Data for the Five Genes of Interest

The bioinformatic data for the GOIs, *Arc, Bdnf, CaMKIIa, Gjd2* and *Grin1*, was retrieved from the National Centre for Biotechnology Information (NCBI) and is listed in Table 1.

Table 1: Gene Data for all Genes of Interest. In alphabetical order, the gene name and accession number are listed for all genes of interest with NCBI accession number, orientation, chromosome location and size of the mRNA transcript (bp).

Gene name	Accession Number	5' – 3' Direction	Chromosome Location	mRNA Size (bp)
Arc	NM_001276684.1	Antisense	Chr15: 74,669,081 – 74,672,570	3,059
Bdnf	NM_007540.4	Sense	Chr2: 109,674,700 – 109,727,043	4,302
CaMKIIα	NM_009792.3	Sense	Chr18: 60,963,554 – 60,988,152	4,268
Gjd2	NM_010290.2	Antisense	Chr2: 114,009,601 – 114,013,619	2,907
Grin1	NM_008169.3	Antisense	Chr2: 25,291,177 – 25,319,187	4,326

1.7 Real-time Quantitative Polymerase Chain Reaction (qPCR)

The polymerase chain reaction (PCR) is a laboratory technique that was developed in 1983 by Dr. Kary Mullis and colleagues [69]. It has since become an increasingly important tool in molecular laboratories by providing a rapid and accurate system for amplifying mRNA in the form of complementary DNA (cDNA) or genomic DNA (gDNA) [70]. Quantitative PCR (qPCR) was introduced in 1992 and is an extension of standard PCR, combining the amplification and detection steps to compare levels of DNA targets [69,71,72]. Real-time imaging of

product amplification is made possible by the addition of fluorescent reporter dyes that are incorporated into the target sequences and visualised in 'real time' [71,73]. The qPCR assay measures increases in fluorescent signals during the assay, which is directly proportional to the amount of product amplified (Figure 18) [73].

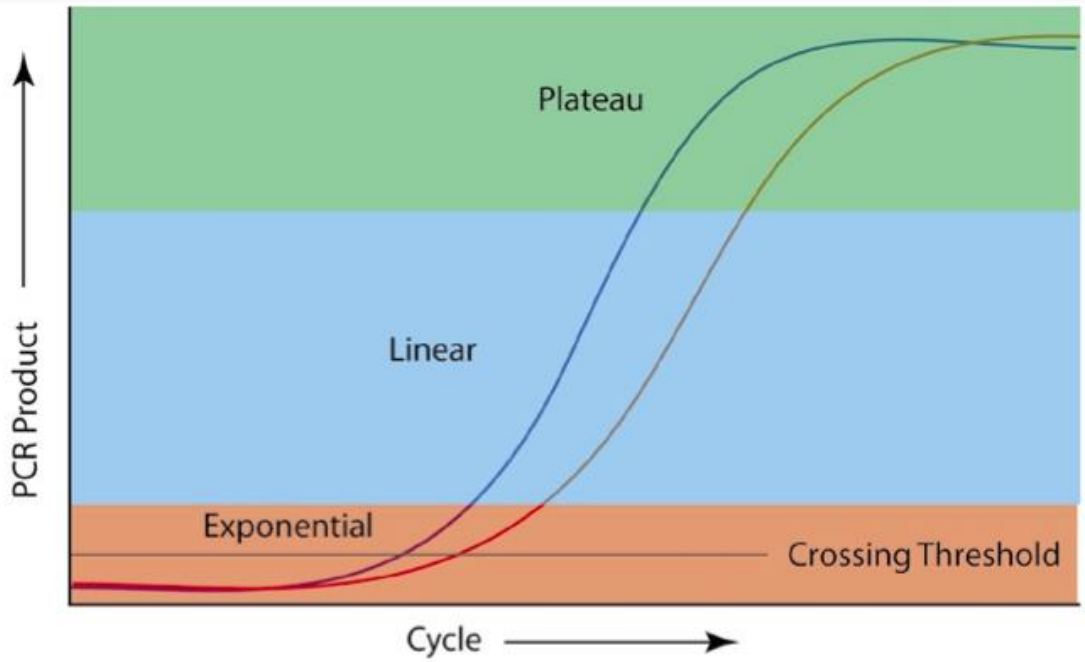

Figure 22: Phases of the qPCR Assay [74]. During the exponential phase of qPCR, the amount of product is relatively small and the reagents are not limited, therefore the reaction efficiency is close to 100%. As the amount of product is small, fluorescence is difficult to detect. During the linear phase, the reagents become more limited and the reaction efficiency begins to decline as the product accumulates. Once the plateau phase is reached, product fails to accumulate any further. The number of cycles at which the fluorescence exceeds the threshold is called the threshold cycle (C_T) or crossing threshold and signals detected above this level are considered 'real'.

Although qPCR was designed for DNA quantification, it is now commonly used to examine mRNA levels [74]. The ability to quantify mRNA amplification in real time has been a major advance in molecular methodologies as it allows determination and quantification of differential gene expression [70]. Due to high sensitivity and specificity, qPCR has become a foundation method in molecular diagnostics [75]. This study aimed to analyse the relative quantification of *Arc*, *Bdnf*, *CaMKIIα, Gjd2* and *Grin1* gene expression between control and anaesthetic treatment samples using qPCR methodologies.

1.8 Animal Model for Exposure Trials

The C57/BL6:129sv strain of mice was used as an animal model for anaesthetic exposure in this research. Mice have been used as a leading model system in biomedical studies of human genes in order to better understand gene function [76]. Over 90% of the mouse and human genomes can be divided into regions of conserved synteny, reflecting conservation of genes and gene function between the two mammalian species [76]. Additionally, both the mouse and human genomes contain approximately 19,000 protein-coding genes, with roughly 80% of mouse genes having an identifiable orthologue in the human genome [76,77]. The mouse model offered a means of investigating gene expression in the cerebral cortex, which would not have been possible in humans.

1.9 Hypothesis, Aims and Objectives

Although memory loss is a common result of general anaesthesia, incidents of intraoperative awareness do occur and there is currently no understanding of why this happens. The cerebral cortex is an important region for the processing of long-term memory and was the region of interest to this research. This data will address the question of whether memory-related gene expression changes during t=2 hour and t=4 hour exposure to general anaesthetics in mice.

1.9.1 Hypothesis

Our hypothesis is that memory-related gene expression will change in the cerebral cortex in response to clinical doses of general anaesthetics.

1.9.2 Aims

The main aims of the research undertaken in this thesis was to 1) investigate and select genes of interest, 2) analyse potential changes in the expression of several memory-related genes in the cerebral cortex using a mouse model, and 3) compare results between exposure to sevoflurane, isoflurane and propofol.

1.9.3 Objectives

The first objective was to determine the changes in gene expression of five GOIs during t=2 hour and t=4 hour exposure to general anaesthetics. Each drug treatment was carried out on six mice: three for the two-hour analysis and three for the four-hour analysis. Six additional control animals were used: three for the zero-hour analysis and three for the four-hour analysis. Molecular techniques were carried out to achieve:

a) Cortical tissue dissection from mouse brain;
b) RNA extraction, quantification and qualification;
c) DNase treatment;
d) cDNA synthesis; and
e) qPCR.

The second objective was to evaluate the qPCR results and carry out statistical analyses using the REST© (V2.0.13, 2009) software to:

a) Generate expression ratios for all GOIs with their corresponding *p*-values;
b) Produce a whisker-box plot to represent data sets;
c) Determine whether gene expression was different to the control; and
d) Validate specificity of product amplification.

Chapter Two

Materials and Methods

All methods were carried out in the C.2.03 Molecular Genetics laboratory at the University of Waikato (UoW), unless stated otherwise. Solutions were made up with autoclaved 15 – 18 megohm-cm double distilled water (mQH_20). The water used for all RNA work was further treated with 0.1% diethylpyrocarbonate (DEPC) for inactivation of RNase enzymes. All glassware was cleaned in a dishwasher, autoclaved and dried overnight in an 80°C oven before use. Recipes for all buffers and solutions used in this research can be found in Appendix 3.

2.1 Preparation of Mammalian Brain Tissue

All animal handling procedures were approved by the UoW Animal Ethics Committee (Hamilton, New Zealand) under approval number 905 (Appendix 1). Eight-week-old male and female C57/BL6:129sv mice were used in this research. Each experiment was conducted at the same time (*t*) of day to reduce temporal variations in the transcription of our GOIs. Four mice were selected for individual experiments to provide a *t*=0 hour control, a *t*=4 hour control, a *t*=2 hour treatment and a *t*= 4 hour treatment. Each experiment was replicated three times to ensure statistical significance of results.

For anaesthesia, two mice were placed in an isolated Perspex container for the anaesthetic exposure (Figure 19), and one mouse was placed in a separate Perspex container as the *t*= 4 hour control. No anaesthetic was applied to the control animal chamber. The animal chambers contained a layer of wood shaving as per normal bedding provided for the mice in their holding facility. A heat lamp

positioned directly above the Perspex chambers was used to maintain a stable and comfortable temperature. All mice were euthanased according to the guidelines outlined in the UoW Standard Operating Procedure (SOP) 9 (Appendix 2).

Figure 23: Experimental Design for Delivery of Volatile Anaesthetics Isoflurane and Sevoflurane. Two animal chambers were set up inside the fume hood; one for the *t*=4 hour control mouse and one for the *t*=2 hour and *t*=4 hour treatment mice.

2.1.1 Volatile Anaesthesia with Isoflurane and Sevoflurane

All experiments involving administration of volatile anaesthetics were carried out in the fume hood at room temperature (RT), due to the inhalation risk. For isoflurane-induced anaesthesia, 0.125 mL of isoflurane was applied to the sealed animal chamber through a rubber stopper for inhalation and the mice lost consciousness within approximately two minutes. Every hour, 0.063 mLs of isoflurane was added to the animal chamber to maintain anaesthesia. As sevoflurane is half as potent as isoflurane, 0.2 mLs of sevoflurane was added at

t=0 hours and another 0.1 mLs every hour for maintenance of sevoflurane-induced anaesthesia [11]. Gas levels of CO_2 and volatile anaesthetics were monitored every ten minutes through a side-port entry to the chamber (that could be rapidly opened and closed) using a Datex Capnomac Ultima Anaesthesia Monitor (Anaesthesia Department, Waikato Hospital, New Zealand). The CO_2 was prevented from exceeding 5% within each animal chamber, so as to comply with the standards outlined in Animal Ethics Approval number 905. If the CO_2 levels reached 5%, the chamber was rapidly opened, flushed with fresh air, resealed and another dose of anaesthetic was applied.

2.1.2 Intraperitoneal Anaesthesia with Propofol

The intraperitoneal (IP) anaesthetic used in this research was 1% propofol 200 mg/20 mL (Provisi MCT-LCT 1%, Claris) and all propofol experiments were conducted in the lab, as there was no inhalation risk that required the use of a fume hood. However, animals were kept under a heat lamp and in the same animal chambers as those used for volatile anaesthesia to reduce environmental variation between the experiments. In this case, the lids were rested on top of the chambers but not sealed, eliminating the build up of CO_2. One mouse was immediately euthanased as the *t*=0 hour control. Initial doses of propofol were administered as 100 mg/kg, based on the weight of each mouse. The mouse was restrained by placing the thumb and forefinger behind the front paws and gripped tightly to prevent any movement of the head. The tail was also pulled back to lengthen the mouse's body for access to the peritoneal cavity on the underside of the mouse. A 0.5 mL BD Ultra-Fine™ insulin syringe (Beckton Dickson and Company, USA) was used to administer propofol to the IP cavity for the *t*=2 hour and *t*=4 hour treatment animals. The initial doses administered to all mice used in

the experiments are outlined in Table 2. The *t*=4 hour control was administered a dose of the intralipid vehicle at 0 hours. The mice were monitored every five minutes to ensure the animals were still under anaesthesia and further "top up" doses were administered when required. Anaesthesia was confirmed by placing the mice on their backs and observing that they were not able to right themselves.

Table 2: Weight and Initial Propofol Dose for Propofol Treatment.

Experiment	Mouse	Sex	Weight (g)	Initial Dose (mL)
1	1	Male	31	0.31
	2	Male	29	0.29
	3	Male	29	0.29
2	1	Female	22	0.22
	2	Female	22	0.21
	3	Female	21	0.21
3	1	Female	23	0.23
	2	Female	31	0.31
	3	Female	21	0.21

2.2 Cortical Tissue Extraction

At the designated time point, each mouse was placed in a carbon dioxide-filled chamber. Following a negative response to the pedal reflex, the mouse was euthanased and whole brain was removed (Figure 20). Cortical tissue was extracted from the whole mouse brain using macro dissection techniques and a sterile scalpel (Swann motion carbon-steel surgical blade, size 21). The cerebral cortex was carefully isolated from underlying subcortical tissue and approximately 50 mg of tissue was obtained from each whole brain sample.

Tissue samples were immediately immersed in a sterile screw cap 2 mL tube (Scientific Specialties, USA) containing 1 mL of TRI Reagent® (Molecular Research Centre, USA), a capful of 0.1 mm zirconia/silica beads (BioSpec Products, USA) and eight 2.5 mm glass beads (BioSpec Products, USA). The capful was measured using the 2 mL tube cap. TRI Reagent® contains phenol and guanidine thiocyanate in a mono-phase solution that inhibits RNase activity, permitting separation of RNA from DNA and proteins whilst maintaining RNA integrity. An RNA extraction protocol was carried out immediately following tissue isolation using the methodologies described in section 2.3.

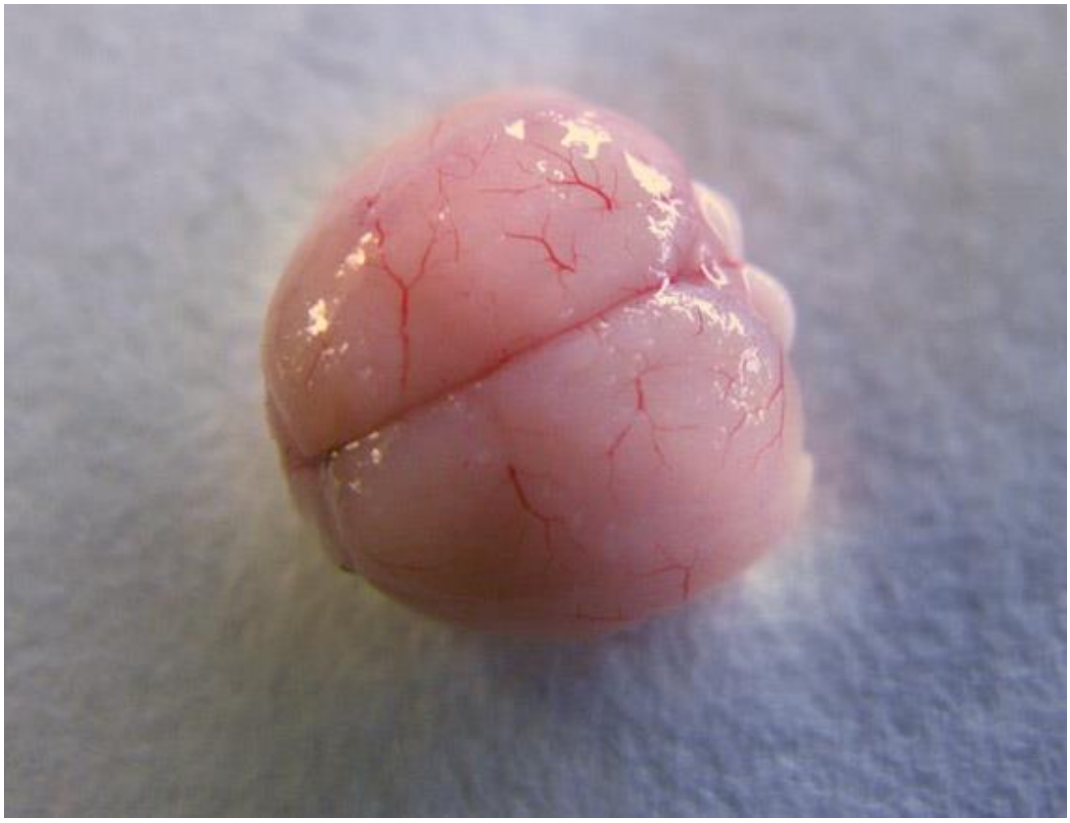

Figure 24: Whole Mouse Brain. Whole mouse brain extracted following euthanasia.

2.3 RNA Extraction

To prevent RNA degradation by RNase enzymes, specific decontamination methods and handling procedures were applied at all times. A dedicated RNA

workspace was created, where only dedicated RNase-free tips, tubes, pipettes, reagents and gloves were used. RNase AWAY® (Invitrogen™, USA) was frequently applied to the surfaces and equipment in the RNA workspace where RNA work was being conducted. Each 50 mg sample of cortex tissue in TRI Reagent® (Molecular Research Centre, USA) was homogenised in a FastPrep® FP120 (Thermo Scientific, USA) at a speed of 6.5 for 25 seconds at RT. Homogenisation was repeated three times with intervals of two minutes in between each cycle to prevent overheating of the machine. All centrifugation for this method was carried out in an Eppendorf 5424R centrifuge at 12,000 x G at RT. Following a one minute centrifugation, the aqueous phase was transferred to a sterile 1.7 mL microcentrifuge tube (Scientific Specialties, USA) and 200 µL of chloroform added for removal of any protein. After fifteen seconds of vigorous shaking by hand, the sample was incubated on a rotating well (Stuart rotator SB2; Thermo Scientific, UK) for fifteen minutes and then centrifuged for a further fifteen minutes. The supernatant was transferred to a new sterile 1.7 mL microcentrifuge tube and RNA precipitated using 500 µL of isopropanol followed by incubation at RT for ten minutes. The sample was centrifuged for eight minutes to pellet the RNA, supernatant was carefully removed and the RNA pellet washed in 1 mL of 75% ethanol to remove any salts. The sample was centrifuged for a further eight minutes to pellet the RNA. After discarding the ethanol, the RNA pellet was air-dried for five minutes at RT and subsequently dissolved in 25 µL of RNase-free DEPC water. The total RNA sample was further incubated in a ThermoMixer® (Scientific Specialties, USA) for fifteen minutes at 65°C to aid suspension and cooled on ice for 5 minutes.

2.3.1 Quality Control of Nucleic Acids and Quantification Methods

During all PCR and qPCR methods, MIQE guidelines were followed so as to produce high quality results for publication [78]. The MIQE guidelines incorporate careful sample acquisition, handling and preparation, quality control (QC) of nucleic acids, consistent reverse transcription, providing all relevant information about amplified genes and stating detailed information on the methods of data analysis [78]. Careful handling of RNA samples was important as this can be the first potential source of sample contamination [78]. Sample handling is especially important with respect to targeting RNA as mRNA profiles can be easily disrupted by poor collection or processing [78]. Cerebral cortex tissue was homogenised immediately following euthanasia and brain extraction to reduce RNA degradation. RNA extractions were carried out following homogenisation to further prevent potential degradation of target RNAs. All samples were subsequently stored in a -80°C freezer.

2.4 Nanodrop Analysis

Total RNA was quantified using a NanoDrop 2000 Spectrophotometer and software (Thermo Scientific™, UK) to analyse the RNA concentration and A_{260}/A_{280} and A_{260}/A_{230} absorbance ratios. An optical density (OD) is the optical spectrometer measurement of absorbance at the wavelengths of 230 nm, 260 nm and 280 nm. An A_{260}/A_{280} ratio of 1.8 - 2.0 is generally accepted as "pure" for RNA [79]. In addition, we sought an A_{260}/A_{230} ratio of 2.0 [79]. Once it was confirmed that the RNA samples were of good quality, each sample was diluted into 1000 ng/µL aliquots prior to storage in a -80°C freezer. All RNA samples were also analysed via gel electrophoresis to confirm the RNA had not degraded. RNA samples were assigned individual codes for ease of reference (Appendix 4). Each

RNA sample was labelled according to its treatment (I, S or P), replicate number (1, 2 or 3) and time point (0, 2, 4T, 4C).

2.5 Denaturing Formaldehyde Gel Electrophoresis

All RNA samples were run in denaturing formaldehyde 1% agarose gel to analyse the integrity of total RNA and provide an indication of the RNA yield. To prepare the gel, 0.5 g of agarose was melted in 31 mL of deionized water (de-I) in a 600W microwave before mixing in 10 mL of 5X 3-(N-morpholino) propanesulfonic acid (MOPS) buffer. When the agarose solution cooled to approximately 60°C, 9 mL of formaldehyde (40%) was added to the solution in a fume hood and the solution was thoroughly mixed by hand. The gel was subsequently poured into a level RNase-free mold (10 cm x 10 cm), inserted with a comb, and left for one hour to set at RT. During this time, RNA samples were prepared in sample buffer for electrophoresis (Table 3) using sterile 1.7 mL microcentrifuge tubes. All samples were incubated at 70°C for 10 minutes to denature the RNA before being cooled on ice for 3 minutes. Two microlitres of formaldehyde gel-loading buffer was added to each sample. The solidified agarose gel was inserted into a gel electrophoresis tank and submerged in 1X MOPS buffer. A sample volume of 20 µL was loaded into the agarose gel wells. Ten microliters of 1 µg/µL RNA ladder (Invitrogen™, USA) measuring fragments of 0.5–10 kB in size was also loaded. Gel electrophoresis was run at 50 V for two hours at RT. The buffer was mixed every 30 minutes to ensure even distribution of ionic components.

Table 3: Components of RNA Sample Buffer. Each RNA sample was added to sample buffer for denaturation and gel electrophoresis. Components were added to 1.7 mL microcentrifuge tubes to a final volume of 21 µL. Before loading into the denaturing formaldehyde gel, 2 µL of RNA loading dye was added to each sample to allow visualisation of the RNA.

Component	**Quantity**
RNA (up to 20 µg)	2 µL
5X MOPS buffer	4 µL
Formaldehyde	4 µL
Formamide	10 µL
Ethidium bromide (200 µg/mL)	1 µL

2.6 DNase Treatment

All RNA samples were DNase treated to eliminate gDNA contamination that may be present. The DNase I enzyme (Zymo Research, USA) catalyzes hydrolytic cleavage of the DNA backbone to degrade any DNA present in the sample and was used at a final concentration of 1 U/µL. A 10 µL reaction was prepared in 0.2 mL microcentrifuge tubes for each RNA sample (Table 4) and incubated in a ThermoMixer® at 37°C for fifteen minutes. To stop the reaction, 1 µL of 500 mM ethylenediaminetetraacetic acid (EDTA) was added to chelate the magnesium (Mg) ions and thus inactivate the DNase I enzyme. In addition, the sample was heat inactivated for ten minutes at 65°C. The samples were incubated on ice for five minutes prior to a thirty-second centrifugation at 12,000 x G at RT. All DNase-treated RNA samples were stored at -80°C until required for cDNA synthesis.

Table 4: DNase Treatment of RNA Samples. The following components and corresponding quantities were used for 10 µL reaction volumes for DNase treatment of all RNA samples.

Component	Quantity (µL)
DEPC water	7
RNA sample 1000 ng/µL	1
10x DNase I buffer	1
DNase I (1 U/µL)	1

2.7 Complementary DNA Synthesis

To prepare a double stranded nucleic acid template for PCR, the conversion of mRNA to cDNA is required. Complementary DNA synthesis involves the reverse transcription of mRNA based on the pairing of RNA base pairs (A, U, G and C) to their DNA complements (T, A, C and G). This was carried out according to the guidelines set out by the manufacturer of Tetro cDNA synthesis kit (Bioline, USA). Briefly, a master mix containing primers, Tetro reverse transcriptase, Ribosafe RNase inhibitor, dNTP mix, 5X reverse transcriptase buffer, and DEPC H_20 was prepared on ice (Table 5). Random hexamer primers were selected as they can simultaneously reverse transcribe all mRNAs and are not biased to the 3′ end of the gene transcript. Nineteen microlitres of master mix was aliquoted into sterile 0.6 mL microcentrifuge tubes and 1 µL of the corresponding RNA sample was added to each allocated tube.

Table 5: Components and Concentrations for Reverse Transcription Reaction. The components were added to a 0.6 mL microcentrifuge tube and mixed by pipetting before centrifugation for 30 seconds at 12,000 x G at RT to collect contents in tube.

Component	**Quantity (µL)**
Random hexamers	1
Tetro reverse transcriptase (200 U/µL)	1
Ribosafe RNase inhibitor (10 U/µL)	1
dNTPs (10 mM)	1
5X reverse transcriptase buffer	4
DEPC H_20	11
DNase-treated RNA (500 ng/µL)	1

Samples were incubated in a thermocycler (PTC-200 Peltier Thermocycler; Geneworks, Australia) for cDNA synthesis, following the program outlined in Table 6. A no reverse transcription (-RT) control was also included to ensure no gDNA contamination was present. This sample substituted RNA with 1 µL of mQH_20. With no RNA template present to transcribe, we expected that the –RT control would produce no cDNA. Complementary DNA samples were subsequently stored at -20°C until required for PCR or qPCR.

Table 6: Reverse Transcription Program for cDNA Synthesis. Synthesis of all cDNA samples was carried out using the following conditions. Reverse transcription of the RNA into cDNA occurs during the initial step. The reverse transcription is followed by a heat inactivation cycle that inactivates the reverse transcriptase enzyme before being cooled briefly at 4°C.

Cycle	**Temperature (°C)**	**Time (min)**
Reverse transcription	45	30
Heat Inactivation	85	5
Final cycle	4	5

2.8 Primer Design

The primers sets used to target *ActB, Bdnf, Gjd2, Gapdh, HPRT1* and *β2m* had been previously published and the target sequence was of optimal length to use in qPCR [72,75,80,81]. Specific *Arc, CamK2a* and *Grin1* primers were designed using the online National Centre for Biotechnology Information (NCBI) primer design tool, and cross referenced with information from the University of California, Santa Cruz (UCSC) Genome Browser. The GenBank sequence for each gene is shown in Table 7. A set of *Bdnf* primers was also designed, as the published set did not target an intron-spanning boundary.

Primers were designed to the following criteria: a) approximately 20 base pairs (bp) in length, b) the GC content was between 40% and 55%, c) the product was no larger than 200 bp for qPCR d) specific targeting of one isoform of each gene, and e) targeted an intron-spanning boundary to exclude the possibility of gDNA amplification. All primers were synthesised by Integrated DNA Technologies (IDT; USA) and the lyophilised pellet resuspended in sterile 1X Tris EDTA (TE) buffer (pH 8.0) to a final concentration of 100 μM. Primers were suspended in TE buffer to make a working stock at a final concentration of 10 μM. All primer solutions were stored at -20°C.

Table 7: Primer Sequences with Corresponding Product Sizes. Primer sequences used for real-time quantitative PCR for specific targeting of *Arc*, *Bdnf*, *CamKIIα*, *Grin1*, *Gjd2* and *Gapdh* mRNAs. The optimal annealing temperature for each set of Forward (F) and Reverse (R) primers has been stated, as well as the final product size of the target sequence and their corresponding accession number.

Gene	Primer Sequence (5' – 3')	Product (bp)	Annealing (°C)	Accession Number
Arc	F:GGTGAGCTGAAGCCACAAAT R:GCTGAGCTCTGCTCTTCTTCA	104	60	NM_018790.3
Bdnf	F:TGAGTCTCCAGGACAGCAAA R:GCCTTCATGCAACCGAAGTA	103	58	NM_007540
Bdnf[80]	F:GTGACAGGCGTTGAGAAAGC R:ATCCACCTTGGCGACTACAG	206	58	NM_007540
CamKIIα	F: CTACTCTGCTGCCTGCAAATG R:ACTGGACTTTCTTTTCTTCACACC	150	59	NM_009792.3
Grin1	F:GTCCTCCAAAGACACGAGCA R:AGCTCTCCCTATGACGGGAA	148	58	NM_008169
Gjd2[81]	F:CCAGTAAGGAGACAGAACCAGAT R:GATGATGTAGAAGCGGGAGATAC	125	59	NM_010290.2
Actβ[81]	F:GATGGTGGGAATGGGTCAGAA R:CTCATTGTAGAAGGTGTGGTGC	151	59	NM_007393.3
Gadph[72]	F:TGCACCACCAACTGCTTAGC R:GGCATGGACTGTGGTCATGAG	87		NM_001289726.1
β2m[75]	F:TTCTGGTGCTTGTCTCACTGA R:CAGTATGTTCGGCTTCCCATTC	104	59	NM_009735.3
HPRT1[72]	F:TGACACTGGCAAAACAATGCA R:GGTCCTTTTCACCAGCAAGCT	94	60	NM_013556.2

2.9 Primer Testing using Standard PCR

The PCR amplification methodologies followed the protocol outlined in the Data Sheet provided by the manufacturer (Solis BioDyne, Estonia). A 20 µL PCR reaction was prepared using a 19 µL volume of master mix that contained the

components outlined in Table 8, and 1 µL of cDNA in a 0.2 mL microcentrifuge tube.

Table 8: Components of PCR Master Mix. A master mix was prepared by adding all the components to a 1.7 mL microcentrifuge tube. The volume was multiplied according to the number of PCR reactions required. The master mix was prepared on ice, vortexed, and briefly centrifuged before aliquoting into individual 0.2 mL microtubes.

Component	**Reaction (19 µL)**	**Final concentration**
10X B2 buffer (Tris-HCl, $(NH_4)_2SO_4$ and detergent)	2 µL	1X
$MgCl_2$ (25 mM)	1.2 µL	1.5 mM
dNTPs (10 mM)	0.4 µL	200 µM
HOT FIREPol® DNA polymerase (5 U/µL)	0.2 µL	0.5 U/µL
Forward primer (10 µM)	0.5 µL	0.25 µM
Reverse primer (10 µM)	0.5 µL	0.25 µM
mQH_2O	14.2 µL	N/A

Samples were placed in the PTC-200 Thermocycler and amplified according to the program outlined in Table 9. Gradient PCR using HOT FIREPol® DNA polymerase (Solis Biodyne, Estonia) with a temperature range of 52°C to 60°C was conducted to validate the primers and identify the optimum annealing temperature of each primer set. Each PCR reaction contained a positive control with template DNA and primers that had known successful amplification, and a negative control that contained mQH_20 rather than template cDNA. A –RT control was also included as a template to ensure no gDNA contamination occurred during cDNA synthesis.

Table 9: Standard PCR Program. PCR was used for validation of primer sets and their targeting of the correct mRNA sequence. The annealing temperature varied for each set of primers, depending on the optimal temperature (Table 7).

Step	Temperature (°C)	Time	Cycles
Initial denaturation	95	15 minutes	1x
Denaturation	95	20 seconds	30x
Annealing	52 – 58	30 seconds	
Elongation	72	40 seconds	
Final elongation	72	5 minutes	1x

Samples were electrophoresed for 10 minutes at 200 volts on a 2% agarose gel made with 1X Superbuffer and stained with 0.1 mg/mL ethidium bromide (EtBr) for UV visualization and confirmation of product size [82]. A 100 bp molecular ladder (Solis BioDyne, Estonia) was also added to estimate size of the resulting PCR products. The resulting bands were visualised under UV light using Scion Image software.

2.10 Sequencing of PCR Products

Quantitative PCR products were visualised using gel electrophoresis and also sent for sequencing to confirm the correct sequence was amplified during qPCR. Prior to sequencing, the qPCR products were purified using a DNA Clean and Concentrator™ kit (Zymo Research, USA). Briefly, DNA Binding Buffer was added to the qPCR product in a 5:1 ratio and vortexed for ten seconds before being added to a Zymo-Spin™ column. The column was centrifuged at 12,000 x G for thirty seconds at RT and the remaining liquid discarded. To wash the DNA binding matrix, 200 μL of DNA Wash Buffer was added to the spin column before centrifuging for thirty seconds and discarding the liquid. The DNA

wash was repeated to ensure a clean sample would be produced. To elute the DNA from the binding matrix, 25 μL of DNA Elution Buffer was added to the column and incubated at RT for one minute. The spin column was centrifuged for a further thirty seconds at 12,000 x G at RT and the liquid transferred to a 1.7 mL microcentrifuge tube. The samples were stored at 4°C until they were required for DNA sequencing at the Waikato DNA Sequencing Facility (UoW, NZ). The sequencing primers were provided at a concentration of 5 μM for each forward and reverse primer. Due to the poor DNA sequencing results, the qPCR products were ligated into a pLUG-Prime® Cloning Vector (Intron Biotechnology, USA) for sequencing analysis.

2.11 Insertion of PCR Products into a Cloning Vector for Target Sequence Analysis

The pLUG-Prime® TA-cloning vector (Intron Biotechnology, USA) is a commercially available 2728 bp plasmid that allows for insertion of a PCR product using the enzyme DNA ligase (Appendix 5). The ligated plasmid is then transformed into chemically competent *Escherichia coli* (*E. coli*) strain DH5α. The bacterial cells were grown in lysogeny broth (LB) media and made chemically competent using a Mix & Go kit (Zymo Research, USA). The advantage of using a Mix & Go kit is that it provided a simple and highly efficient DNA transformation (>10^8) without requiring heat shock, incubation or growth. All genetically modified *E. coli* was created under the HSNO approval code GMD101146.

2.11.1 Preparation of Chemically Competent *E. coli* Cells

LB agar was prepared as per the recipe in Appendix 3. Approximately 30 - 40 mLs of LB agar was poured onto each sterile petri dish and left to set at RT before being stored in a sterile media-only 4°C fridge. DH5α *E. coli* cells grown on an LB+ agar was kindly gifted by Sarah Hardie, UoW. The genotype of this strain is as follows: F– Φ80*lac*ZΔM15 Δ(*lac*ZYA-*arg*F) U169 *rec*A1 *end*A1 *hsd*R17 (rK–, mK+) *pho*A *sup*E44 λ– *thi*-1 *gyr*A96 *rel*A1[83]. A single colony was selected using a flame sterilised inoculation loop and was used to inoculate a 14 mL Greiner culture tube containing 5 mLs of LB media. The bacterial culture was incubated at 37°C overnight at 200 RPM.

The following day, a 0.1 mL aliquot of overnight-cultured DH5α *E. coli* was used to inoculate 5 mL of ZymoBroth™ (Zymo Research, USA) in a 50 mL Erlenmeyer flask that was sealed with cotton wool and covered with foil. The culture was grown at 37°C, shaking at 200 RPM until the OD_{600nm} had reached between 0.4 and 0.6. This ensured that the bacterial cells were captured during the log phase of growth. During this time, 0.82 mL working stocks of 1X Wash Buffer and 1X Competent Buffer (Zymo Research, USA) were prepared on ice according to the concentrations listed in Table 10. When the bacterial cells had reached an OD_{600nm} between 0.4 and 0.6, 2 mLs was aliquoted into two sterile 1.7 mL microcentrifuge tubes and incubated on ice for 10 minutes.

Table 10: Buffer Preparation for Cell Harvesting. The 1X buffers were prepared and kept on ice to ensure all buffers were ice-cold when added to the *E. coli* DH5α cells.

Buffer	**Component**	**Quantity**
1X Wash Buffer	Dilution buffer	0.41 mL
	2X stock wash buffer	0.41 mL
1X Competent Buffer	Dilution buffer	0.41 mL
	2X stock competent buffer	0.41 mL

The bacterial cells were pelleted by centrifuging at 12,000 x G for 10 minutes at 4°C. The supernatant was removed and the cells resuspended in 0.4 mL of ice-cold 1X Wash Buffer. The cells were re-pelleted with a further round of centrifugation at 12,000 x G for 10 minutes at 4°C. The supernatant was completely removed and the remaining cells were resuspended in 0.4 mL of ice-cold 1X Competent Buffer and mixed gently by pipetting the solution up and down several times. On ice, 0.1 mL volumes of the chemically competent cells were aliquoted into eight sterile microcentrifuge tubes for DNA transformation. The remaining *E. coli* DH5α cells chemically competent cells were stored at -80°C.

2.11.2 DNA Ligation of Purified PCR Products and pLUG-Prime® Cloning Vector

Thymine adenine (TA) cloning is a technique that avoids the use of restriction enzymes and instead relies on complementary base pairing between different DNA fragments. In the presence of a ligase, the DNA fragments hybridise and become ligated together. This method was used to hybridise our purified PCR products (section 2.9) into a pLUG-Prime® Cloning Vector (Intron Biotechnology, USA) for DNA sequencing purposes. Some DNA polymerases

used in standard PCR can preferentially add an adenine to the 3' end of the product. The pLUG-Prime® Cloning Vector has a complementary 3' thymine overhang, which hybridises to the adenine during ligation. The molar ratio of the insert (such as the PCR product) had to be optimised for the ligation reaction by using a 5 – 10 fold molar excess of PCR product over the TA-cloning vector. The concentration of each product used for insertion into the vector was determined using Equation 1.

Equation 1: Formula for Optimising Insert to Vector Ratio for Ligation Reaction.

$$ng\ PCR\ product\ required = \frac{50\ ng\ x\ PCR\ product\ (bp)}{Vector\ size\ (2729\ bp)} x\ molar\ ratio$$

Before preparing the ligation reaction, PCR products and components of the vector kit were centrifuged at 12,000 x G for 30 seconds at RT to collect the contents to the bottom of the tube. The ligation buffer was also vortexed and centrifuged at 12,000 x G for 30 seconds at RT. Each 10 µL ligation reaction mix was prepared as outlined in Table 11 in a 0.2 mL microcentrifuge tube (Scientific Specialties, USA). The reaction was mixed gently by pipetting before incubation for 15 minutes at 4°C. Ligation reactions were stored at -20°C or 2 uL was used for transformation into *E. coli.*

Table 11: Components and Corresponding Quantities for the Ligation Reaction Mix. The PCR products for *Arc*, *Bdnf*, *Gjd2*, *Grin1*, *β2m* and *Gapdh* were ligated into a pLUG-Prime® Cloning Vector (Intron Biotechnology, USA) prior to transformation into chemically competent *E. coli* α5 cells.

Components	**Quantity (µL)**
10X Ligation Buffer A	1
10X Ligation Buffer B	1
TA-Cloning Vector (25 ng/µL)	2
T4 DNA Ligase (2 U/µL)	1
PCR product	*
mQH_20	2

Positive and negative insert controls were also prepared. The positive control was a plasmid containing a VMO1 insert, kindly donated by Hannah Crossan (UoW, NZ). The VMO1 insert produced a product 354 bp in length when extracted from the plasmid using M13 primers [85]. The negative control was a ligation reaction prepared according to Table 11 with 2 µL of mQH_20 added in substitution for a purified PCR product.

For the transformation reaction, 2 µL of ligated DNA was added to the competent bacterial cells that were prepared in section 2.11.1. The transformation reaction was gently mixed by pipetting and 100 µL was spread onto a pre-warmed (37°C) LB+ agar plates using a flame sterilised glass spreader. The LB+ agar contained ampicillin at a final concentration of 50 µg/µL. Each LB+ agar plate contained 40 µL of XGal and 40 µL of IPTG for blue/white colony screening. The plates were then incubated upside down at 37°C overnight to allow the colonies to grow and prevent condensation. All agar plates were subsequently stored at 4°C. Blue/white colony screening allowed detection of positive vector cloning.

Bacterial cells transformed with the vector containing the purified PCR insert were expected to produce white colonies and those only containing the vector were expected to produce blue colonies. Any colonies that were not transformed would not contain the ampicillin resistant gene and would therefore be unable to grow on LB+ agar. The positive control was expected to produce only white colonies. The negative control was expected to produce no colonies as it had not been transformed with the ampicillin resistant gene and would therefore not survive on LB+ agar plates. White colonies were selected for colony PCR to validate the presence of recombinant DNA containing the purified PCR insert. The transformation efficiency for the positive transformation control was calculated by using Equation 2 [84].

Equation 2: Formula for Calculating Transformation Efficiency of Transformed *E. coli* Colonies [84].

$$\frac{\#\,colonies\ on\ agar\ plate}{ng\ of\ DNA\ plated} x\ 1000\ ng/uL$$

2.11.3 Colony PCR

Colony PCR was used to evaluate whether the PCR products had been successfully inserted into the pLUG-Prime® Cloning Vector (Intron Biotechnology, USA). A standard PCR mastermix was prepared (Table 8) using M13 primers (10 μM) provided with the pLUG-Prime® Cloning Vector kit that targeted a 178 bp target in the plasmid. As Table 8 only made 19 μL reaction volumes, an extra 1 μL per tube of mQH_20 was added. Four PCR reactions were prepared; test insert, positive insert control, positive ligation control and negative ligation control. An isolated white colony from LB+ agar plate containing the transformed plasmid DNA (section 2.10.2) was removed using a sterile pipette tip

and dipped in the corresponding PCR tube before being spread onto an LB+ agar plate. This allowed growth of the selected colony for later use. The plates were then incubated upside down at 37°C overnight. At least ten different isolated colonies containing the PCR insert were selected for amplification via colony PCR. The PCR conditions were carried out to the conditions outlined in Table 12 and the products visualised on a 1% agarose gel made in 1X Superbuffer stained with EtBr (0.25 μg/mL). The size of each product was compared to a 100 bp molecular weight ladder (Solis BioDyne, Estonia).

Table 12: Thermocycler Conditions for Colony PCR.

Step	**Temperature (°C)**	**Time**	**Cycles**
Initial denaturation	95	5 minutes	1x
Denaturation	94	20 seconds	25x
Annealing	55	30 seconds	
Elongation	72	30 seconds	
Final elongation	72	5 minutes	1x

The positive ligation plasmid had a product of 354 bp in length [85]. The predicted product size of the plasmids containing the purified PCR inserts are outlined in Table 13. Colonies were selected for DNA extraction and sequencing based on visualization of the correct plasmid size using gel electrophoresis.

Table 13: Expected Product Size of Vector Containing PCR Insert Following Amplification with M13 Primers.

Vector Containing PCR Insert (gene)	Expected Size (bp)
β2m	282
Gapdh	265
Arc	282
Bdnf	281
Gjd2	303
Grin1	326
VMO1	354

2.11.4 Plasmid DNA Extraction

One white colony from the corresponding LB+ agar plate (section 2.10.3) was selected using a sterile pipette tip and inoculated in a sterile 14 mL culture tube (Greiner Bio-One, USA) containing 2 mL of LB^+ media and 4 µL of 25 mg/mL ampicillin. The LB+ media was incubated overnight at 37°C, shaking at 200 RPM. The next day, the media was streaked onto a LB^+ agar plate and further incubated at 37°C, shaking at 200 RPM overnight. To be certain that a single colony was selected for DNA extraction, one colony was isolated from the LB+ plate following overnight incubation and grown overnight at 37°C, 200 RPM before being streaked onto another LB^+ agar plate. One colony was selected and incubated in 5 mL of LB media containing 10 µL of ampicillin (25 mg/mL) in a sterile culture tube.

DNA was extracted from the transformed *E. coli* cells using a Zyppy™ Plasmid Miniprep Kit (Zymo Research, USA). All centrifugation for this process was carried out at 12,000 x G at 4°C in an Eppendorf 5424R centrifuge. Briefly,

2 mLs of cell culture was centrifuged for 30 seconds, supernatant was discarded and the cells were resuspended in 600 µL of sterile mQH_2O in a sterile 1.7 mL microcentrifuge tube. The 7X Lysis Buffer was pre-warmed at 37°C before 100 µL was added to the resuspended cells. The solution was mixed by gently inverting the tube six times. A colour change from opaque to clear blue indicated that the cells had undergone complete lysis. Following cell lysis, 350 µL of 4°C Neutralization Buffer was added and mixed thoroughly by inversion. When the neutralization was complete the sample changed to a yellow colour with a yellowish precipitate, which was centrifuged for 3 minutes. The supernatant was transferred to a Zymo-Spin™ IIN column, which was placed into a collection tube and centrifuged for 30 seconds. Following centrifugation, 200 µL of Endo-Wash Buffer was added to the column and centrifuged for 30 seconds before 400 µL of Zyppy™ Wash Buffer was added to the column and further centrifuged for one minute. The column was transferred into a sterile 1.7 mL microcentrifuge tube and 30 µL of elution buffer (pre-warmed to 55°C) was added directly to the column matrix and left to stand at RT for one minute. The column was centrifuged for 30 seconds and the flow-through re-applied to the matrix and centrifuged for a further 30 seconds to maximise plasmid DNA extraction. The DNA was analysed using the Nanodrop 6000 Spectrophotometer to estimate the concentration for sequencing. Plasmid DNA was stored at 4°C until it was required for sequencing.

2.11.5 Restriction Digest of Plasmid DNA using HindIII and EcoRI

The restriction enzymes HindIII and EcoR1 were used to cut the pLUG-Prime® cloning vector. HindIII and EcoR1 are site-specific restriction enzymes that cleave DNA sequences at 5'-A^AGCTT-3" and two recognition sequences are

available for each in the pLUG-Prime® Cloning Vector (Appendix 5). Individual plasmid DNA was digested overnight at 37°C in the reaction volumes outlined in Table 14.

Table 14: Components and Corresponding Quantities for Restriction Digest of Plasmid Containing pLUG-Prime® Vector.

Component	Restriction Digest	Control
Plasmid DNA	6 µL	6 µL
EcoR1 (10 U/µL)	1 µL	-
HindIII (10 U/µL	1 µL	-
Buffer	2 µL	2 µL
mQH_2O	-	2 µL

The restriction digest products were visualised using gel electrophoresis. Due to the low concentration of some plasmid DNA samples, all samples were run on a 2% agarose gel to validate the presence of DNA and estimate concentration using the 100 bp molecular ladder (Genscript™, USA).

2.11.6 Sequencing of Plasmid DNA Containing Purified PCR Insert

Once the presence of the ligated cloning vector in plasmid DNA was confirmed by restriction digest and gel electrophoresis, individual plasmid DNA was sent to the Waikato DNA Sequencing Facility (UoW, NZ). All sequencing results were relayed in FASTA and ABD formats. Geneious software (Version 7) was used to analyse all sequences and align them with the reference mRNA sequences (Appendix 4).

2.11.7 Optimised Methods for Sequencing Results

The plasmid DNA containing *Arc*, *Bdnf*, *Gapdh*, *Gjd2* or *Grin1* produced poor sequencing results that could not be used to validate the target sequences. Due to time constraints, only the two genes that showed a change in gene expression (*Arc* and *Bdnf*) and the two reference genes (*β2m* and *Gapdh*) were optimised further to improve DNA quality and yield. Briefly, the low concentration plasmid DNA extracted previously was transformed directly into chemically competent DH5α *E. coli* cells. As the plasmid DNA had already shown it contained the vector insert, there was no need for blue/white colony screening or colony PCR. Instead, the transformed cells were spread onto LB+ agar plates and grown overnight at 37°C. Following incubation, 10 mL (rather than 2 mL) of LB^+ media was inoculated with a colony and grown overnight at 37°C. The media was spilt into two sterile 14 mL culture tubes to maximise aeration during incubation. Following 24 hours of incubation, plasmid DNA extraction was carried out according to the method outlined in section 2.11.4. After Nanodrop analysis, the plasmid DNA was sent to the Waikato DNA Sequencing Facility (UoW, NZ) for sequencing.

2.12 Quantitative Polymerase Chain Reaction (qPCR)

The qPCR reactions were carried out according to the manufacturer's instructions for HOT FIREPol® EvaGreen® qPCR mastermix (Solis Biodyne, Estonia). Briefly, a mastermix was prepared to the final concentrations described in Table 15. A separate master mix was made to amplify each GOI, and each reference gene. Negative controls that replaced cDNA with mQH_20 and –RT controls were also included for each qPCR assay.

Table 15: Components of the qPCR Master Mix. Components and their final concentrations for the master mix used in all qPCR experiments. Each master mix contained a separate primer set, which was aliquoted into 0.2 mL microcentrifuge tubes (Scientific Specialties, USA) for the qPCR reaction. Two microliters of cDNA template that had been diluted 1:20 with sterile H_20 was added to the appropriate tube to make a final concentration of 0.002 ng/µL. Primer sequences are listed in The 5X HOT FIREPol® EvaGreen® qPCR Mix was kept in an amber tube away from light to prevent contamination and reduce exposure to light.

qPCR Master Mix Component	Quantity (µL)	Final Concentration
5X HOT FIREPol® EvaGreen® qPCR Mix Plus	4	1X
Forward primer (5 µM)	0.4	400 nM
Reverse primer (5 µM)	0.4	400 nM
mQH_2O	13.2	N/A

The qPCR analysis was conducted using a *t*=0 hour control against a *t*=2 hour or *t*=4 hour anaesthetic treatment. During the qPCR assay, expression of GOIs were analysed against expression of the reference genes, *β2m* and *Gapdh,* for normalisation. Each sample was processed as a triplicate for internal standardization, and each qPCR assay was repeated the following day as a technical control. Samples were amplified in a Rotor-Gene 6000™ Thermocycler designed specifically for quantitative analysis (Table 16). The wavelength absorption was set to "green" for use with the EvaGreen® dye in the qPCR master mix.

Table 16: Standard qPCR Program. The thermocycler program used for all qPCR experiments included an initial denaturation step before completing 40 cycles of denaturation, annealing, elongation and final melt. An annealing temperature of 65°C was used for all qPCR experiments.

Step	Temperature (°C)	Time	Cycles
Initial denaturation	95	12 minutes	1x
Denaturation	95	15 seconds	40x
Annealing	65	30 seconds	
Elongation	72	30 seconds	
Final melt	80	10 seconds	

2.12.1 Generating Statistical Data

The Rotor-Gene™ 6000 software produced raw quantitative data derived from the amplification plots and melting curve profiles to validate the specificity of the products amplified. The raw take-off and amplification data was extracted from Rotor-Gene™ 6000 software and entered into REST© (V2.0.13, 2009) software for statistical analysis. The take-off values represented the first significant cycle of the exponential region, where 'noise' had ended and exponential amplification began. The second derivative of the amplification plot was the amplification values, which corresponded with the maximum rate of fluorescence increase during each reaction. REST© was set to 'RG' mode and all GOI and reference genes were added individually for each treatment (sevoflurane or propofol) and time point (t=0 hours compared with t=2 hour or t=4 hour). The isoflurane treatment was not analysed in real-time qPCR due to time restrictions. REST© uses the $\Delta\Delta C_T$ method described by Livak et al. (2001) to compare the C_T value of target genes to a reference gene(s) and thus analyse relative changes in gene expression from real-time qPCR experiements. The $\Delta\Delta C_T$ method is shown in Equation 3.

Equation 1: The $\Delta\Delta C_T$ Method used by REST©.[71] Here, $\Delta\Delta C_T$ is the ΔC_T of any sample normalised to the reference gene minus the ΔC_T of the reference gene.

$$\Delta\Delta C_T = \Delta_{CT(sample)} - \Delta_{CT(reference)}$$

REST© can compare multiple target genes to reference gene(s) in two data groups (control and treatment) [86]. Using the $\Delta\Delta C_T$ method, REST© calculates expression ratios based on take-off values and the mean crossing point deviation between sample and control groups [86]. The expression ratios are subjected to a randomisation test to ensure significance and are represented on whisker-box plots [86]. REST© automatically computed the results into expression ratios, which were calculated using Equation 4 and displayed on a whisker-box plot that plotted the expression ratios for each gene on a logarithmic scale.

Equation 2: Relative Expression Ratio. When using multiple reference genes, the geometric mean of all reference gene concentrations (conc.) can be used to calculate the relative expression of individual GOIs.

$$\text{Relative expression} = \frac{\text{Conc. of GOI}}{\text{Geometric mean (conc. of reference gene 1, conc. of reference gene 2)}}$$

2.12.2 Analysis of Statistical Data

Along with the generation of expression ratios, REST© also carried out other statistical analyses including the Pair Wise Fixed Reallocation Randomisation Test©, which was performed to assess the statistical signifcance of differences in gene expression between control and treatment groups [86]. Each REST© analyses contained 10000 randomisations (iterations) that served to avoid making any assumptions about the distributions. Instead, the Pair Wise Fixed Reallocation Randomisation Test© repeatedly and randomly reallocates observed values within the two groups, recording the apparent effect (expression ratio) after each randomisation. Furthermore, the *p*-value for each GOI is calculated by obtaining

the proportion of random allocations of the mean observed data to the control and treatment groups. The result is a better indication of the treatment effect than what is actually observed. If more than 2000 samples are reallocated, a good estimate of p is obtained [86]. A p-value of less than 0.05 ($p<0.05$) lead to the rejection of the null hypothesis (H_0). Therefore, if $p<0.05$, H_0 is rejected and the alternative hypothesis (H_1), that gene expression between the control and treatment samples changed, is accepted. In conclusion, the Pair Wise Fixed Reallocation Randomization Test© allows us to state that the difference between control and treatment samples is real and statistically significant [86].

2.12.3 Whisker-Box Plots

REST© automatically generated expression ratios from the raw take-off and amplification data derived from the qPCR amplification plots. The expression ratios for individual GOIs were displayed in whisker-box plots. Each whisker-box plot conveyed data about the mean, the 1st and 3rd quartile ranges and the minimum and maximum value of each group, demonstrating the skew of distributions around the sample mean. The 'box' area encompasses 50% of all values while the 'whiskers' represent the outer 50% of values. Using the Pair Wise Fixed Reallocation Randomization Test©, REST© produces whisker-box plots based on the expression data (y-axis), rather than raw C_T values [86].

Chapter Three

Results

This section outlines the results from the molecular methodologies used to extract RNA from cortical mouse brain tissue and convert it to a cDNA template, which was subsequently used to analyse gene expression during a two or four hour anaesthetic drug exposure.

3.1 Anaesthetic Exposure Trials using a Mouse Model

Male and female eight-week-old wildtype C57/BL6:129sv mice were used for all experiments in this study that involved adult mice. The aged mice used for this research were eighteen months old and were of the individual C57 and BL6:129sv parent strains. Mice were subject to controlled treatments of isoflurane, sevoflurane and propofol before euthanisation, followed by extraction of cortical brain tissue. RNA was extracted from the cortical brain tissue, reverse transcribed into cDNA and used as a template to measure mRNA expression using qPCR.

3.1.1 Volatile Anaesthesia

Animals were placed in their respective chambers in the fume hood for the duration of the experiment (Figure 19). Following administration of volatile anaesthetic (sevoflurane or isoflurane), animals were anaesthetised within two minutes. Analysing the inability to roll over when placed on their backs confirmed complete anaesthesia of the mice. The CO_2 levels approached 5% approximately every hour during the volatile anaesthetic exposure at which time the animal chamber was opened and flushed with fresh air. This did not result in rousing of

the animals and a "top-up" dose of anaesthetic was administered immediately followed flushing. Monitoring of the CO_2 and anaesthetic gas levels inside the animal chambers every ten minutes indicated that the isoflurane and sevoflurane levels declined at a similar rate (Figure 21), with the addition of a further half-dose at the two-hour and three-hour time points required to maintain anaesthesia.

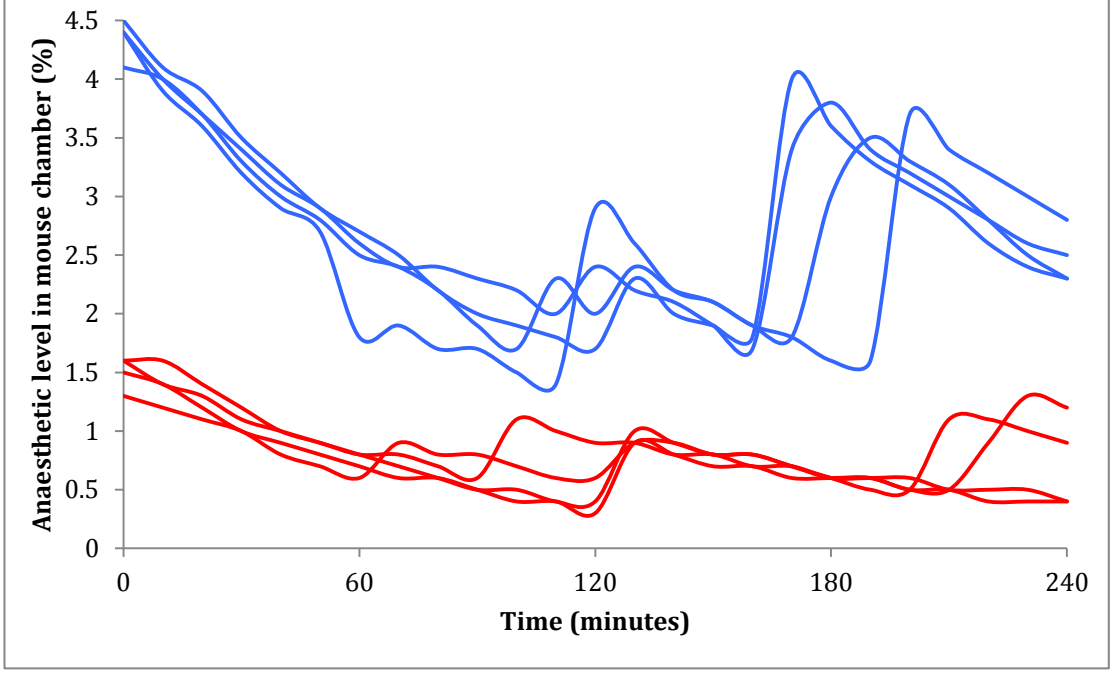

Figure 25: Comparison of Sevoflurane and Isoflurane Gas Levels During Mouse Anaesthesia. The isoflurane (red) and sevoflurane (blue) gas levels followed a similar rate of decline and required additional anaesthetic to be added approximately every hour during the four-hour exposure. Mice were euthanised at the two and four hour time-points. For each drug treatment *n*=12 mice were used.

3.1.2 Intraperitoneal Anaesthesia

The administration of IP anaesthetic was not carried out in the fume hood but the animals were kept in the same animal chambers to prevent variation in surroundings. The anaesthetic treatment mice were injected with 1% propofol (Provisi MCT-LCT 1%, Claris) at *t*=0 hours. To reduce variation between the treatment and control samples, mice used for the *t*=4 hour control were injected

with an equivalent dose of the intralipid vehicle that the propofol was suspended in. The initial dose administered to the treatment mice was 100 mg per kg of weight (Table 17). "Top up" intralipid doses were not administered to the control animals because of the additional stress that it would have caused.

Table 17: Weight and Initial Propofol Dose for Propofol Treatment. Mice used for propofol treatments were weighed at *t*=0 hours to calculate the correct initial dose of propofol for each individual animal.

Experiment	Mouse	Sex	Weight (g)	Initial Dose (mL)
1	1	Male	31	0.31
	2	Male	29	0.29
	3	Male	29	0.29
2	1	Female	22	0.22
	2	Female	22	0.21
	3	Female	21	0.21
3	1	Female	23	0.23
	2	Female	31	0.31
	3	Female	21	0.21

During the anaesthetic exposure experiments, it was observed that the effect of propofol wore off much faster than the isoflurane or sevoflurane anaesthetics. The required dose of propofol was also variable between each animal, some requiring "top-up" doses of propofol more frequently than others. A 0.1 mL dose of propofol initially lasted 25 minutes but gradually required more frequent doses, with some as often as five minutes in the last hour of exposure. The "top-up" doses were increased from 0.1 mLs to 0.15 mLs for experiments 2 and 3, which

lasted 20 – 25 minutes for the first three hours and decreased to ten minutes in the last hour.

3.2 RNA Qualifications and Quantification Analysis

Following anaesthetic exposure for two or four hours, mice were immediately euthanased with CO_2 and cortical brain tissue was removed. The RNA extracted from mouse cortical brain tissue required qualitative and quantitative analysis before proceeding with downstream applications. RNA quantification of all samples is important when ensuring that approximately the same amount of RNA template is used for downstream experiments [78]. Specific RNA-handling and processing techniques were carried out at all times. The Nanodrop 2000 Spectrophotometer was used to examine the concentration and A_{260}/A_{280} and $A_{260}/_{230}$ absorbance ratios of all RNA samples prior to storage in the -80°C freezer. The absorbance ratios provided an indication of RNA purity, as the ratio is altered when contaminating DNA or phenols are present [78]. Furthermore, all RNA samples were electrophoresed in denaturing formaldehyde gels to analyse the integrity of total RNA.

3.2.1 Analysis of Processed RNA Samples from Mouse Cortical Brain Tissue

Analysis of RNA extracted from cortical brain tissue indicated that all RNA extractions resulted in high quantity and quality of nucleic acid products, with concentrations greater than 500 ng/µL. The concentration of RNA obtained ranged from 512 ng/µL to 5034 ng/µL, with a total yield ranging from 25 µg to 252 µg, respectively. Absorbance readings were taken prior to DNase treatment and those values greater than 2000 ng/µL may have resulted from gDNA contamination.

3.2.1.1 Nanodrop Results for Sevoflurane Exposure and Controls

An A_{260}/A_{280} ratio of 2.0 is generally accepted as pure for RNA. The A_{260}/A_{230} ratio is usually higher, with a value of 2.0 – 2.2 considered ideal. The A_{260}/A_{280} ratio for all RNA samples from the sevoflurane exposure ranged from 1.4 – 2.2 and A_{260}/A_{230} ranged from 1.7 – 2.6. Data for all absorbance readings can be found tabulated in Appendix 4. The values obtained from the absorbance readings indicated that all sevoflurane-treated RNA samples had A_{260}/A_{280} and A_{260}/A_{230} ratios within the preferable range. Although some values were lower than 1.8, when displayed on a graph clear peaks can be seen at 260 nm (Figure 22).

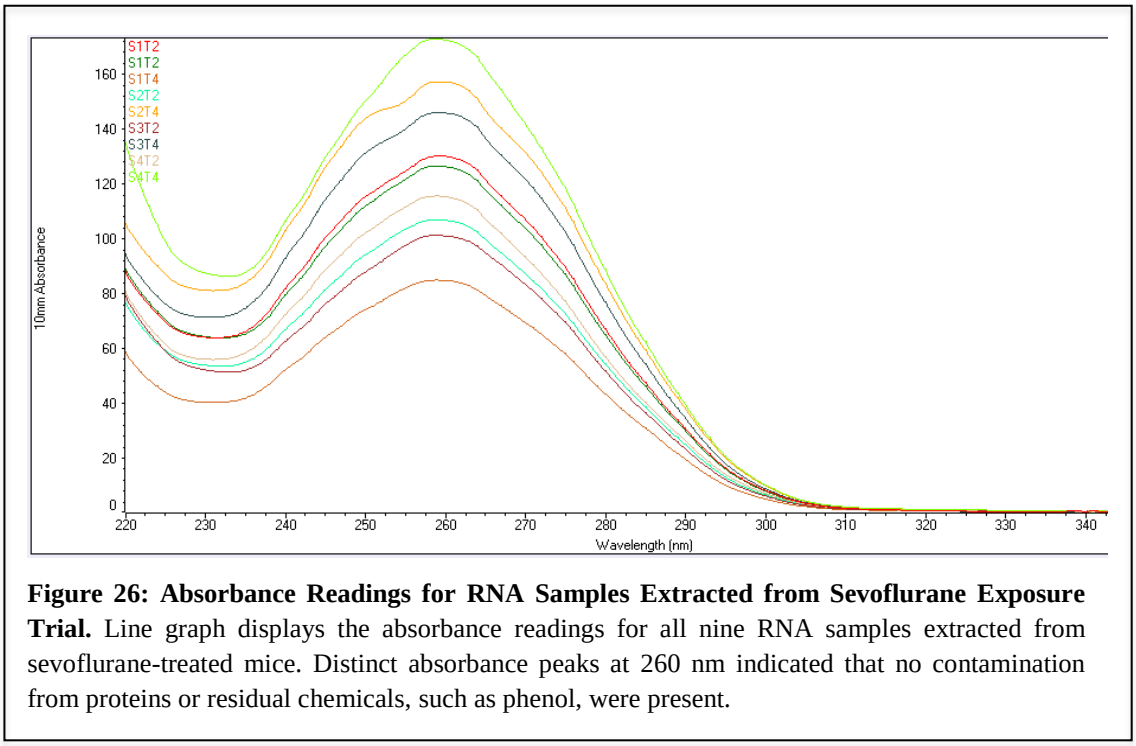

Figure 26: Absorbance Readings for RNA Samples Extracted from Sevoflurane Exposure Trial. Line graph displays the absorbance readings for all nine RNA samples extracted from sevoflurane-treated mice. Distinct absorbance peaks at 260 nm indicated that no contamination from proteins or residual chemicals, such as phenol, were present.

3.2.1.2 Nanodrop Results for Propofol Exposure and Controls

Absorbance readings of the propofol-treated RNA samples also demonstrated clear peaks at 230 and 260 nm for nine out of twelve of the RNA samples (Figure 23). The P2T4C and P2T4T RNA samples displayed a slight shift in the 230 and 260 peaks, which may have been caused by residual contamination from the RNA extraction. The P2T4C RNA displayed a very high peak at 230 nm that is

indicative of phenol contamination from the TRI Reagent®. Subsequent analysis of these RNA samples in a denaturing formaldehyde gel indicated the RNA had maintained integrity and was used for later qPCR analysis.

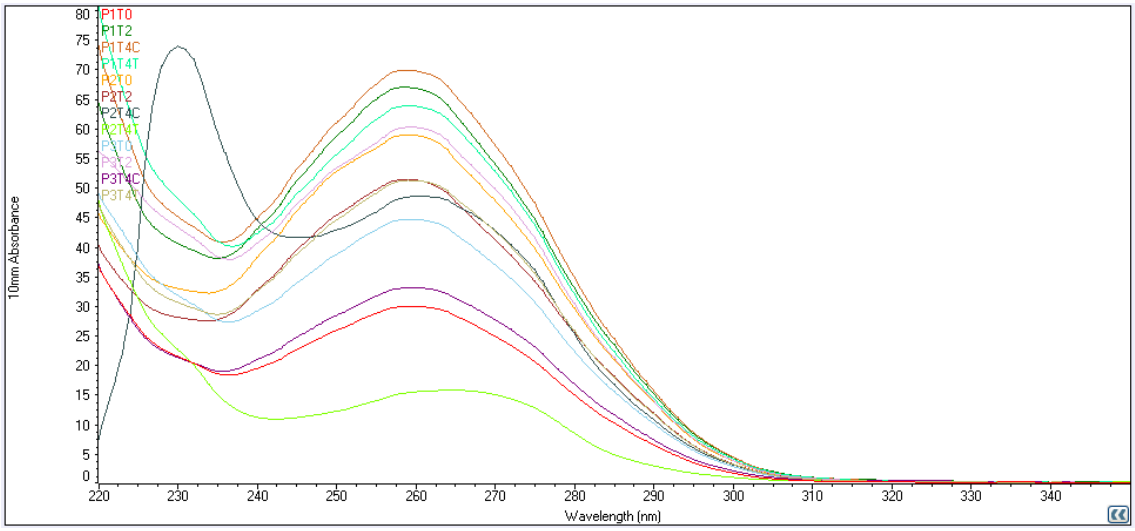

Figure 27: Line Graph of Absorbance Readings for Propofol Exposure Trial. The absorbance readings for the all RNA samples displayed clear A_{260}/A_{280} and A_{260}/A_{230} peaks, apart from the P2T4C sample. P2T4C RNA (black) exhibited absorbance at 230 nm, which was likely due to residual phenol contamination. The number of treatment and control mice used in this trial was *n*=12.

3.2.2 Denaturing Formaldehyde Gel Electrophoresis

A denaturing formaldehyde gel was prepared in order to analyse the size and integrity of the eukaryotic 28S and 18S ribosomal RNA (rRNA) bands. Intact total RNA is expected to result in two distinct bands on the electrophoresis gel in a 2:1 ratio. Partially degraded RNA will appear as smeared bands. An RNA molecular ladder was also loaded into the denaturing formaldehyde gel in order to provide an indication of the size of the single stranded rRNA bands present.

3.2.2.1 Denaturing Gel Electrophoresis for Sevoflurane-Treated RNA

Initially, two RNA samples were analysed to ensure the denaturing formaldehyde gel electrophoresis method was effective. A comparison was made between the

S4T2 RNA sample before and after DNase treatment. A new RNA ladder was also tested. Gel electrophoresis results (Figure 24) showed that the RNA sample pre-DNase treatment produced distinct 28S and 18S bands; indicating good quality RNA was present. The DNase-treated sample did not display any bands, which may be due to interference from residual DNase I enzyme or the lower concentration of RNA resulting from diluting it 1:10 during DNase treatment. Absorbance readings indicated that the DNase-treated sample still maintained clear peaks at 230 and 260 nm. The RNA ladder (3 µg) was overly fluorescent (Figure 24C) and did not result in the migration of nine clear bands ranging 0.5 - 10 kB in size with the observation of the 1.5 kb band being more intense than other ladder bands.

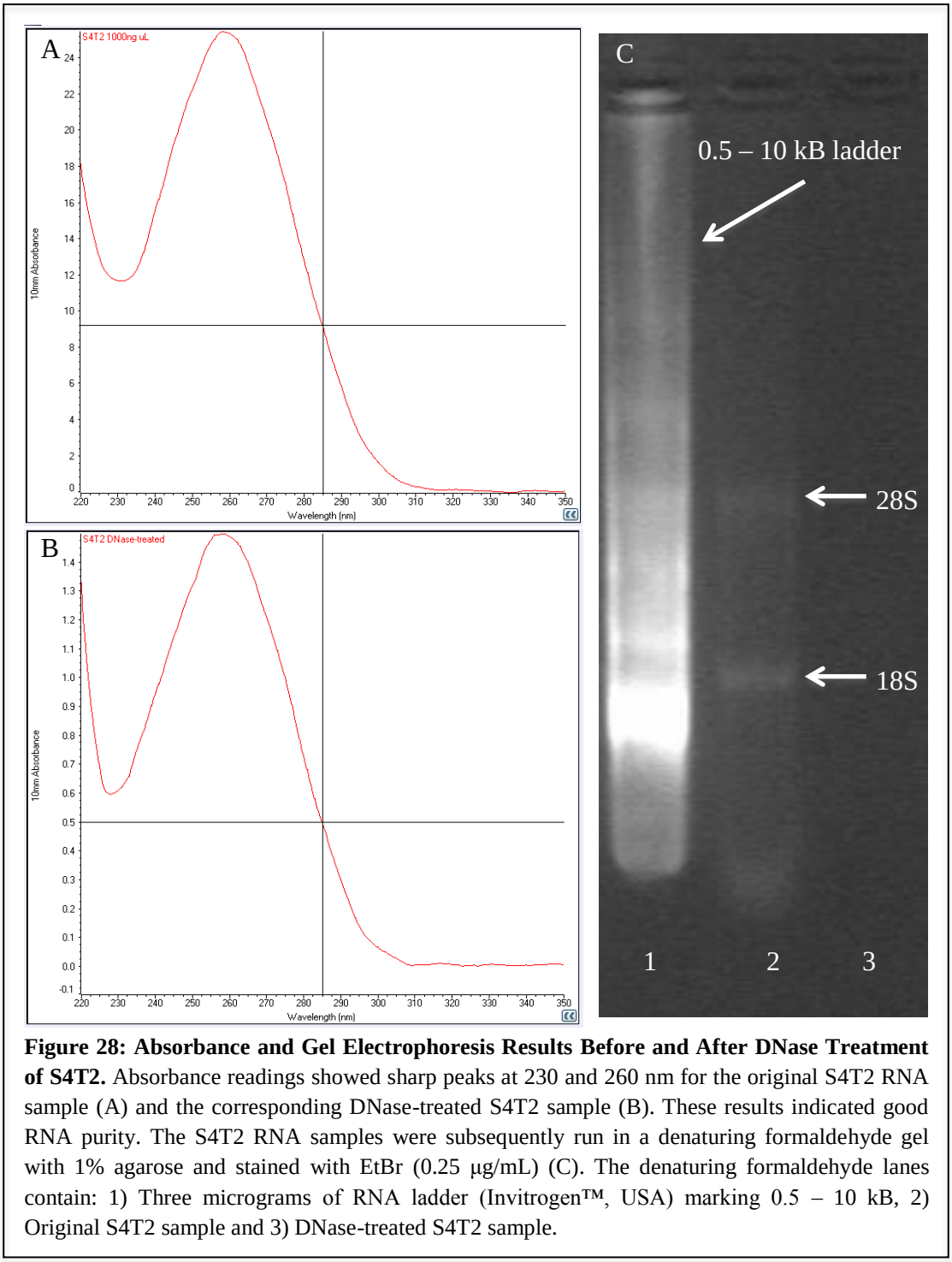

Figure 28: Absorbance and Gel Electrophoresis Results Before and After DNase Treatment of S4T2. Absorbance readings showed sharp peaks at 230 and 260 nm for the original S4T2 RNA sample (A) and the corresponding DNase-treated S4T2 sample (B). These results indicated good RNA purity. The S4T2 RNA samples were subsequently run in a denaturing formaldehyde gel with 1% agarose and stained with EtBr (0.25 µg/mL) (C). The denaturing formaldehyde lanes contain: 1) Three micrograms of RNA ladder (Invitrogen™, USA) marking 0.5 – 10 kB, 2) Original S4T2 sample and 3) DNase-treated S4T2 sample.

After analysis of the S4T2 samples, further denaturing formaldehyde gel electrophoresis was carried out to analyse all remaining RNA samples. The electrophoresis results for the RNA from the sevoflurane exposure trials are shown in Figure 25. Only 2 µg of the RNA ladder was loaded into the formaldehyde gel, as previous results (Figure 24C) displayed strong fluorescence, making it difficult to visualise the different sized molecular markers. The RNA

samples S1T2, S1T4, S2T2, S2T4, S3T2 and S3T4 were added to sample buffer and loaded into the subsequent lanes. Ultraviolet illumination of the formaldehyde gel showed that all RNA samples displayed intact 28S and 18S bands. Some smeared bands can be seen towards the bottom of the gel image that may represent degraded RNA or smaller 5S rRNA. However, the 28S and 18S bands were both still clearly present. Thus, it was concluded that the RNA was of good quality to use in qPCR. Although a lesser quantity of the RNA ladder was used, the ladder was still too fluorescent and removed from Figure 25. Therefore, a dilution of the RNA ladder should be tested for an optimised loading concentration in future experiments.

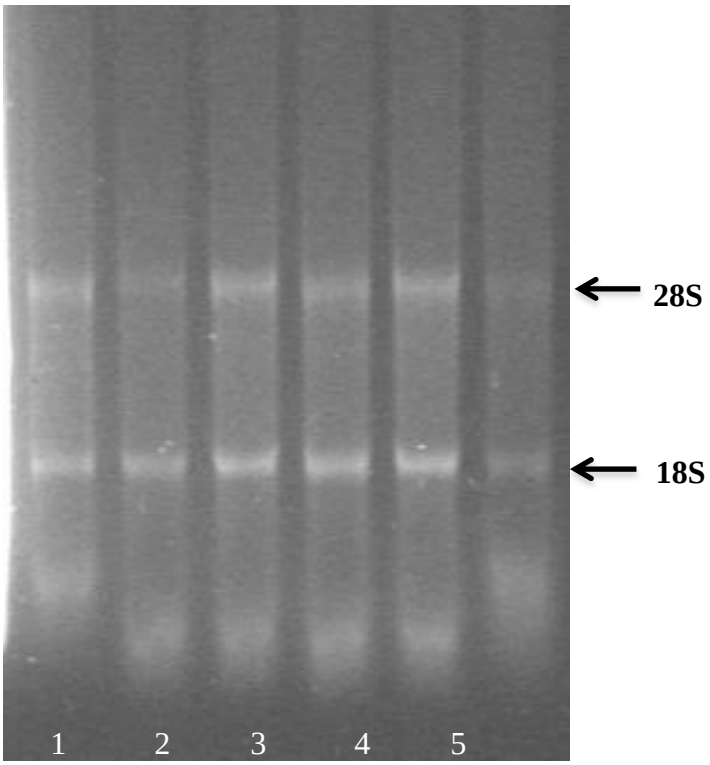

Figure 29: Gel Electrophoresis Image for RNA Samples from Sevoflurane Exposure. Gel electrophoresis of a denaturing formaldehyde gel made with 1% agarose was used to visualise RNA integrity of all sevoflurane-treated RNA samples. The individual lanes contain the following six 1 µg RNA samples: 1) S1T2, 2) S1T4, 3) S2T2, 4) S2T4, 5) S3T2 and 6) S3T4. Electrophoresis was carried out at 50V for 1.5 hours.

3.2.2.2 Denaturing Gel Electrophoresis for Propofol-Treated RNA

All propofol-treated RNA samples were analysed using denaturing formaldehyde gel electrophoresis (results not shown). The resulting gel image displayed undefined 28S and 18S rRNA bands. This may have been the result of poor methodology or the RNA was indeed degraded and of poor quality. Therefore, the denaturing formaldehyde gel and RNA sample preparation was further optimised. Briefly, the concentration of RNA analysed was increased from 1 µg to 3 µg and the denaturation heat step was increased from 70°C to 85°C. Gel electrophoresis was also run at a slower voltage over a longer time interval; 30V for 3 hours, rather than 50V for 1.5 hours to prevent the gel from overheating. In addition, during gel electrophoresis, the 1X MOPS buffer was circulated by pipetting every 30 minutes. Despite optimisation of the denaturing formaldehyde gel electrophoresis method, the resulting image still indicated undefined 28S and 18S rRNA bands and poor definition of the RNA ladder (Figure 26). Due to the small quantity of RNA, all samples were subsequently run in a non-denaturing 1% agarose gel to validate the presence of intact 28S and 18S rRNA.

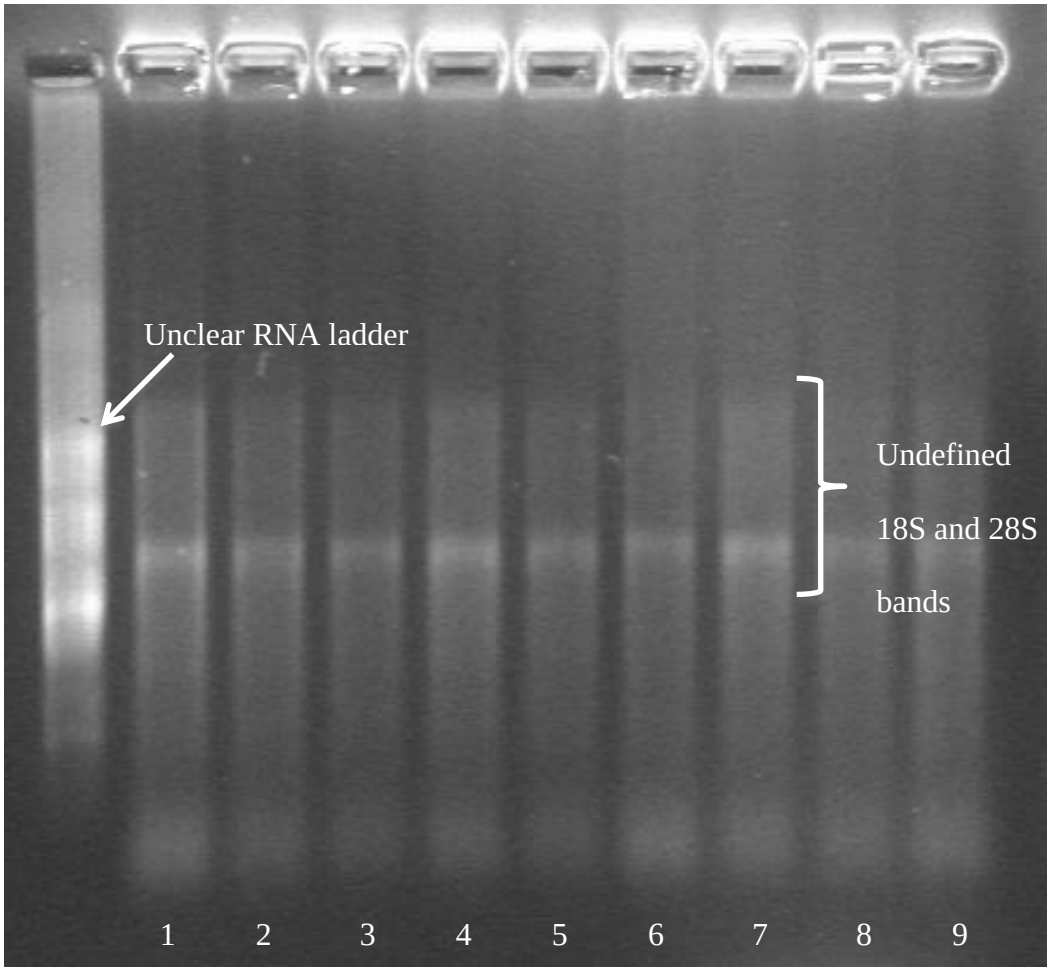

Figure 30: Denaturing Gel Electrophoresis Image for Propofol-Treated RNA Samples. Denaturing formaldehyde gel electrophoresis was used to visualise RNA integrity of all propofol-treated RNA samples. The lanes contain the nine 3 µg RNA samples: 1) P1T0, 2) P1T4C, 3) P1T4T, 4) P2T0, 5) P2T4C, 6) P2T4T, 7) P2T0, 8) P3T4C and, 9) P3T4T. None of the RNA samples loaded were able to produce clearly defined 28S or 18S rRNA bands. The RNA ladder was loaded at a concentration of 2 µg and did not produce clear resolved bands of 0.5 – 10kB. Gel electrophoresis was conducted at 30V for three hours.

3.2.2.3 Non-Denaturing Gel Electrophoresis for Propofol-Treated RNA

Using the optimised gel electrophoresis method, 3 µg of each propofol-treated RNA sample was loaded in a non-denaturing 1% agarose gel made in 1X Superbuffer stained with EtBr (0.25 µg/mL) for confirmation that the 28S and 18S rRNA bands were present for cDNA synthesis. A 1 kB+ molecular ladder at a final concentration of 5 µg/mL was also loaded to compare the RNA bands against. The secondary structure of RNA alters its migration pattern in native gels and may not migrate according to its expected size of 4712 and 1869 bp, respectively. Figure 27 shows the 28S rRNA band just below the 5000 bp marker

on the agarose gel. Similarly, the 18S rRNA band was observed just below the 2000 bp marker

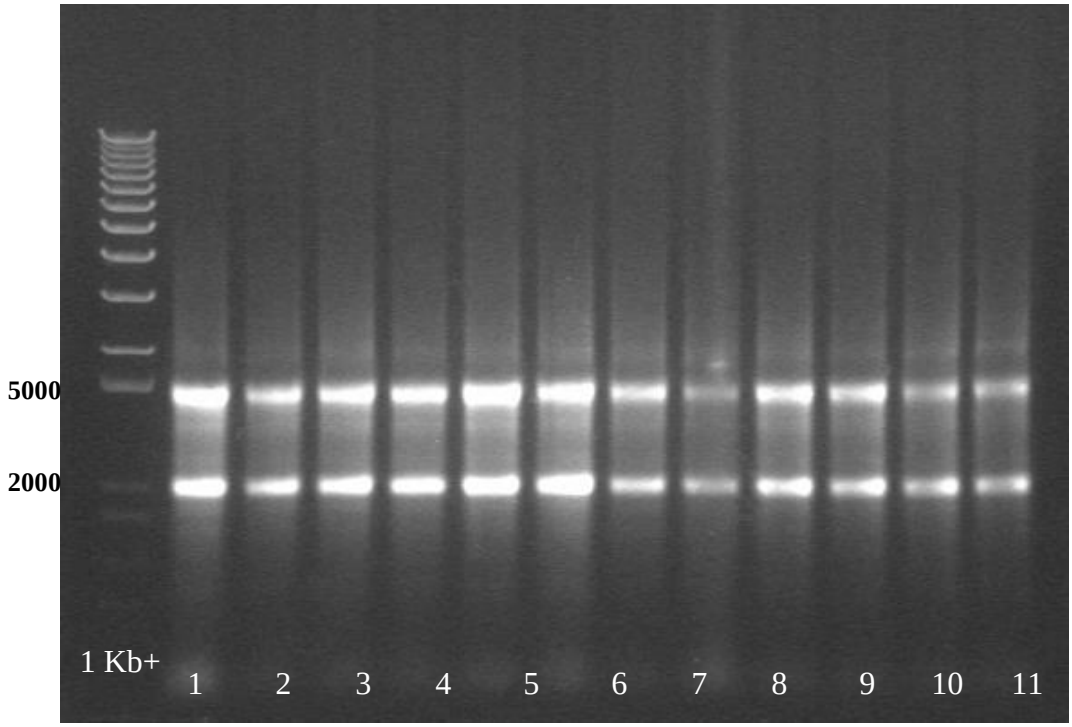

Figure 31: Visualisation of Propofol-Treated RNA Samples in Non-Denaturing Gel Electrophoresis. RNA extracted from propofol-treated mice was run in a non-denaturing 1% agarose gel made in 1X Superbuffer and stained with EtBr (0.25 µg/mL). Electrophoresis was carried out at 200 V for ten minutes. Ten microliters of 1 kB+ molecular ladder (Invitrogen™, USA) at a final concentration of 5 µg/mL was loaded for comparison with the 28S and 18S rRNA bands. The 28S rRNA band was visualised at the expected size of 4712 bp and the 18S rRNA band was also visualised at the expected size of 1869 bp.

3.3 Primer Design and Bioinformatic Analysis

In accordance with the MIQE guidelines, it was preferable to use primer sets that had demonstrated successful amplification in previous publications [78]. The *Actβ*, *β2m*, *Gapdh*, *Gjd2*, *HPRT1* and one set of *Bdnf* primers were selected from published data [72,75,81]. Primer sets targeting the remaining mouse GOIs in this study (*Arc*, *CaMKIIα*, and *Grin1*) with optimal length for qPCR (100 – 200 bp) were not available. Therefore, primers for these GOIs were designed using the NCBI Basic Local Alignment Search Tool (BLAST®) software. All primers were designed to specific criteria (stated in section 2.8), the most important of which

was the targeting of an intron-spanning region. Since mRNA transcripts do not contain introns, the targeting of a boundary where the intron has been spliced out ensures mRNA, not DNA, is targeted. As the published *Bdnf* primer set did not target an intron-spanning region, an alternative *Bdnf* primer set was designed with NCBI. All target sequences can be found in Appendix 6.

The NCBI BLAST® tool was also used to analyse sequence homology between the target mouse sequences and the corresponding human genes. The identity value generated by BLAST® represented the extent to which the human and mouse nucleotide sequence of the GOIs had the same residues at the same positions in an alignment. High sequence homology was anticipated for relevance of our results to human research and the identification of genes involved in memory loss during general anaesthesia.

3.3.1 *Arc* Primers

The *Arc* gene is located at position qD3 on chromosome 15 in *Mus musculus* and spans 3490 bp. Two transcript variants are generated via alternate splicing and transcript variant 1 (NM_018790), an mRNA transcript that is 3059 bp in length, was targeted for the purpose of this research study. The *Arc* primer set was designed using BLAST® to target an intron-spanning region between exon 1 and exon 2 of the *Arc* mRNA transcript resulting in the amplification of a 104 bp PCR product (Figure 28A). The target sequence had a guanine cysteine (GC) content of 57% and an expected melting temperature of 82°C. The mRNA sequences of human and mouse *Arc* transcript variant 1 were 2948 bp and 3059, respectively.

Alignment of these sequences in BLAST® indicated that 80% of the sequence was homologous between the species.

3.3.2 *Bdnf* Primers

The *Bdnf* gene is located at qE3 on chromosome 2 in *Mus musculus*, spanning 78,516 bp and producing eleven transcript variants through alternate splicing. The primers designed for this research targeted transcript variant 1 (NM_007540.4), which is 4302 bp in length. The target sequence was 103 bp in length, spanning the boundary between exon 1 and exon 2 and also contained part of the ORF in exon 2 (Figure 28B). The target sequence had a GC content of 46% and an expected melting temperature of 77°C. The BLAST® tool was used to analyse sequence homology between transcript variant 1 of the human and mouse *Bdnf* gene. The mRNA sequence of human and mouse *Bdnf* are 4747 bp and 4302 bp, respectively, and the ORF spans 744 bp in both human and mouse. Transcript variant 1 of mouse *Bdnf* displays 80% identity with human *Bdnf* transcript variant 1.

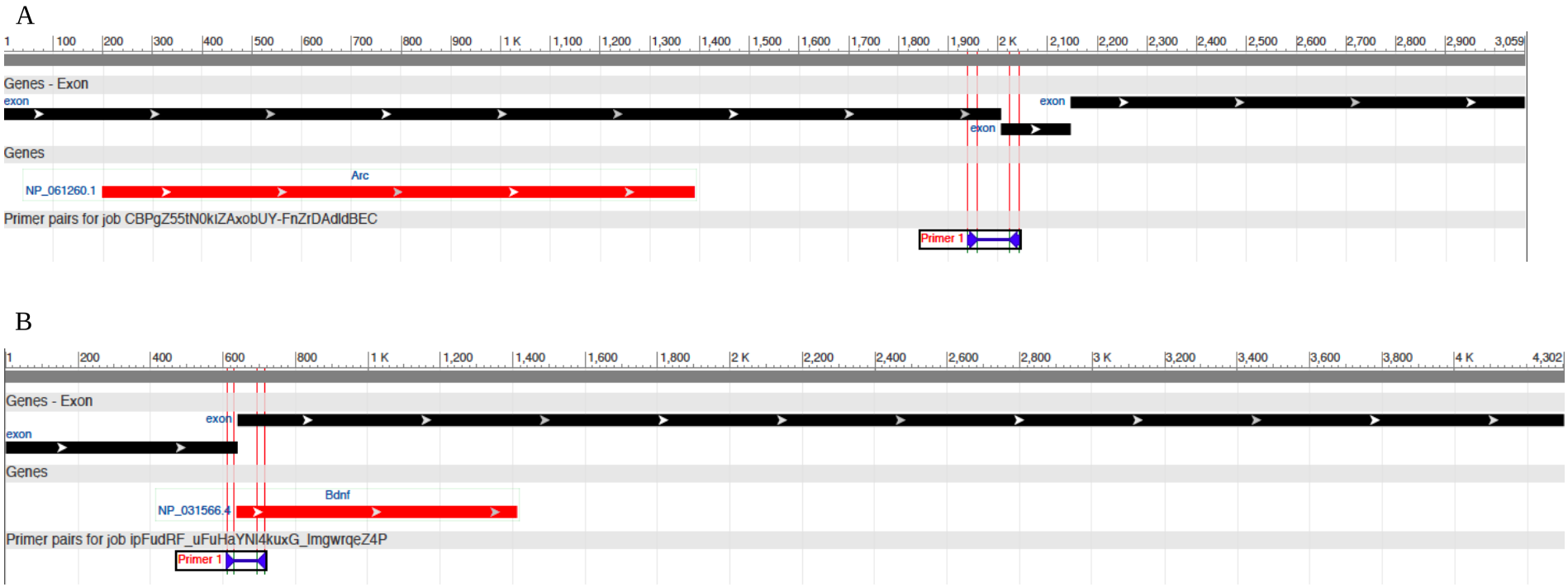

Figure 32: *Arc* and *Bdnf*. The grey bar illustrates the complete mRNA sequence; Black bar, the exons; and the red bar the ORF of the translated mRNA seqeunce. The *Arc* and *Bdnf* primer sets used in qPCR were designed using the NCBI primer design tool. Each set was designed to target an intron-spanning boundary so as to ensure that mRNA was targeted. (A) The *Arc* primers target the boundary between exon one and exon two. (B) The *Bdnf* primers target the boundary between exon one and exon two.

3.3.3 *CaMKIIα* Primers

The *CaMKIIα* gene spans 62,521 bp at position qE1 on chromosome 18 in *Mus musculus*. Three transcript variants of *CaMKIIα* are produced through alternate splicing. Transcript variant 1 (NM_009792.3) is 4268 bp in length and was targeted in this research with the primers designed using BLAST®. The target sequence was 157 bp in length, crossing the boundary between exon 1 and exon 2 (Figure 29A). Part of the ORF located on exon 1 was also targeted by the *CaMKIIα* primer set. The target sequence had a GC content of 53% and an expected melting temperature of 82°C. Transcript variant 1 for mouse and human *CaMKIIα* mRNAs was 4268 bp and 4918 bp in length, respectively. Sequence alignment in BLAST® showed a 78% identity between the two species.

3.3.4 *Grin1* Primers

The *Grin1* gene is located at position qA3 on chromosome 2 in *Mus musculus*, spanning 27,987 bp and producing three transcript variants through alternate splicing. Transcript variant 1 (NM_008169.3) is 4326 bp in length and was targeted by the *Grin1* primer set to produce a PCR product 148 bp in length. The target sequence spanned the boundary between exon 19 and exon 20 and included part of the ORF (Figure 29B). It contained a GC content of 49% and had an expected melting temperature of 80°C. Transcript variant 1 of the mouse and human *Grin1* gene were 4326 bp and 4289 bp in length, respectively. Alignment of these sequences in BLAST® demonstrated 90% identity between the two species.

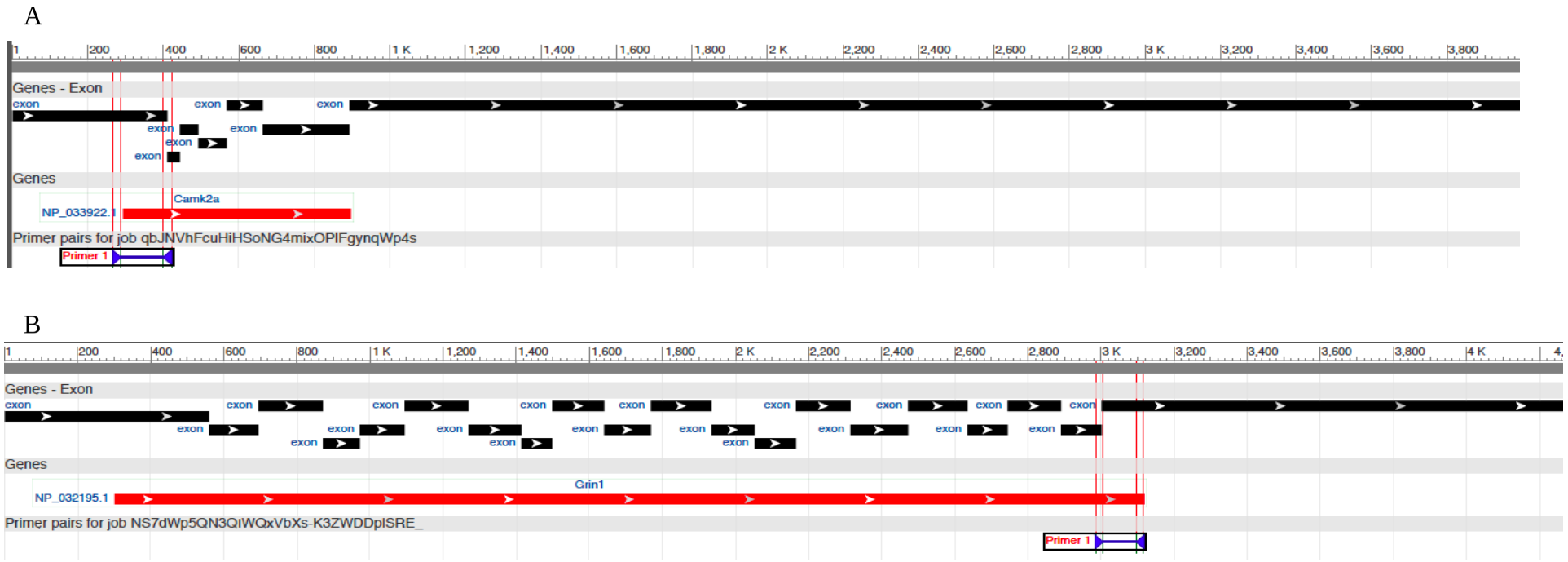

Figure 33: *CaMKIIα* and *Grin1*. The grey bar illustrates the complete mRNA sequence; Black bar, the exons; and the red bar the ORF of the translated mRNA seqeunce. The *CaMkIIα* and *Grin1* primer sets used in qPCR were designed using the NCBI primer design tool. Each set was designed to target an exon/exon boundary so as to ensure that mRNA was targeted. (A) The *CamkIIα* primers target the boundary between exon one and exon two. (B) The *Grin1* primers targeted the boundary between exon 19 and exon 20.

3.3.5 Reference Gene Primers

Reference genes provide a means of internal normalisation in qPCR assays. Four reference genes were selected for use in this study based on validation in previous studies; *Actβ, β2m, Gapdh* and *HPRT1* [72,75,81]. After testing these primer sets in standard PCR, *β2m* and *Gapdh* were selected for further use in this research. Primers for the target gene, *Gjd2*, had been tested in a brain slice model (*in vitro*) by Keiran Oxton (UoW, NZ). Therefore, this primer set was included for targeting the GOI, *Gjd2*, for *in vivo* validation of previous results.

The *Gjd2* primer set targeted part of the ORF in exon 2 to produce a 125 bp PCR product (Figure 30C). The sequence had a GC content of 52% and an expected melting temperature of 81°C. The *β2m* primer set targeted a sequence 104 bp in length that crossed the boundary between exon 1 and exon 2 and also contained part of the ORF (Figure 30A). The targeted sequence had a GC content of 51% and an expected melting temperature of 79°C. The *Gapdh* primers targeted an 87 bp sequence that included the boundary between exon 4 and exon 5 and was inside the ORF (Figure 30B). The sequence had a GC content of 56% and an expected melting temperature of 80°C.

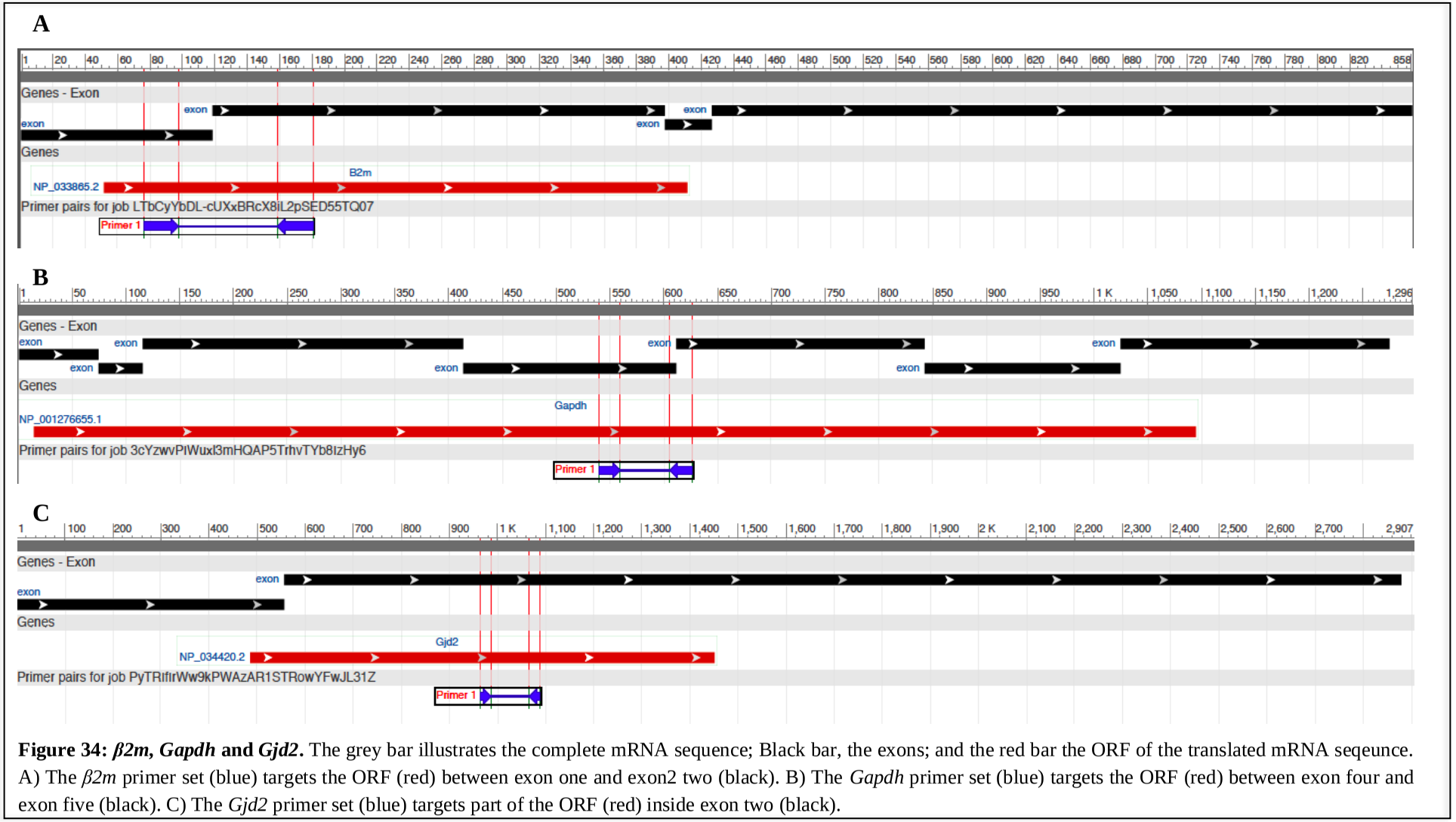

Figure 34: *β2m, Gapdh* and *Gjd2*. The grey bar illustrates the complete mRNA sequence; Black bar, the exons; and the red bar the ORF of the translated mRNA seqeunce. A) The *β2m* primer set (blue) targets the ORF (red) between exon one and exon2 two (black). B) The *Gapdh* primer set (blue) targets the ORF (red) between exon four and exon five (black). C) The *Gjd2* primer set (blue) targets part of the ORF (red) inside exon two (black).

3.4 Evaluation of Primers and Synthesised cDNA using Standard PCR

All primer sets were tested using standard PCR to examine the target product size and determine the optimal annealing temperature for each primer set. The PCR products were visualised using gel electrophoresis for experimental confirmation of the target sequence preceding qPCR analysis. All PCR assays were carried out with -RT and NTC controls. These controls provided evidence that the experiment was not DNA contaminated during synthesis of cDNA samples or PCR set up.

3.4.1 *Actβ* Primer Testing

The *Actβ* primer set amplified the expected product of 150 bp in length for both cDNA samples tested, however, the negative control also showed evidence of amplification (Figure 33). Amplification in the negative control may have resulted from contaminated primer stock, mQH_20 or pipette tips or carryover contamination during PCR set up. Further testing of the *Actβ* primer set was carried out. Procedures to eliminate contamination issues included replacing all tips, gloves and reagents, re-making diluent solutions such as mQH_20 and TE buffer and leaving spaces between the tubes when in the thermocycler. The contamination in the *Actβ* negative control was unable to be eliminated. Therefore, it was concluded that the primers were not suitable and primers targeting other reference genes were investigated.

3.4.2 *Arc* Primer Testing

The *Arc* (NM_018790.3) primers were also tested using standard PCR. The *Arc* PCR products were electrophoresed in a 1.5% agarose gel made with 1X Superbuffer stained with EtBr (0.25 μg/mL) to visualise the size of DNA products

amplified during PCR. Amplified *Arc* products visualised using gel electrophoresis showed two fluorescent bands positioned near the 100 bp and 400 bp markers (Figure 31). Thus, the primers resulted in the expected amplicon size of 104 bp. Bioinformatic analysis revealed that the additional 349 bp band was a genomic product, indicating gDNA contamination of the RNA samples. Thus, TRI Reagent™ was not sufficient for removing DNA from the samples and DNase treatments of all RNA samples was subsequently carried out.

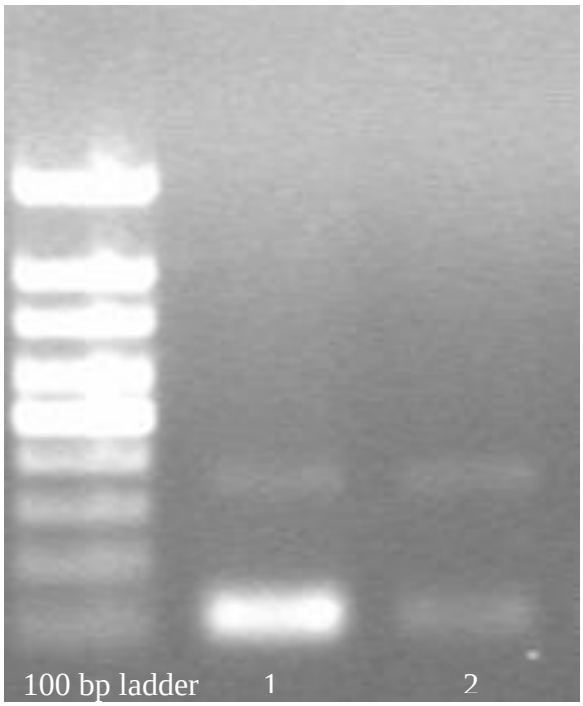

Figure 35: *Arc* Primer Testing with S1T2 and S3T4 cDNA. Standard PCR testing of the *Arc* primers with two cDNA samples; S1T2 (1) and S3T4 (2). PCR products were loaded on to a 1.5% agarose gel made in 1X Superbuffer stained with EtBr (0.25 µg/mL) and electrophoresed for 10 minutes at 200 V. A 100 bp DNA ladder was added to visualise size of the PCR products. Both S1T2 and S3T4 with *Arc* primers showed the expected product of 104 bp with an additional product at 349 bp. Bioinformatic analysis indicted the 349 bp product was the result of amplified genomic DNA. All RNA samples were subsequently DNase-treated.

3.4.3 Elimination of Genomic DNA Contamination

All RNA samples were treated with DNase I enzyme to eliminate genomic DNA contamination and produce accurate results by ensuring only mRNA was amplified during qPCR. A control cDNA sample with known gDNA

contamination was also tested in PCR for comparison. The results demonstrated that treatment of RNA samples with DNase I enzyme was sufficient for the removal of gDNA. This is shown in Figure 32, where the 349 bp gDNA product has not been amplified by the *Arc* primers. Additionally, the negative controls did not amplify any product, indicating the reverse transcription process and PCR set up was not contaminated.

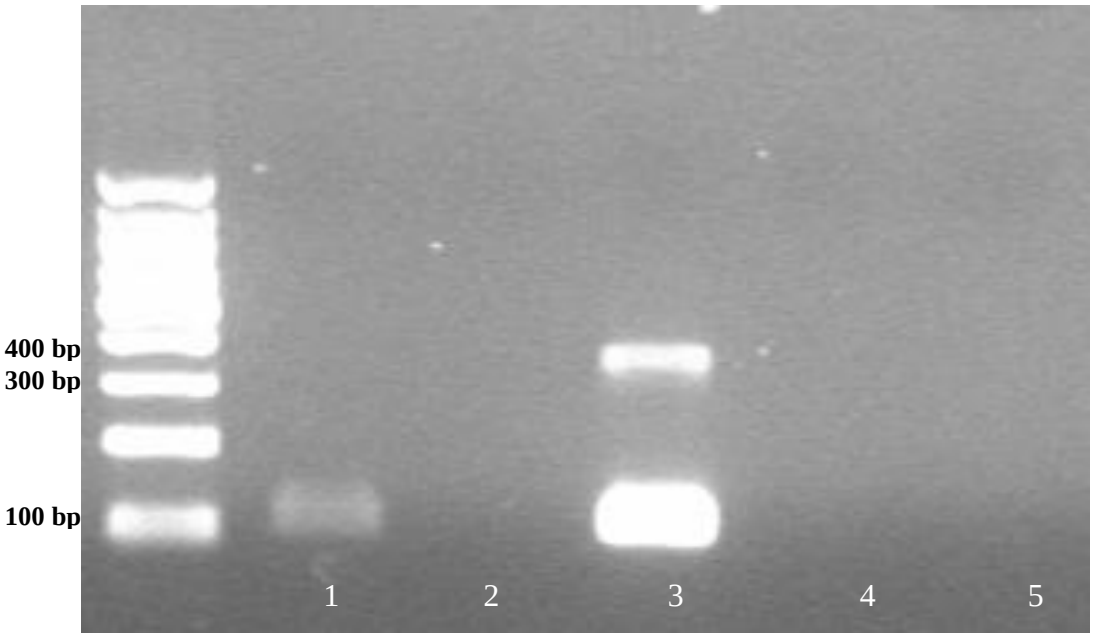

Figure 36: Removal of Genomic DNA Contamination. A 1.5% agarose gel made with 1X Superbuffer and stained with EtBr (0.25 µg/mL) was used to visualise *Arc* PCR products. The gel was electrophoresed for ten minutes at 200 V. The PCR products were compared with a 100 bp molecular ladder (Solis BioDyne, Estonia). The lanes represent: 1) DNase treated S1T2 cDNA sample with *Arc* primers, displaying one band at approximately 104 bp, 2) blank 3) non-DNase treated S1T2 cDNA sample with *Arc* primers, displaying bands at approximately 104 bp and 349bp, 4) -RT control and 5) NTC. The gDNA band present in lane 3 has been eliminated, as shown in lane 1. Due to DNase treatment, there is a 10x dilution difference between the loading template between lane 1 and lane 3 however, lane 1 demonstrates that there is clearly a lack of the larger band seen in lane 3.

3.4.4 *Bdnf* Primer Testing

Both the previously published and experimentally designed *Bdnf* primer sets were tested in standard PCR. The resulting gel electrophoresis image (Figure 33) indicated that both sets of *Bdnf* primers amplified products of the expected size (103 bp and 205 bp). Similarly, the negative controls for the *Bdnf* primer sets

displayed no fluorescent bands, indicating no contamination was present. However, the published *Bdnf* primer set did not target an intron-spanning boundary and was therefore not ideal for qPCR.

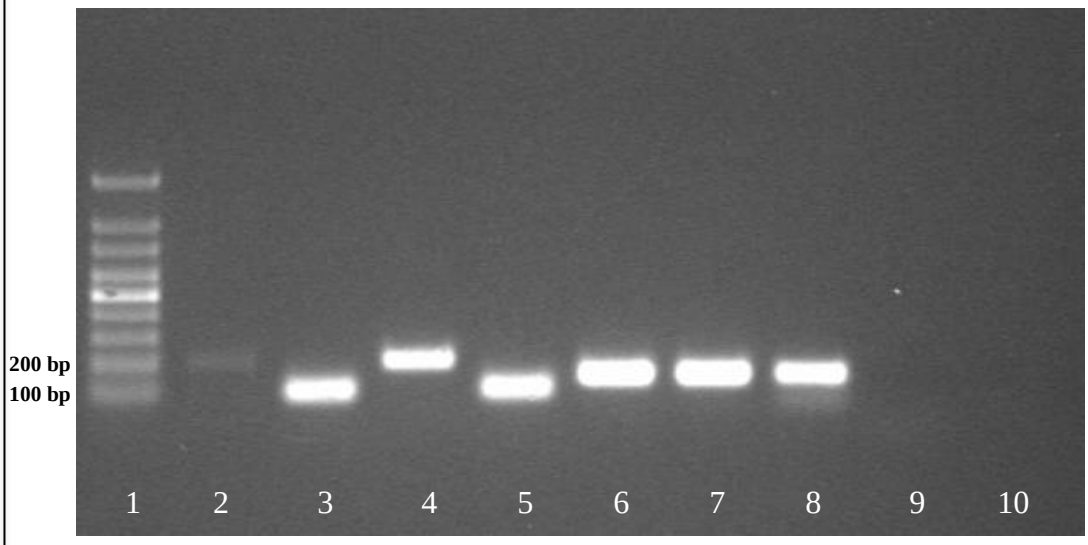

Figure 37: Gel Image of Amplified cDNA using *Bdnf* and *Actβ* Primer Sets. The image shows a gel electrophoresis image of 1.5% agarose gel made in 1X TAE and stained with EtBr (0.25 µg/mL). The gel was electrophoresed at 90 V for 30 minutes. Two cDNA samples were validated; S1T2 and C1T0. Each lane is as follows: 1) 100 bp ladder (Solis Biodyne, Estonia), 2) published *Bdnf* primer set with S1T2, 3) designed *Bdnf* primer set with C1T0, 4) published *Bdnf* primer set with S1T2, 5) designed *Bdnf* primer set with C1T0, 6) *Actβ* primers with S1T2, 7) *Actβ* primers with C1T0, 8) *Actβ* primer set with H_20 (negative control), 9) published *Bdnf* primer set with H_20 (negative control) and 10) designed *Bdnf* primer set with H_20 (negative control). The published primers showed a fluorescent band where expected at approximately 205 bp. Similarly, the designed primer set indicated a fluorescent band at the predicted 103 bp size and *Actβ* at 150 bp.

3.4.5 Testing of *CaMKIIα* and *Grin1* Primer Sets

The primer sets used to target the *CaMKIIα* and *Grin1* genes were designed using the BLAST® primer design tool and tested using a gradient PCR ranging from 52°C - 56°C to determine the optimal annealing temperature of each primer set. Both sets of primers amplified a product of expected size at all three temperatures, with the negative controls clear of any amplification (Figure 34).

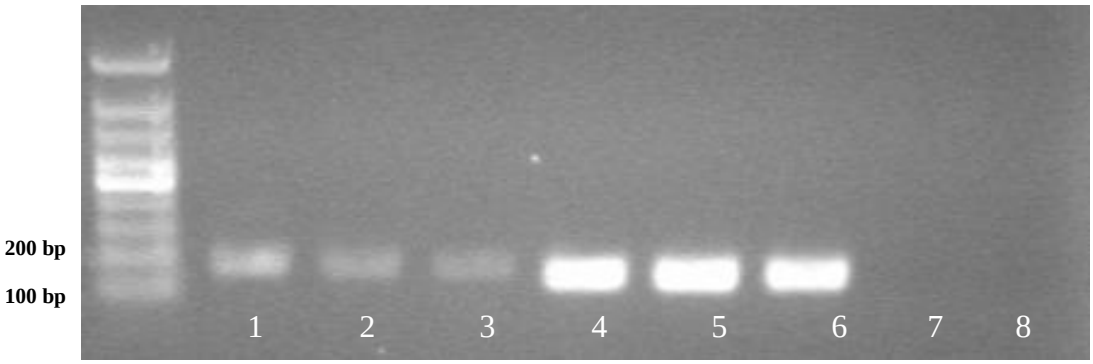

Figure 38: Gel Electrophoresis Image for *CaMKIIα* and *Grin1* Primers. The *CaMKIIα* and *Grin1* primers were tested with C1T0 RNA in gradient PCR and electrophoresed in a 1.5% agarose gel made with 1X Superbuffer and stained with EtBr (0.25 μg/mL). The gel was electrophoresed at 90 V for 30 minutes. 1) *Grin1* at 52°C. 2) *Grin1* at 54°C. 3) *Grin1* at 56°C. 4) *CaMKIIα* at 52°C. 5) *CaMKIIα* at 54°C. 6) *CaMKIIα* at 56°C. 7) Negative control with *Grin1* primers. 8) Negative control with *CaMKIIα* primers. The *CaMKIIα* primers amplified the expected target at 85 bp. Similarly; the *Grin1* primers amplified the expected 148 bp product.

3.4.6 *β2m, Gjd2* and *HPRT1* Primer Testing

The *β2m* primers had been previously published by Rijn et al. (2014) to target a 104 bp sequence within the *β2m* mouse gene. Similarly, the *Gjd2* primer set used in this research had been previously published by Wang et al. (2012) to target a 125 bp sequence in the *Gjd2* mouse gene and the *HPRT1* primers had been validated by Gilsbach et al. (2006) to produce a 94 bp PCR product. Gradient PCR ranging from 55 to 62°C was conducted for all three sets of primers to validate amplification of the expected PCR product before moving on to qPCR (results not shown). The *β2m* and *Gjd2* primer sets indicated optimal amplification at 58°C and no contamination was present in the negative controls. However, the *HPRT1* primer set failed to amplify cDNA template at annealing temperatures of 55 to 62°C. Multiple cDNA templates were tested but no amplification of the expected 94 bp product occurred. Therefore, *HPRT1* was not targeted as a reference gene in this research.

3.5 PCR Product Sequencing for Target Sequence Confirmation

In order to confirm that the correct mRNA sequences were amplified, the PCR products were purified and then ligated into individual cloning vectors, which were subsequently transformed into chemically competent *E. coli* cells. Plasmid DNA that tested positive via PCR was extracted from the *E. coli* cells and then sent to the Waikato DNA Sequencing Facility (UoW, New Zealand) for DNA sequencing.

3.5.1 Purification of PCR Products for DNA Sequencing

Positive PCR reactions of the expected size were purified for DNA sequencing analysis (Figure 35). The *β2m*, *Gapdh*, *Gjd2* and *Grin1* PCR products were purified using a DNA Clean and Concentrator™ kit to remove residual chemicals from the PCR reaction including polymerases, primers and free dNTPs. When visualised in a 2% agarose gel made in 1X Superbuffer stained with EtBr (0.25 μg/mL), fluorescent bands of the expected size were present and the fluorescence gave an estimation of the DNA concentrations. The *Arc* and *Bdnf* primers initially failed to amplify the cDNA template. Therefore, the PCR was repeated. Following a positive PCR reaction, the *Arc* and *Bdnf* PCR products were similarly purified (results not shown).

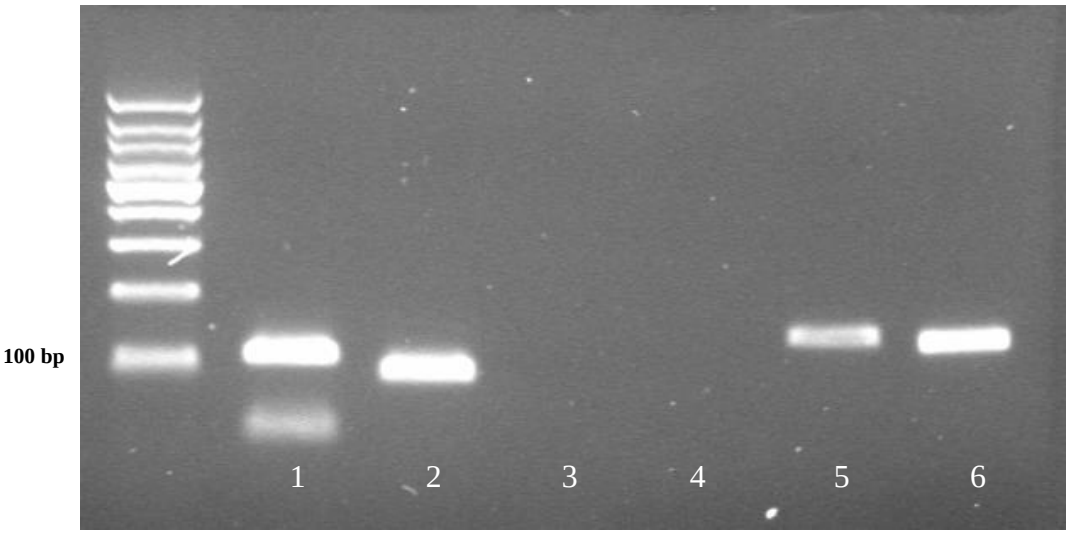

Figure 39: Gel Electrophoresis Image of *β2m*, *Gapdh*, *Arc*, *Bdnf*, *Gjd2* and *Grin1* PCR Products. All PCR products were electrophoresed in a 1% agarose gel made in 1X TAE, stained with EtBr (0.25 μg/mL) and run at 90V for 30 minutes. The *β2m, Gapdh, Gjd2* and *Grin1* primers amplified the expected product size and were subsequently purified for DNA sequencing. The lanes represent the following: 1) 104 bp *β2m* product and primer dimer, 2) 87 bp *Gapdh* product, 3) *Arc* primers that failed to amplify template, 4) *Bdnf* primers that failed to amplify template, 5) 148 bp *Grin1* product and 6) 125 bp *Gjd2* product. Further PCR was carried out to obtain amplified *Arc* and *Bdnf* products.

3.5.2 Ligation and Transformation of PCR Products

Initially, the purified *β2m* PCR product was sent to the Waikato DNA Sequencing Facility (UoW, New Zealand) for DNA sequencing, however the resulting electropherogram did not have well defined peak resolution or uniform peak spacing and contained a large amount of background noise (results not shown). Therefore, the purified *β2m* product was ligated into a pLUG-Prime® TA Cloning vector to produce a larger template size for sequencing.

3.5.2.1 Ligation of Purified *β2m* PCR Product into pLUG-Prime® Cloning Vector and Transformation into Chemically Competent *E. coli* cells

Initial vector cloning was carried out with the purified *β2m* PCR product (section 2.9). Three controls were included for the cloning strategy; a positive transformation control (pLUG-Prime® TA Cloning vector containing a *VMO1*

insert), a positive ligation insert control (provided with the pLUG-Prime® TA Cloning vector kit), and a negative ligation control (mQH_20 in place of any DNA). Chemically competent *E. coli* cells (strain DH5α) were prepared for transformation as outlined in section 2.11.1. Following transformation, *E. coli* cells were streaked out onto LB^+ agar plates containing XGal and IPTG and incubated overnight at 37°C for blue/white colony screening. The positive transformation control displayed greater than $1x10^8$ cfu/μg white colonies and no blue colonies, as expected. The positive insert control displayed 59 blue colonies and greater than $1x10^8$ cfu/μg. Similarly, the *β2m* insert had 87 blue colonies and greater than $1x10^8$ cfu/μg of white colonies. Thus, these transformations had resulted in false positives where the vector with no PCR insert had self-ligated. For this reason, multiple colonies were selected for colony PCR to confirm which were indeed true positives. The negative insert control had 13 blue colonies but was surrounded by few white colonies. Although we expected to observe no white colonies in the negative insert control, there were considerably less colonies present than what had been observed in both the positive and test insert controls (Figure 36).

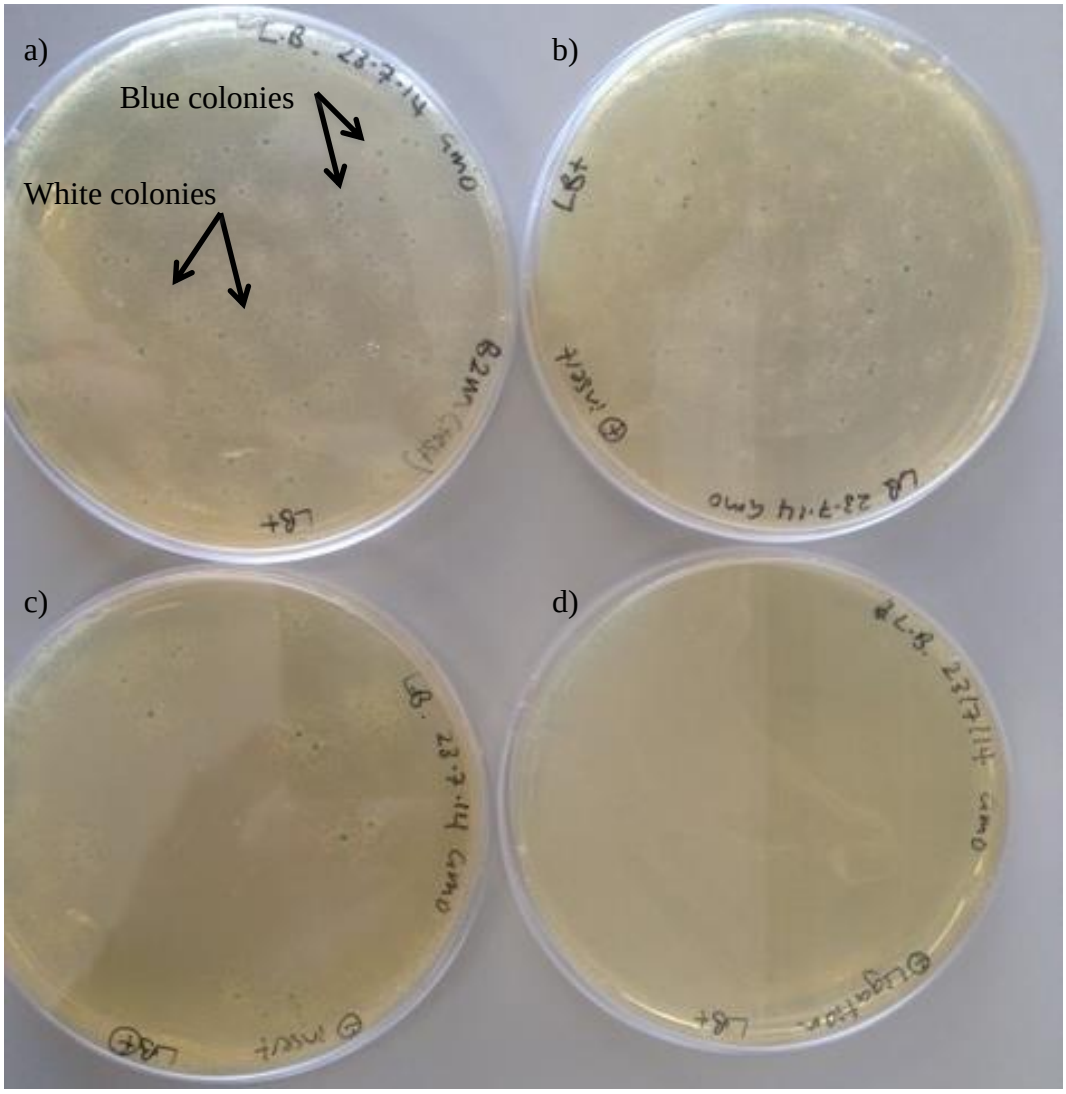

Figure 40: Blue/White Colony Screening of Transformed DH5α *E. coli* with Ligated Vector Containing Purified *β2m* Insert. After spreading the colonies onto LB+ agar plates containing XGal and IPTG and incubating overnight, the agar plates displayed the following: a) *β2m* insert displayed a large number of blue and white colonies, b) the positive insert displayed a large number of blue and white colonies, c) the negative control displayed blue and white colonies but considerably less than the previous plates and d) the positive transformation control displayed a large number of white colonies.

Due to the large number of colonies that grew on all plates, the volume of transformed cells spread onto the agar plates for the remaining PCR inserts to be cloned was reduced from 100 µL to 50 µL and plated out in 1:10 and 1:100 dilutions. This allowed a single colony to be selected more easily as well as allowing more accurate counting of cells.

3.5.3 Colony PCR

Following blue/white colony screening, individual colonies were selected for colony PCR with the M13 primers so as to confirm presence of the vector containing the *β2m* insert. The M13 primers targeted a 178 bp sequence in the pLUG-Prime® Cloning Vector. Therefore, with the *β2m* PCR product inserted, the expected product would be 282 bp. Figure 37 showed that the one of the ten white colonies tested contained the cloning vector of the expected size. The other colonies were likely false positives where self-ligation of the vector had occurred.

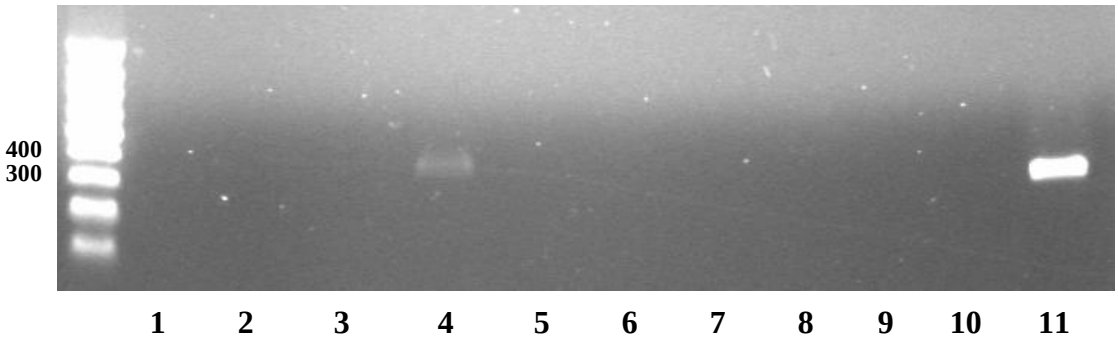

Figure 41: Gel Electrophoresis Image of *β2m* Colony PCR. Ten colonies from the *β2m* ligation were selected for colony PCR from the blue/white colony screening, with one positive ligation control colony. The plasmid DNA was visualised in a 1% agarose gel made with 1X TAE and stained with EtBr (0.25 µg/mL). Electrophoresis was carried out at 90V for 30 minutes. Lane 4 shows the presence of a single band at the expected size of 282 bp. Lane 11 shows a single band for the positive ligation control containing *VMO1* insert at the expected size of 354 bp.

3.5.4 Plasmid DNA Extraction

Colonies testing positive for the cloned vector were grown overnight in LB+ media and plasmid DNA was extracted using a Zyppy™ Plasmid Miniprep Kit. The concentration and integrity of the extracted DNA was analysed using the Nanodrop 2000 Spectrophotometer. Plasmid DNA was analysed in duplicates to ensure accuracy of the spectrophotometer. DNA extracted from the *β2m* colonies produced ideal A_{260}/A_{280} and A_{260}/A_{230} ratios of 1.88 and 2.18, respectively. The plasmid DNA concentration was 100.9 ng/µL, producing a total yield of 3027 ng.

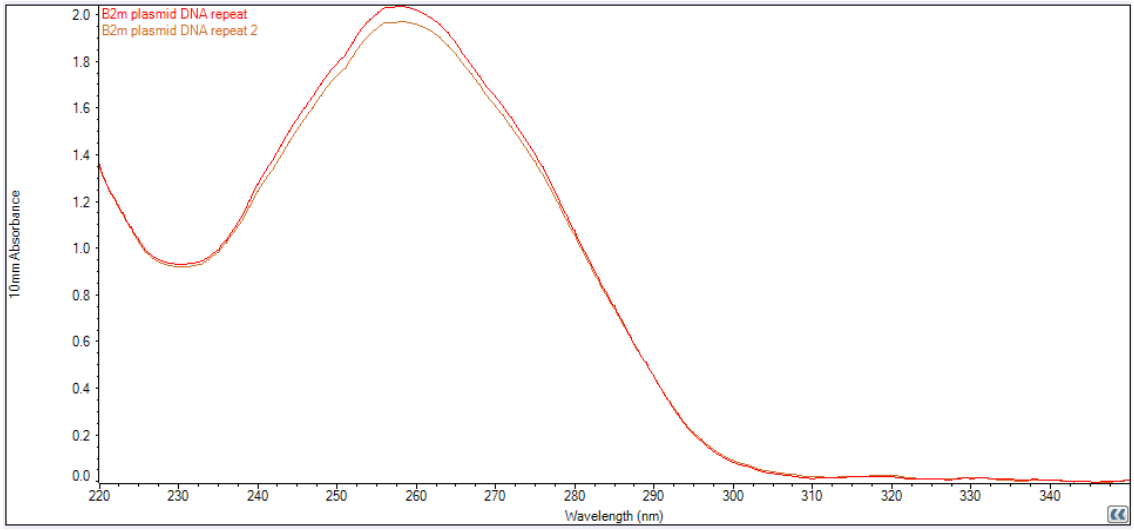

Figure 42: Absorbance Readings for *β2m* Plasmid DNA. The two absorbance readings displayed clear peaks at 260 nm. The reading at 260 nm allows calculation of the concentration of nucleic acid in the sample.

3.5.5 Restriction Digest of Plasmid DNA

For secondary validation that the *β2m* insert had been successfully ligated into plasmid DNA, a restriction digest with the HindIII and EcoRI restriction enzymes was carried out. The pLUG-Prime® Cloning Vector has both HindIII and EcoRI cut sites that fall before and after the *β2m* insert site, producing an expected product of approximately 300 bp. Initially, two restriction digests were carried out to include the plasmid DNA containing the *β2m* insert and a negative control of plasmid DNA with no restriction enzymes. The resulting products were electrophoresed and visualised under UV light (Figure 39). The plasmid DNA cut by the HindIII and EcoR1 enzymes resulted in fluorescent bands at the expected sizes of 2728 bp (cut plasmid DNA) and 282 bp (cut plasmid DNA containing vector with *β2m* insert). The negative control displayed three bands representing nicked, linear and supercoiled DNA.

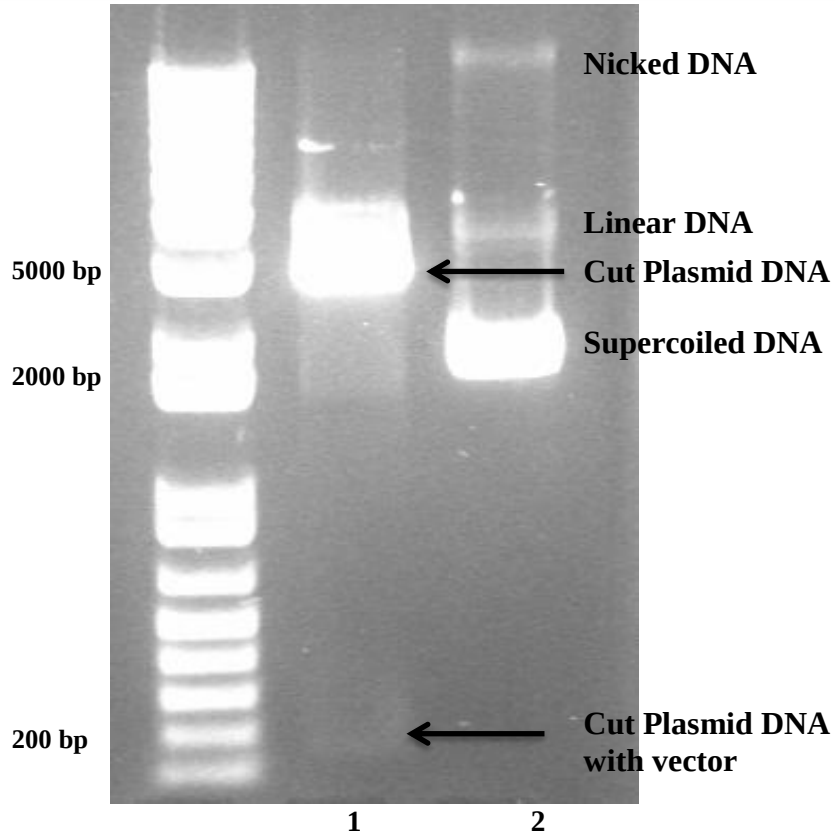

Figure 43: Gel Electrophoresis Image of Restriction Enzyme Digest. One microgram of *β2m* plasmid DNA was run in a restriction enzyme digest with HindIII and EcoR1 to cut the cloning vector. The resulting DNA was electrophoresed in a 2% agarose gel made with 1X TAE buffer and stained with EtBr (0.25 μg/mL) and compared with a 1 kB+ molecular ladder (Invitrogen™, USA). The gel was electrophoresed at 90V for 30 minutes. (1) Cut plasmid DNA at 282 bp and 2728 bp. (2) Undigested plasmid DNA with three bands representing the nicked, linear and supercoiled plasmid DNA.

In conclusion, the Nanodrop results indicate that a high purity and yield of plasmid DNA containing the *β2m* insert was achieved, and that the insert could be cut out of the plasmid using a double restriction digest. Therefore, this plasmid was sent to Waikato DNA Sequencing Facility (UoW, New Zealand) for DNA sequencing.

3.5.6 Sequencing Results

Plasmid DNA samples were sent to the Waikato DNA Sequencing Facility (UoW, NZ) for sequencing of the region targeted by the M13 primers, which contained

the PCR insert. All sequencing results were received in FASTA and ABD formats for analysis in Geneious (Version 7, 2014).

3.5.6.1 Sequencing Results for the *β2m* Insert

The *β2m* sequence targeted by M13 primers was aligned to the consensus *β2m* sequence (NM_009735.3) using Geneious (Version 7, 2014). The *β2m* sequence aligned 100% with the consensus nucleotide sequence (Figure 40).

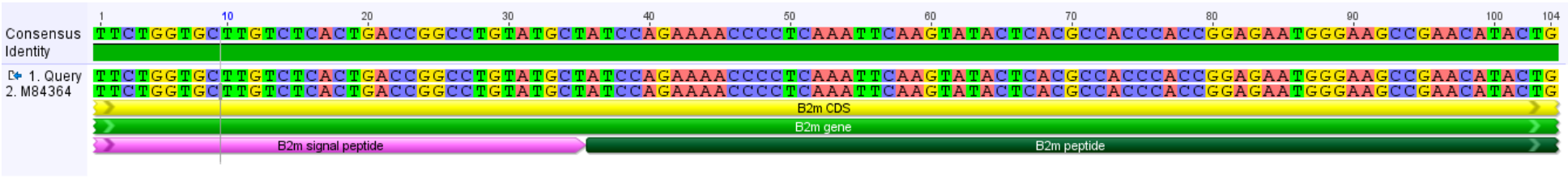

Figure 44: *β2m* Sequence Alignment. The *β2m* PCR product was ligated into a pLUG-Prime® Cloning Vector (Zymo Research, USA), grown up in competent DH5α *E. coli* cells and plasmid DNA was extracted to confirm the *β2m* nucleodtide sequence (Query), which aligned 100% to the consensus identity (NM_009735.3). The diagram also demonstrates that the targeted *β2m* sequence is within in ORF (yellow bar).

3.5.7 DNA Sequencing of Remaining Purified PCR Products

Following the success of *β2m* sequencing, ligation and transformation reactions were carried out with the remaining purified *Arc, Bdnf, Gjd2, Grin1* and *Gapdh* PCR products. Due to initial difficulty amplifying a single *CaMKIIα* product during qPCR, there was no purified *CaMKIIα* for sequencing purposes. The PCR products were ligated into individual pLUG-Prime© Cloning Vectors and initially produced colonies under blue/white colony screening. However, the transformation efficiencies were low (less that $1x10^4$ cfu/μg). Colony PCR indicated that several colonies analysed for each transformation contained the vector however, when selected for growth in LB+ media the colonies failed to grow or produced very low yields of DNA (30 – 40 ng/μL) after plasmid extraction. The ligation reactions had been stored at -20°C and were thawed on ice to trial transformation of chemically competent *E. coli* cells with 4 μL of vector, rather than the 2 μL previously used. When grown on an LB+ agar plate with XGal and IPTG for blue/white colony screening, the colonies indicated an improved transformation efficiency of approximately $1x10^6$ cfu/μg. Colonies were grown in LB+ media overnight before plasmid DNA extraction was carried out. The plasmid DNA samples had concentrations ranging from 30 - 134 ng/μL (Table 18).

Table 18: Inserted Sequence with Corresponding DNA Concentration and Absorbance Ratios for all Plasmid DNA Extractions.

Plasmid DNA (with insert)	**Concentration (ng/µL)**	**A_{260}/A_{230}**	**$A_{260}/_{280}$**
Arc	111	1.7	1.5
Bdnf	107	1.8	1.7
Gjd2	45	1.7	1.8
Grin1	134	1.8	2
β2m	101	2.1	1.9
Gapdh	30	2.1	2.5

Due to the low concentrations of plasmid DNA, the remaining *Arc, Bdnf, Gjd2, Grin1* and *Gapdh* DNA products were not digested with restriction enzymes, as it would require too large a quantity of DNA. Typically 500 ng is enough for checking most restriction digests on a gel however, most protocols advise at least 1 µg [87]. Instead, all products were electrophoresed in an agarose gel to confirm the presence of plasmid DNA (Figure 41). Each plasmid DNA product produced two bands; the brighter larger one representing supercoiled plasmid DNA and the smaller, less bright band representing circular, single-stranded plasmid DNA.

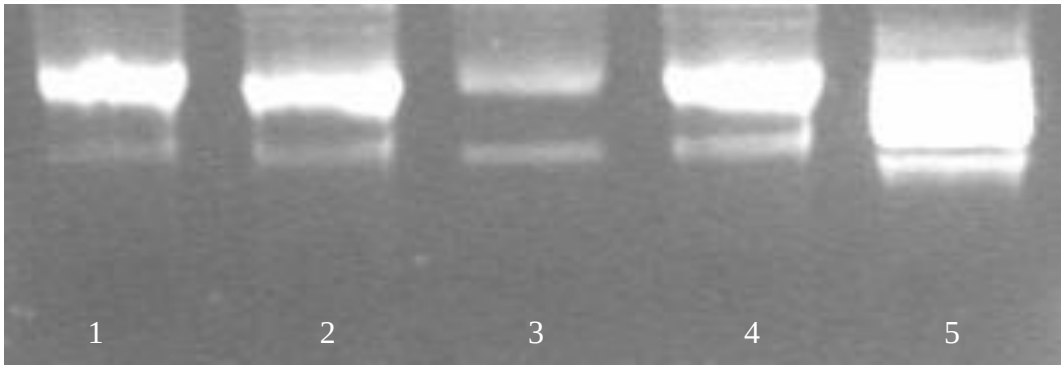

Figure 45: Gel Electrophoresis Image of Five Uncut Plasmid DNA Samples. 1) Plasmid DNA with *Arc* insert. 2) Plasmid DNA with *Bdnf* insert. 3) Plasmid DNA with *Gjd2* insert. 4) Plasmid DNA with *Grin1* insert. 5) Plasmid DNA with *Gapdh* insert. All plasmid DNA samples display a brighter, larger supercoiled plasmid DNA band and a smaller, less fluorescent single-stranded circular plasmid DNA band. The DNA ladder was removed from the image due to too large a quantity being loaded.

Once the presence of plasmid DNA was confirmed, all remaining plasmid DNA samples were sent to the Waikato DNA Sequencing Facility (UoW, NZ) for sequencing. Unfortunately, the resulting sequences did not have well defined peak resolution or uniform peak spacing and contained a large amount of background noise, similar to the original negative sequencing results. Therefore, optimisation of the plasmid DNA extraction was required to obtain higher yields of plasmid DNA for sequencing. The plasmid DNA extraction method was optimised further for sequencing of the purified *Arc, Bdnf* and *Gapdh* PCR products only.

3.5.7.1 Optimised Plasmid DNA Extraction and Sequencing Results for the Cloned *Arc, Bdnf* and *Gapdh* PCR Inserts

Following optimisation of the plasmid DNA extraction method (section 2.11.7), higher yields of plasmid DNA ranging from 156 – 185 ng/µL were obtained (Table 19) and subsequently sent to the Waikato DNA Sequencing Facility (UoW, NZ) for sequencing.

Table 19: Concentration of Plasmid DNA Containing the *Arc, Bdnf* and *Gapdh* PCR Inserts. The optimised method for plasmid DNA extraction produced higher yields of plasmid DNA that were optimal for sequencing. Concentration and absorbance readings were measured using the Nanodrop 2000 Spectrophotometer.

Plasmid DNA (with insert)	**Concentration (ng/µL)**	**A_{260}/A_{230}**	**$A_{260}/_{280}$**
Arc	160	1.88	1.63
Bdnf	185	1.85	2.05
Gapdh	156	1.84	1.94

The vectors containing *Arc, Bdnf* and *Gapdh* sequences were targeted using the M13 primers. The resulting nucleotide sequences were aligned using Geneious (Version 7, 2014) and compared to the corresponding consensus sequence. The overlapping *Bdnf* sequence displayed 100% alignment with the consensus sequence (NM_007540.4). The sequencing image can be viewed in Appendix 8. The target *Arc* sequence was unable to be located within the sequenced plasmid DNA, which was also considerably shorter than previous sequences (approximately 350 bp compared to 600 – 700 bp). Therefore, a false positive may have occurred that led to sequencing of a self-ligated vector with no PCR insert. Sequencing of the plasmid DNA containing the *Gapdh* PCR insert failed, preventing alignment with the consensus sequence.

3.6 Quantitative PCR Analysis

Quantitative PCR was used to analyse the gene expression of *Arc, Bdnf, CaMKIIα, Gjd2* and *Grin1* in the mouse cortex between *t*=0 hour controls and *t*=2 hour and *t*=4 hour exposure to sevoflurane or propofol anaesthetics. Due to time constraints, the isoflurane exposure trials were not analysed by qPCR. *β2m* and *Gapdh* were the reference genes used as an internal control to normalise qPCR

results. Where the negative controls (-RT and NTC) produced any amplification, the data was not included and the experiment was repeated.

3.6.1 Testing of Reference Genes for qPCR Analysis

The MIQE guidelines recommend the use of at least two reference genes for normalisation of qPCR[78]. Primer sets targeting *Actβ*, *β2m*, *Gapdh*, and *HPRT1* had been used successfully in previous publications and were tested for efficiency in qPCR [72,75,81]. The *Actβ* primers proved too sensitive, often amplifying the negative control where other primers did not (section 3.4.1). This may have resulted from carry-over contamination during qPCR set-up or very high expression levels in mouse brain tissue. There was also difficulty in acquiring consistent amplification with the *HPRT1* primer set, which may have been due to SNPs or low expression levels in the mice tested. For these reasons, *HPRT1* and *Actβ* were not used as reference genes in qPCR. *β2m* and *Gapdh* were selected for their consistent amplification and efficiency in qPCR (Figure 42). Amplification data was displayed on a graph that plotted the level of fluorescence for each cycle of the qPCR reaction.

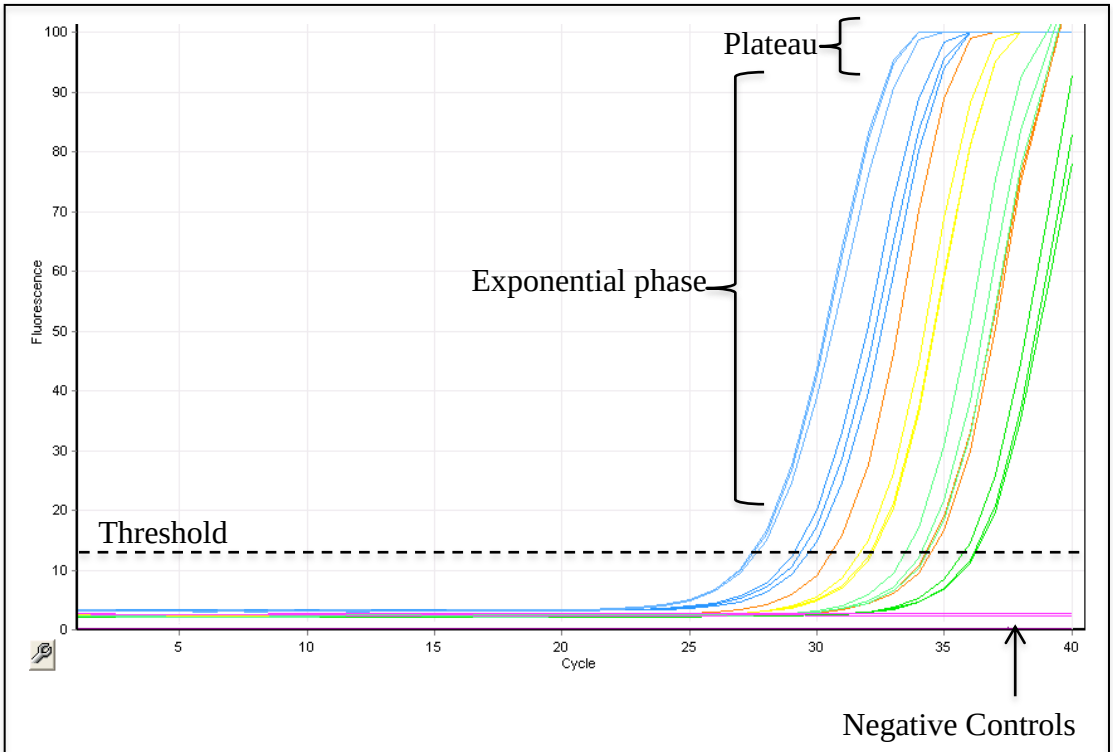

Figure 46: Amplification Plot on Logarithmic Scale. Signals that are detected above the threshold (dashed black horizontal line) are considered 'real' as they cross the C_T. Amplification plot displays signals from *β2m* (green), *Gapdh* (blue), *Gjd2* (orange) and *Grin1* (yellow). The increases in the number of DNA transcripts each cycle is shown by an increase in fluorescent signal during the exponential phase. The negative controls (pink line) did not display fluorescent above baseline levels, indicating the absence of any contamination.

Following completion of the qPCR assay, take off and amplification values derived from the amplification plots were entered into REST® (V2.0.13, 2009) to generate relative expression ratios for the individual GOIs. This data was displayed in whisker-box plots that showed the spread of expression data around the mean. Rotor-Gene™ 6000 software also produced melting curve profiles to validate the melting temperature of amplified products and reveal whether any non-specific amplification had occurred. All raw data is located on the accompanying disc in Appendix 9.

3.6.2 Melting Curve Profiles

Melting curve profiles and gel electrophoresis were used following qPCR to identify the melting temperature of amplified products and validate the specificity of qPCR amplification. The Rotor-Gene™ 6000 software generated melting curves for each set of primers by plotting the inverse of the difference in fluorescence divided by the difference in temperature (-dF/dT) against temperature (T) [88]. Melting peaks occurred at the equilibrium temperature for each duplex and a clear single peak was expected for each primer set. Initially, some non-specific amplification was observed (Figure 43). Therefore, the template dilution was adjusted from 1:20 to 1:5 and the annealing temperature was increased from 60 – 65 °C. Following optimisation, single, clear peaks were observed in the melt curve analysis (Figure 44).

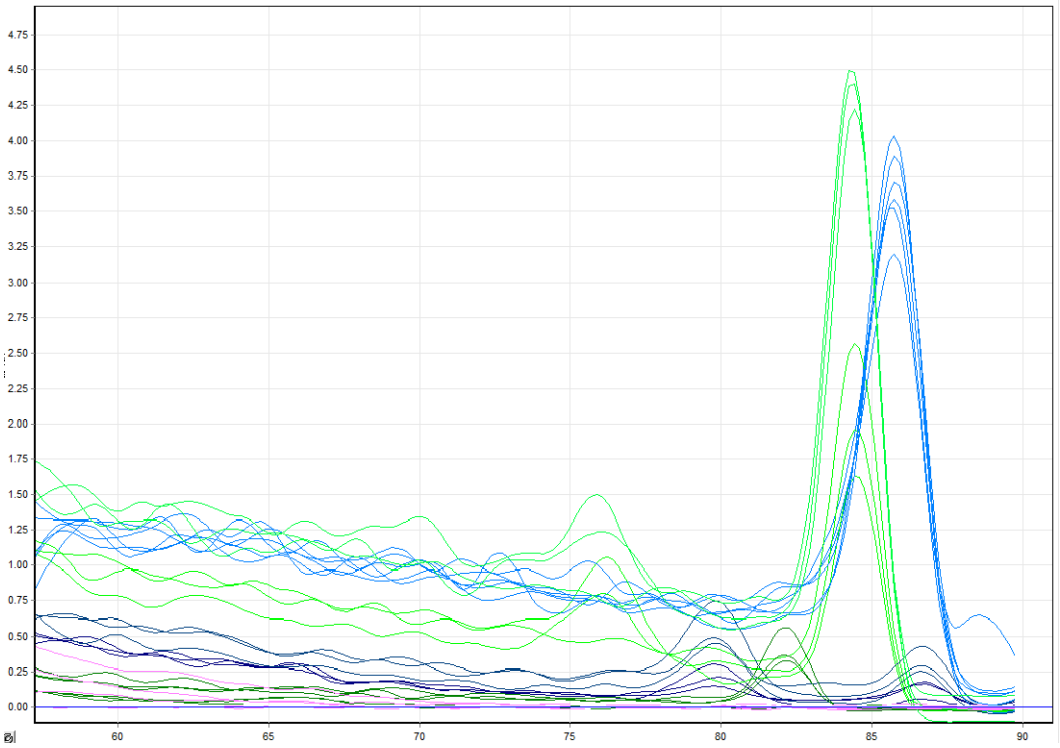

Figure 47: Melting Curve Analysis after Adjusting Template Concentration and Annealing Temperature. A) *β2m* amplification (light green) shows sharp peaks at 84°C but also shows smaller, less defined peaks at 76°C that may be indicative of non-specific amplification. *Arc* amplification (dark blue) also displayed peaks at both 79°C and 87°C. B) After changing the cDNA concentration from 1:20 to 1:5, non-specific amplification did not occur and single peaks were produced at the corresponding T_m.

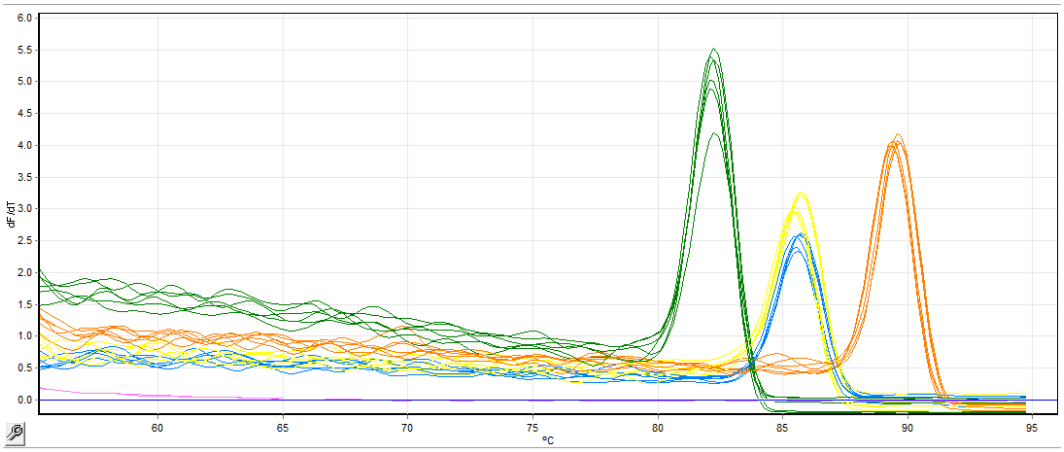

Figure 48: Melting Curve for *Bdnf, Gapdh, Gjd2* and *Grin1* Amplification. One defined peak was present for each amplified product. *Gapdh* (blue) and *Gjd2* (yellow) had a melting temperature of 86°C, *Grin1* (orange) was 89°C and *Bdnf* (green) was 83°C.

3.6.2.1 Multiple Melting Peaks for *Arc* Primers

Amplification of the *Arc* mRNA transcript during qPCR for the sevoflurane treatment produced two peaks at 80°C and 87°C. Agarose gel electrophoresis was carried out to analyse whether there was more than one product amplified during qPCR. The resulting gel electrophoresis image (Figure 45) indicated that there was an expected band at 104 bp and no genomic (or other) band was present at 349 bp.

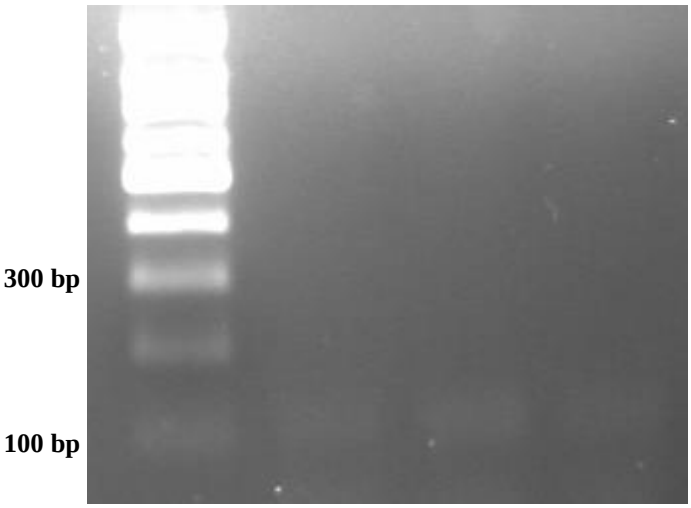

Figure 49: Gel Electrophoresis Image of *Arc* qPCR Products. The three replicative amplified *Arc* products were electrophoresed at 90V for 30 minutes in a 2% agarose gel made with 1X TAE and stained with EtBr (0.25 µg/mL) to confirm whether non-specific amplification was occurring during qPCR. The results indicated that the only the *Arc* PCR product at the expected size of 104 bp was amplified. There was no 349 bp band that would indicate gDNA contamination and no bands of any other size. The fluorescent bands are faint, possibly due to low levels of amplification.

3.6.2.2 Multiple Melting Peaks for *Bdnf* Primers

Two melting temperature of 66°C or 83°C were observed for *Bdnf* amplification however, each sample only showed a peak at either 66°C or 83°C, not both (Figure 46).

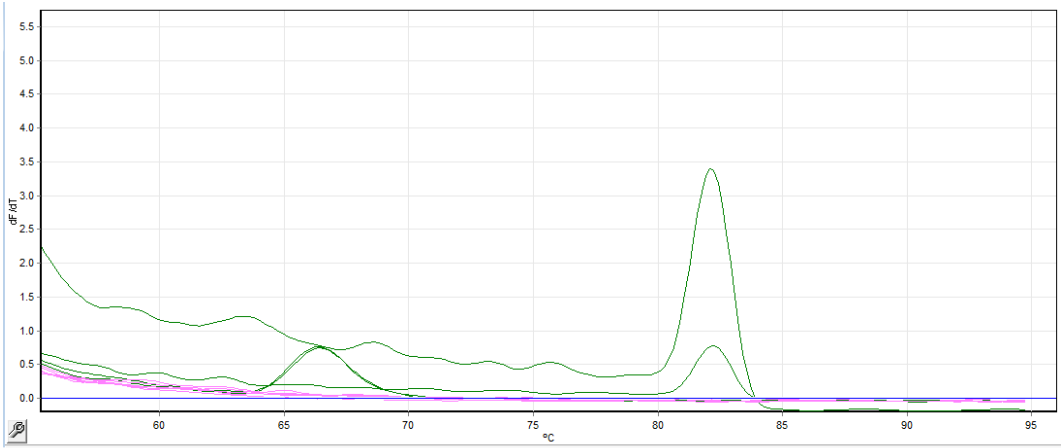

Figure 50: Melting Profile for *Bdnf* Amplification. The *Bdnf* primers produced amplified products that had T_m values of 66°C and 83°C. These qPCR products were analysed using gel electrophoresis to estimate the size of each product and exclude the possibility of non-specific amplification.

Three out of the four samples analysed using gel electrophoresis displayed fluorescent bands below the 100 bp molecular marker, with one sample displaying a fluorescent band at both the expected 103 bp size and one below the 100 bp marker (Figure 47). Due to their small size, the fluorescent bands visualised below the 100 bp molecular marker were likely a result of primer dimer formation. Primer dimers generally melt at a much lower temperature that the PCR product therefore, it was concluded that the melting peak at 66°C was the result of primer dimer formation.

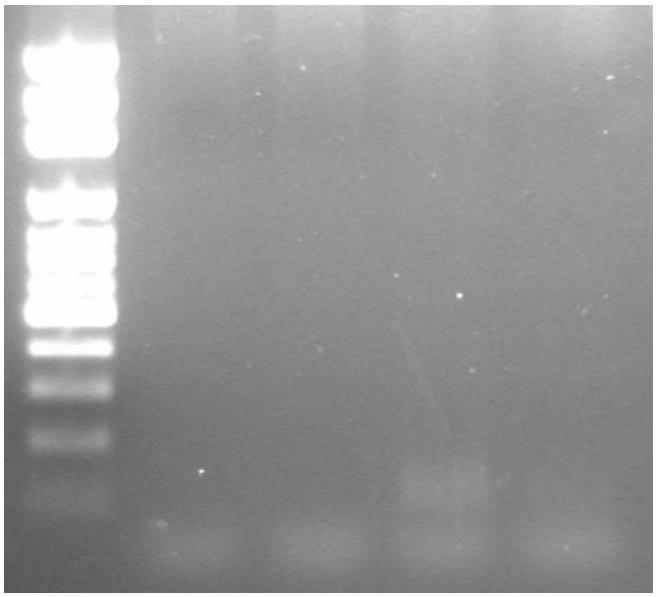

Figure 51: Gel Electrophoresis Image of Amplified *Bdnf* Products. Quantitative PCR products amplified by the *Bdnf* primers were electrophoresed at 90V for 30 minutes in a 2% agarose gel made in 1X TAE and stained with EtBr (0.25 μg/mL) to estimate product size against a 100 bp molecular ladder (GenScript™, USA). All samples displayed bands below the 100 bp marker that were likely indicative of primer dimer formation. Lane 3 displayed an additional band at the expected size of 103 bp.

3.6.2.3 Multiple Melting Peaks for *CaMKIIα* Primers

Two melting peaks at 64°C and 87°C were also observed for amplification with the *CaMKIIα* primers. Gel electrophoresis indicated that fluorescent bands were present at the expected size of 150 bp and also at approximately 1750 bp (Figure 48).

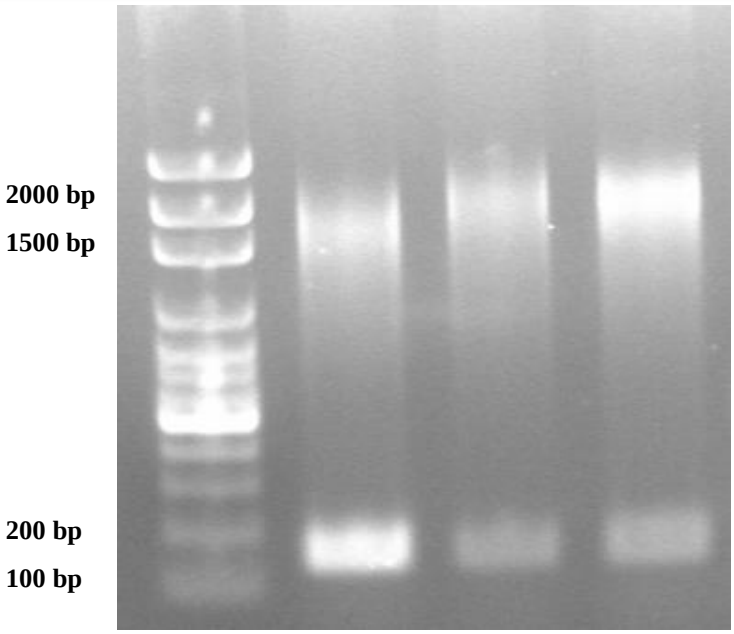

Figure 52: Gel Electrophoresis Image of Amplified *CaMKIIa* Products. Three *CaMKIIa* qPCR products were electrophoresed at 90V for 30 minutes in a 2% agarose gel made with 1X TAE and stained with EtBr (0.25 µg/mL) to analyse PCR product size and primer specificity. The primers had produced the expected 150 bp product as well as a product approximately 1750 bp in length. Bioinformatic analyses were carried out to identify the second, larger qPCR product.

3.6.3 Actual Melting Temperatures

Melting temperatures for each target sequence were obtained from the melting curve profiles generated by Rotor-Gene™ 6000. The observed T_m for all primer sets is recorded is Table 20 and are consistently 5°C higher than the expected T_m.

Table 20: Primer Target Sequences and the Corresponding Melting Temperature. The melting temperature for each primer set was estimated according to the peak observed in melting curve profiles generated by Rotor-Gene™ 6000.

Primer Target	**Expected T_m (°C)**	**Actual T_m (°C)**
Arc	82	87
Bdnf	77	83
CaMKIIα	82	86
Gjd2	81	86
Grin1	85	89
β2m	79	84
Gapdh	80	86

3.7 Statistical Analysis of Relative Expression Data

Each anaesthetic experiment used n=12 animals: six controls and six treatments. Raw take-off and amplification data was entered into REST© and expression ratios were calculated relative to the control group and normalised to reference gene expression. The reaction efficiency (E) and p-values for all GOIs were key features for statistical risk analysis in this research. Examination of statistical significance (p<0.05) was done by a Pair Wise Fixed Reallocation Randomization Test© as previously described [86]. The results were displayed in a box and whisker format that conveyed data about the mean and upper and lower quartile ranges of the relative expression data. As the expression values are ratios, they often have lopsided ratios with greater variability in the upper quartile. The ratio populations are also subject to large and uneven variability, which better reflects characteristics of gene expression that would otherwise go unnoticed in bar graph visualisations. Even though a large spread of values is present in the upper

'whiskers' of all plotted data (Figures 49 – 52), the lower 'whiskers' are smaller and more stable. Therefore, statistically significant alteration of gene expression can still be concluded as the variances are found mostly on one side of the distribution.

3.7.1 Gene Expression Results for Four Hour Sevoflurane Exposure

The relative expression results for *Arc, Bdnf, CaMKIIα, Gjd2* and *Grin1* after exposure to sevoflurane are shown in Table 21. The *p*-values for the *Arc, CaMKIIα, Gjd2* and *Grin1* transcripts were 0.226, 0.131, 0.543 and 0.914, respectively. These values were higher than 0.05, allowing us to accept the null hypothesis (H_0) that there was no change in mRNA expression during exposure to the general anaesthetic, sevoflurane. Down-regulation of *Bdnf* mRNA transcripts between the t=0 hour control and t=4 hour sevoflurane treatment was observed, represented by a final *p*-value of 0.007. Replicate animals, triplicate samples and technical qPCR repeats provided a large data set for analyses and the Pair Wise Fixed Reallocation Test© showed that there was statistically significant down-regulation of *Bdnf* during exposure to sevoflurane. Therefore, the alternate hypothesis (H_1) was true for *Bdnf* expression after a four-hour exposure to sevoflurane. The expression ratios generated for the four hour sevoflurane treatment are displayed on a whisker-box plot (Figure 49).

3.7.2 Gene Expression Results for Four Hour Propofol Exposure

The relative expression results for *Arc, Bdnf, CaMKIIα, Gjd2* and *Grin1* after propofol treatment are shown in Table 22. The *p*-values for the *Bdnf, CaMKIIα, Gjd2* and *Grin1* transcripts were 0.880, 0.305, 0.885 and 0.717, respectively.

These values were higher than 0.05, allowing us to accept H_0 that there was no change in mRNA expression, compared to the reference genes, during a *t*=4 hour exposure to propofol. However, up-regulation of *Arc* mRNA was also observed, represented by a final *p*-value of 0.000. A *p*-value of zero is not theoretically possible however, REST© did not display more than three decimal places and this was unable to be modified. Therefore, we were unable to view the final *p*-value past three decimal places. Statistical analyses carried out by REST© did produce a final result of "up-regulated" for *Arc* expression. It was concluded that the actual *p*-value was less than 0.001, therefore the alternate hypothesis (H_1) was true for *Arc* expression after a four-hour exposure to propofol. Replicate animals, triplicate samples and technical qPCR repeats provided a large data set for analyses and the Pair Wise Fixed Reallocation Test© showed that there was statistically significant up-regulation of *Arc* during exposure to propofol. The expression ratios generated from the take-off and amplification values for this treatment are displayed on a whisker-box plot (Figure 50).

3.7.3 Quantitative PCR for Two Hour Drug Exposure

To further validate our results, qPCR was carried out with cDNA from *t*=2 hour time point of the drug exposures. Only *Arc, Bdnf* and the reference genes *β2m* and *Gapdh* were analysed as previous results showed there was no change in expression of *CaMKIIα, Gjd2* or *Grin1* at *t*=4 hour.

3.7.3.1 Gene Expression Results for Two Hour Exposure to Sevoflurane

Quantitative PCR was carried out to analyse the expression of *Arc* and *Bdnf* after a *t*=2 hour exposure to sevoflurane and used for comparison with the *t*=4 hour

data. The relative expression results confirmed that *Bdnf* was also down-regulated at *t*=2 hour, represented by a *p*-value of 0.000 (Table 23). Replicate animals, triplicate samples and technical qPCR repeats provided a large data set for analyses and the Pair Wise Fixed Reallocation Test© showed that there was statistically significant down-regulation of *Bdnf* following exposure to propofol ($p<0.05$). *Arc* expression was unchanged during this treatment. Therefore, the alternate hypothesis (H_1) was true for *Bdnf* expression after a two-hour exposure to sevoflurane. The expression ratios generated from the take-off and amplification for treatment are displayed on whisker-box plots (Figure 51).

3.7.3.2 Gene Expression Results for Two Hour Exposure to Propofol

Quantitative PCR was carried out to analyse the expression of *Arc* and *Bdnf* after a *t*=2 hour exposure to propofol and used for comparison with the *t*=4 hour results. The relative expression results indicated that *Bdnf* was down-regulated after a two hour exposure to propofol, represented by a *p*-value of 0.001 (Table 24). Replicate animals, triplicate samples and technical qPCR repeats provided a large data set for analyses and the Pair Wise Fixed Reallocation Test© showed that there was statistically significant down-regulation of *Bdnf* during exposure to sevoflurane ($p<0.05$). *Arc* expression was unchanged during this treatment. Therefore, the alternate hypothesis (H_1) was true for *Bdnf* expression after a two hour exposure to sevoflurane. The expression ratios generated from the take-off and amplification for treatment are displayed on a whisker-box plot (Figure 52).

Table 21: Statistical Data From Quantitative PCR Analysis of Four-Hour Exposure to Sevoflurane. The results demonstrated down-regulation of *Bdnf* expression, represented by a *p*-value of 0.007. There was no change in the expression of target genes *Arc, CaMKIIα, Gjd2* or *Grin1*.

Gene	***p*-value**	**Normalised Result**
Arc	0.226	No change
*Bdnf**	0.007	Down-regulated
CaMKIIα	0.131	No change
Gjd2	0.543	No change
Grin1	0.914	No change

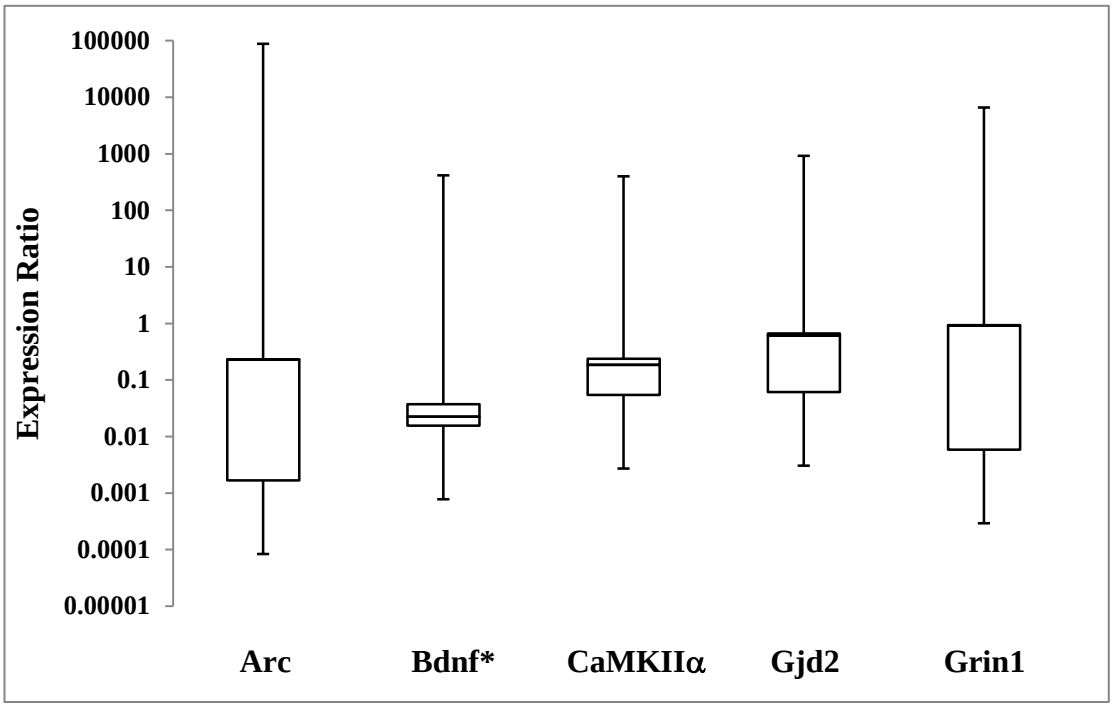

Figure 53: Whisker-Box Plot Representing the Spread of Statistical Data from Sevoflurane Treatment at Four Hours. *Bdnf* gene expression was down-regulated after a four hour exposure to sevoflurane while there was no change observed for *Arc, CaMKIIα, Gjd2* or *Grin1* expression. The whisker-box plot reports the mRNA expression ratio on the *y*-axis of given genes denoted in the *x*-axis. Relative expression data for *Arc, Bdnf, CaMKIIα, Gjd2* and *Grin1* mRNA transcripts was generated by REST® (V2.0.13, 2009). When $p<0.05$, the null hypothesis that gene expression had not changed in response to anaesthetic exposure was rejected.

Table 22: Statistical Data From Quantitative PCR Analysis of Four-Hour Exposure to Propofol. The results demonstrated up-regulation of *Arc* expression, represented by a *p*-value of 0.000. Although it is not theoretically possible to have a *p*-value of zero, the REST© software did not provide more than three decimal places. There was no change in the expression of target genes *Bdnf, CaMKIIα, Gjd2* or *Grin1*.

Gene	***p*-value**	**Normalised Result**
*Arc**	0.000	Up-regulated
Bdnf	0.880	No change
CaMKIIα	0.305	No change
Gjd2	0.885	No change
Grin1	0.717	No change

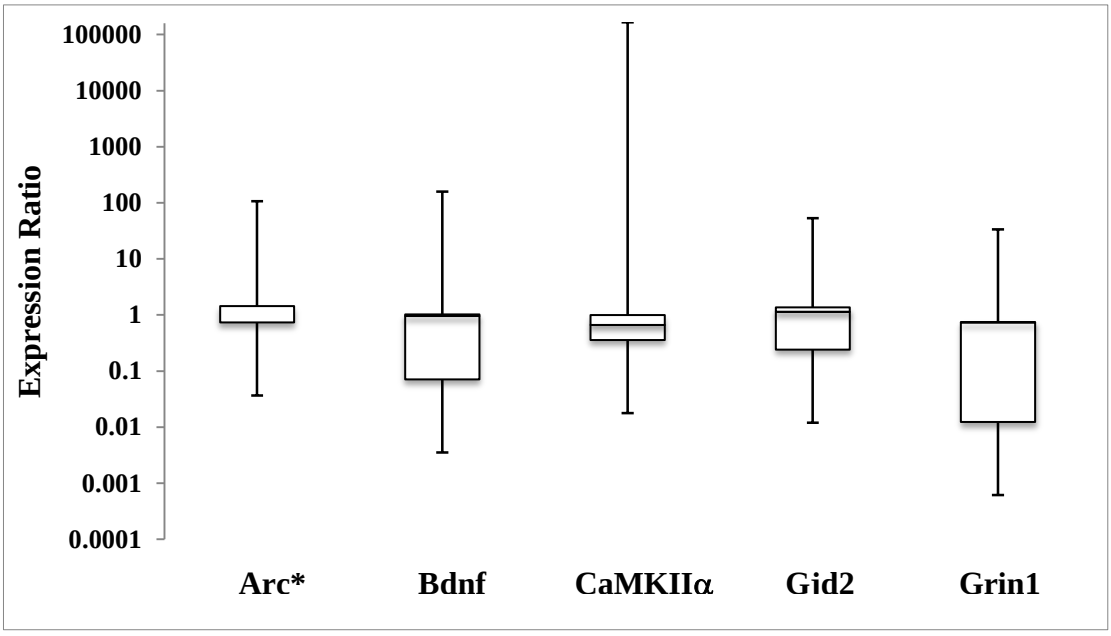

Figure 54: Whisker-Box Plot Representing Spread of Statistical Data from Propofol Treatment at Four Hours. *Arc* gene expression was up-regulated after a four hour exposure to propofol while there was no change observed for *Bdnf, CaMKIIα, Gjd2* or *Grin1* expression. The whisker-box plot reports the mRNA expression ratio on the *y*-axis of given genes denoted in the *x*-axis. Relative expression data for *Arc, Bdnf, CaMKIIα, Gjd2* and *Grin1* mRNA transcripts was generated by REST® (V2.0.13, 2009).

Table 23: Statistical Data From Quantitative PCR Analysis of Two-Hour Exposure to Sevoflurane. The results demonstrated down-regulation of *Bdnf* gene expression, represented by a *p*-value of 0.000. Although it is not theoretically possible to have a *p*-value of zero, the REST© software did not provide more than three decimal places. There was no change in the expression of *Arc*. The target genes *CaMKIIα, Gjd2* and *Grin1* were not analysed at the two-hour time point.

Gene	***p*-value**	**Normalised Result**
Arc	0.556	No change
*Bdnf**	0.000	Down-regulated

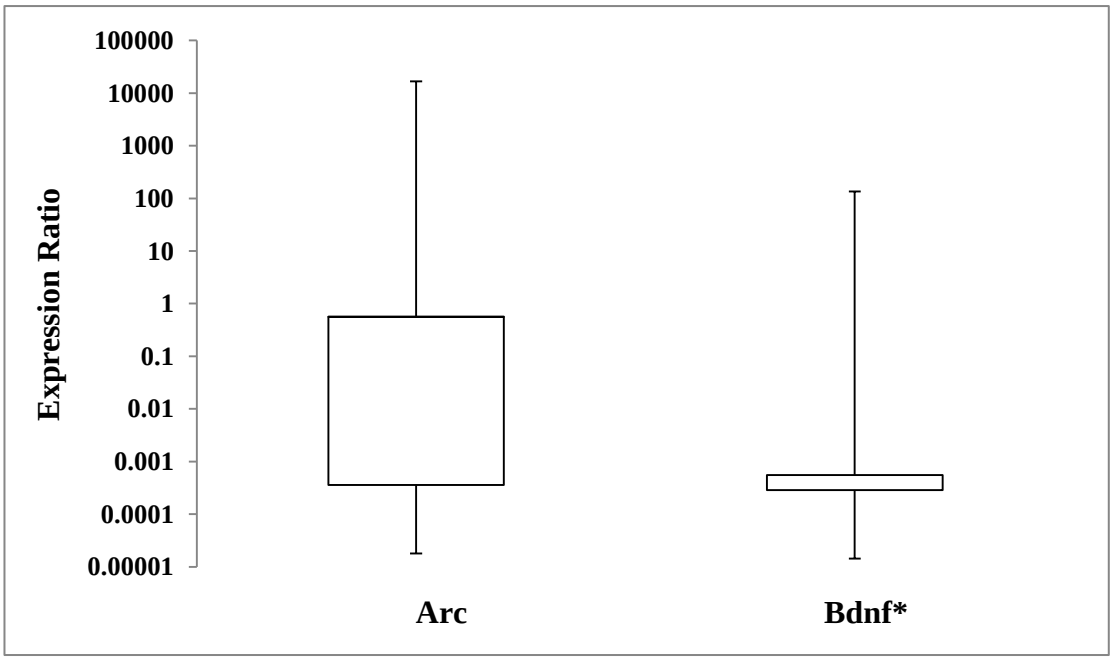

Figure 55: Whisker-Box Plot Representing the Spread of Relative Expression Data for Sevoflurane Treatment at Two Hours. *Bdnf* gene expression was down-regulated after a two hour exposure to propofol, while there was no change observed for *Arc, CaMKIIα, Gjd2* or *Grin1* expression. The whisker-box plot reports the mRNA expression ratio on the *y*-axis of given genes denoted in the *x*-axis. Relative expression data for *Arc, Bdnf, CaMKIIα, Gjd2* and *Grin1* mRNA transcripts was generated by REST® (V2.0.13, 2009).

Table 24: Statistical Data From Quantitative PCR Analysis of Two-Hour Exposure to Propofol. Statistical Data From Quantitative PCR Analysis of Two-Hour Exposure to Sevoflurane. The results demonstrated down-regulation of *Bdnf* gene expression, represented by a *p*-value of 0.001. There was no change in the expression of *Arc*. The target genes *CaMKIIα, Gjd2* and *Grin1* were not analysed at the two-hour time point.

Gene	***p*-value**	**Normalised Result**
Arc	0.303	No change
*Bdnf**	0.001	Down-regulated

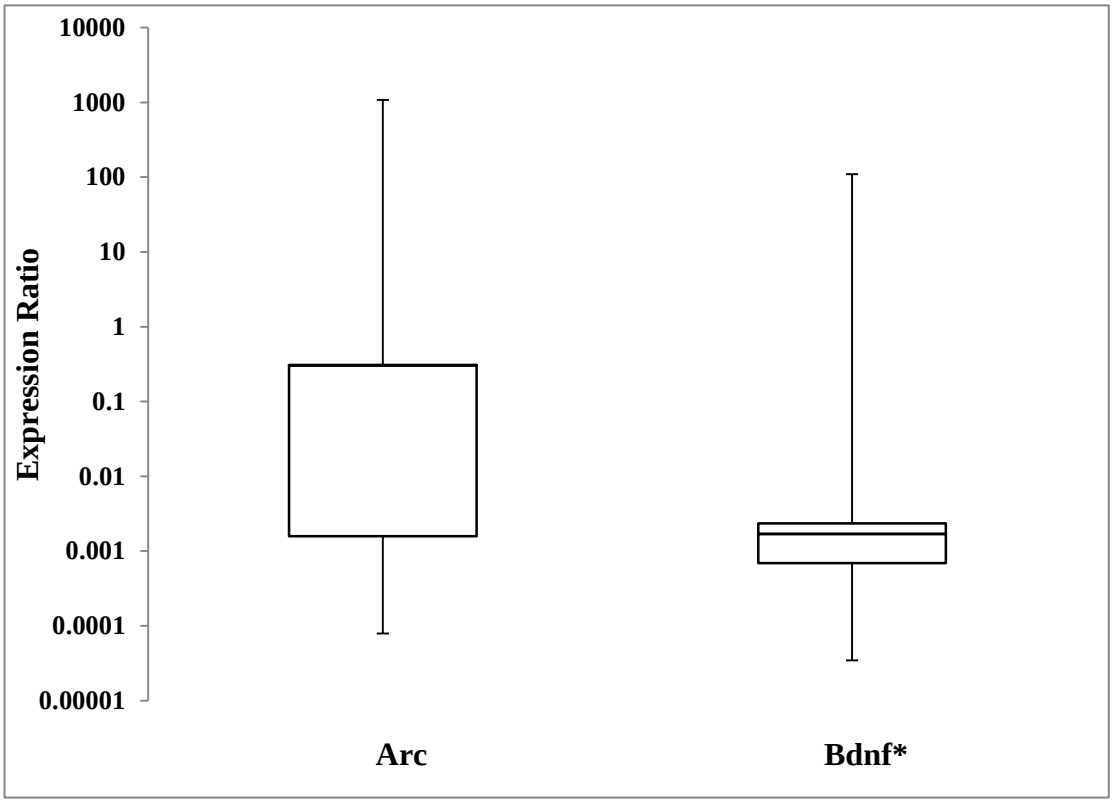

Figure 56: Whisker-Box Plot Representing the Spread of Relative Expression Data for Propofol Treatment at Two Hours. *Bdnf* gene expression was down-regulated after a two hour exposure to propofol, while there was no change observed for *Arc, CaMKIIα, Gjd2* or *Grin1* expression. The whisker-box plot reports the mRNA expression ratio on the *y*-axis of given genes denoted in the *x*-axis. Relative expression data for *Arc, Bdnf, CaMKIIα, Gjd2* and *Grin1* mRNA transcripts was generated by REST® (V2.0.13, 2009).

Chapter Four

Discussion

The aim of this research was to investigate the effects of three commonly used general anaesthetics on the expression of five memory-related genes in the cerebral cortex of mice. The memory-related genes selected for this research were *Arc, Bdnf, CaMKIIα, Gjd2* and *Grin1*. An *in vivo* mouse model was used for two and four hour exposures to anaesthetic agents. Real-time qPCR was the method used to analyse mRNA expression and statistical analysis of the resulting data was carried out using REST© (V2.0.13, 2009). Our hypothesis stated that genes with memory-related function would change in response to a clinical dose of general anaesthetic.

4.1 Experimental Set Up for Anaesthesia

The volatile and IP anaesthetics used in this research required different experimental set-ups due to the nature of administration. However, attempts were made to reduce variation between these experiments. For example, all experiments were conducted at the same time of day to reduce temporal variation. The animals were anaesthetised in animal chambers, which were kept under a heat lamp to provide a warmer environment for the mice after observing behaviour in the first experiment that indicated they were too cold. The sample number of animals for each treatment was twelve (n=12), which was carried out in three replicate experiments. Each replicate consisted of a t=0 hour control, t=2 hour treatment, t=4 hour control and t=4 hour treatment.

4.1.1 Sevoflurane Exposure Trials

Sevoflurane is a volatile anaesthetic that was administered to the animals via inhalation. The *t*=0 hour control animal was euthanased immediately and the *t*=4 hour control animal was held in a separate animal chamber to the treatment mice for the duration of the experiment. The *t*=2 hour and *t*=4 hour anaesthetic treatment mice were held in an animal chamber in which the sevoflurane was injected into. It took approximately two minutes for the animals to become completely anaesthetised, which was monitored by analysing their inability to correct themselves when placed on their backs. The CO_2 and sevoflurane gas levels were monitored every ten minutes to ensure the CO_2 did not exceed 5% and to record the sevoflurane levels. All animals for the sevoflurane treatment followed a similar trend, requiring a half dose of sevoflurane at approximately the two and three hour time points (section 3.1.1).

4.1.2 Intraperitoneal Propofol Exposure Trials

The initial dose of propofol administered to the *t*=2 hour and *t*=4 hour mice was calculated based on the animals' weight and administered to the IP cavity. Similar to the sevoflurane treatment, the *t*=0 hour control was euthanased immediately. The *t*=4 hour control was administered an equivalent dose of the intralipid vehicle that the propofol was contained in and held in a separate chamber throughout the duration of the experiment. During the anaesthetic exposure, it was observed that propofol wore off much faster than sevoflurane. It was also highly variable between mice and required close monitoring for administration of further doses (section 3.1.2). The initial dose lasted approximately 25 minutes, with subsequent doses varying between five and 25 minutes in duration between mice in the initial experiment. The "top-up" doses were adjusted to 0.15 mL for experiments two

and three, which lasted 25 minutes initially but gradually decreased down to ten minutes.

In conclusion, there were difficulties administering and maintaining a consistent and predictable dose of IP anaesthetic to the mice used in this research. The initial dose of propofol administered was 100 mg per kg of body weight however, the "top-up" doses were an estimation loosely based on the relative amount of volatile anaesthetic previously used. This resulted in a variation of responses from the animals and a somewhat inconsistant dose of propofol. Therefore, an optmised method for administration of IP anaesthetic is required before further research can be carried out. The most effective means of maintaining a controlled dose of anaesthetic would be through the use of an intravenous drip. Unfortunately this would require constant restraint of the mice, which would likely result in elevated levels of stress. Similarly, the control animal would also have to be restrained. Thus, the most effective outcome would result from identifying an optimal initial and "top-up" dose for mice. Our recommendation would be to trial 0.2 mLs for the "top-up" doses or investigate alternative methods of IP administration, which are discussed in more detail in the next section.

4.1.2.1 Alternative Intraperitoneal Administration Methods

In order to administer a more controlled dose of IP anaesthetic, other approaches such as an indwelling catheter or implantable pumps should be investigated. An indwelling catheter is a tubular device that allows prolonged infusion of drugs into a body cavity, such as the IP cavity [89]. Although an indwelling catheter would provide a cost-effective and reliable method for prolonged and controlled drug

delivery, they may result in local or system infections due to disruption of epidermal integrity [89]. Alternatively, an implantable pump such as the iPRECIO® fusion pump could be used to administer propofol. The iPRECIO® fusion pump is an implantable and refillable device that can be implanted subcutaneously in laboratory animals such as mice and rats [90]. The implant removes the need for animal restraint and allows full control over drug dosage. Over 12,500 published studies have demonstrated that implantable pumps provide reliable delivery of a wide range of compounds [91]. Therefore, our recommendation is to trial the iPRECIO® fusion pump for future experiments that require administration of IP anaesthetics.

4.2 RNA Analysis

Accurate qualification and quantification of RNA was important to ensure an acceptable quality and concentration of RNA was present across all RNA samples extracted from mouse brain tissue. Ribonucleases (RNases) rapidly degrade RNA and are one of the major issues affecting RNA integrity [92]. These enzymes are found in both eukaryotes and prokaryotes and can be dispersed throughout the air and secreted from the human body [92]. RNases are extremely resilient and can remain active at pH 2 – 10, extreme temperatures ranging from 15 – 80°C and boiling for 30 minutes [92]. Contamination of RNA samples by RNases can compromise later analyses; therefore precautions must be taken to prevent degradation of RNA [92]. The Nanodrop 2000 spectrophotometer was initially used to analyse the concentration and A_{260}/A_{280} and A_{260}/A_{230} absorbance ratios of all RNA samples. To further validate RNA integrity, the RNA samples were also

electrophoresed in a denaturing formaldehyde agarose gel to visualise the 28S and 18S rRNA bands and ensure that a similar concentration was present across all samples. The use of formaldehyde in the agarose gel denatured secondary structure of RNA, which allowed for accurate analysis of the rRNA bands. Failing adequate visualisation of some of the RNA samples in a denaturing formaldehyde gel, samples were run in a non-denaturing agarose gel to confirm the 28S and 18S rRNA bands were present.

4.2.1 Spectrophotometer Analysis

The concentration (ng/μL) and absorbance ratios (A_{260}/A_{280} and A_{260}/A_{230}) of all RNA samples was analysed using the Nanodrop 2000 spectrophotometer. The absorbance maxima for nucleic acids is 260 nm and the absorbance ratios indicate the nucleic acid purity [79]. Ratios that fall close to 2.0 for A_{260}/A_{230} and 2.2 for A_{260}/A_{280} are accepted as "pure" for RNA. Absorbance at 230 nm is also measured to provide an indication of other potential contaminants such as proteins or phenol, which will produce sharp absorbance peaks at 230 nm [79]. Eleven RNA samples extracted (I3T2, I4T2, C1T0, C1T4, C3T4, P1T0, P1T4T, P1T4C, P1T4T, P3T0 and P3T2) out of a total 36 displayed A_{260}/A_{280} ratios lower than 1.8, ranging from 0.6 – 1.58. No samples were higher than 2.0. The low A_{260}/A_{280} ratios were likely caused by residual phenol from the TRI Reagent® used in the RNA extraction protocol. Therefore, the RNA extraction protocol needs optimising to reduce the residual phenol that remained in RNA samples. To confirm that the RNA samples would be of good quality for downstream applications, including qPCR, they were analysed using gel electrophoresis. All RNA samples were electrophoresed in a denaturing formaldehyde gel to confirm the presence of clear 28S and 18S rRNA bands.

4.2.1.1 Contamination of RNA

The RNA samples I3T2, I4T2, C1T0, C1T4, C3T4, P1T0, P1T4T, P1T4C, P1T4T, P3T0 and P3T2 all displayed A_{260}/A_{280} ratios lower than 1.8, ranging from 0.6 – 1.58. No samples were higher than 2.0. A low A_{260}/A_{280} ratio was likely caused by residual phenol from the TRI Reagent® used in the RNA extraction protocol. Low A_{260}/A_{280} ratios can also be caused by very low concentrations of nucleic acids (<10 ng/μL). However, the lowest concentration of RNA extracted was 264.7 ng/μL. The RNA sample A2T4C had an A_{260}/A_{230} ratio significantly lower than the acceptable range, giving a reading of 1.48. The low value is also indicative of phenol contamination from the RNA extraction. Therefore, the RNA extraction protocol needs optimising to reduce the residual phenol that remained in RNA samples. Usually, a 75% ethanol wash can be added to at the end of an extraction to improve the overall quality of an RNA sample for absorbance readings, however our extraction protocol already included an ethanol wash [93]. We recommend adding an extra ethanol wash and/or an extra chloroform extraction step to aid in isolation of more pure RNA. To confirm that the RNA samples would be of good quality for downstream applications, including qPCR, they were also analysed using gel electrophoresis. All RNA samples were electrophoresed in a denaturing formaldehyde gel to confirm the presence of clear 28S and 18S rRNA bands.

4.2.2 Denaturing Gel Electrophoresis

The sevoflurane-treated RNA samples were electrophoresed in a 1% agarose gel made with 5X MOPS buffer with added formaldehyde. Although the fluorescence of the 28S band was not twice that of the 18S band, both displayed clearly separated fluorescent bands. The RNA molecular ladder used for estimation of

RNA size was run at the recommended quantity of 3 μg. However, the resulting bands were overly fluorescent and the individual molecular markers were unable to be clearly visualised. Two micrograms of the RNA molecular ladder was loaded in a subsequent gel but this also resulted in over-fluorescence and undefined molecular markers. Therefore, the RNA molecular ladder should be tested in a dilution series to determine an optimal loading concentration.

4.2.3 Denaturing Gel Electrophoresis Analysis of Propofol-Treated RNA

The propofol-treated RNA samples were also electrophoresed in a denaturing formaldehyde gel however; the rRNA bands were not clearly defined or separated. The electrophoresis of propofol-treated samples was repeated using twice the quantity of RNA (2 μg) but produced similar results, with unclear rRNA bands and large smear present towards the bottom of the gel image. The poor separation of rRNA may have been a result of poor quality reagents, such as the formaldehyde or MOPS. Due to the limited amount of RNA available (<25 μg), 2 μg of each propofol-treated RNA sample was electrophoresed in a standard non-denaturing gel. The samples were heat-denatured at a higher temperature of 85°C prior to electrophoresis and run at 50V for two hours. The 1X MOPS running buffer was regularly circulated to maintain an even ion balance. A standard 1 kB+ ladder was used for comparison of rRNA band size. The resulting image showed clearly defined rRNA bands with minimally degraded RNA. The 28S band was visualised at the correct estimated size of 4712 bp and the 18S at the correct estimated size of 1869 bp. The presence of clearly defined rRNA bands and ideal absorbance ratios allowed us to conclude that the RNA from both sevoflurane and propofol treatments was of good quality to use in downstream applications including qPCR. The results also showed that although heat

denaturation of RNA at 70°C for ten minutes was sufficient, an increased temperature 85°C demonstrated better separation of rRNA bands.

Negatively charged groups found in agarose polymers, such as pyruvte and sulphate, can create a flow of water in the opposite direction to the movement of DNA in a process called electroendosmosis (EEO) [93]. This movement can decelerate the movement of DNA, resulting in blurring of bands. EEO may have caused blurring of the RNA molecular ladder used in the denaturing gel electrophoresis that resulted in undefined molecular markers under UV visualisation. Low EEO agarose or low-melting point agarose can be used to reduce the occurance of EEO [93]. Additionally, reducing the agarose concentration from 1% to 0.5% may be sufficient for reducing the electroosmotic flow.

For an improved estimation of the concentration and integrity of RNA, other electrophoresis methods, such as the use of a TAE bleach gel, should be further investigated and they are described in more detail in the next section.

4.2.4 Bleach Gel Electrophoresis

Denaturing formaldehyde gel electrophoresis is a time-intensive procedure that requires the use of toxic reagents such as formaldehyde and formamide [92]. Aranda et al. (2011) describe the use of a TAE gel with added bleach (6% sodium hypochlorite) to denature the secondary structure of RNA through the destruction of hydrogen bonds. The results demonstrated the protective effects of bleach on RNA quality, with increasing rRNA band integrity occurring with increasing

bleach concentration (0.1 – 0.5%). This method did not require the addition of toxic reagents such as formaldehyde and minimised preparation and running time in comparison with the denaturing formaldehyde method. Therefore, the TAE bleach gel provides a much simpler method for RNA analysis and we recommend trialling this method for future RNA analysis. Time constraints and limited quantities of RNA did not allow this trial to be carried out during this research.

An alternative to this method and a more expensive option is the purcahse and use of an RNA analyser. The RNA analyser utilises parallel capillary electrophoresis (CE) to separate RNA, which is then detected using fluroescent light.

4.3 DNA Sequencing for Target Sequence Analysis

In order to validate amplification of the expected mRNA transcripts, individual PCR products were purified and inserted into a cloning vector. Chemically competent *E. coli* were transformed with the cloning vectors and grown for plasmid DNA extraction. Once the concentration and integrity of plasmid DNA had been confirmed, M13 primers were used to target the cloning vector in a sequencing reaction.

4.3.1 Ligation of Purified PCR Products into Cloning Vectors and Transformation of *E. coli*

In order to verify that the correct sequence was targeted and amplified by the primers during PCR analysis, individual PCR products were sequenced at the Waikato DNA Sequencing Facility (UoW, NZ). Due to the short length of the

PCR products (approximately 100 – 150 bp), they were ligated into cloning vectors to provide a larger template for sequencing.

4.3.2 Plasmid DNA Extraction

Plasmid DNA containing the cloning vector ligated with PCR insert was extracted from DH5α *E. coli* cultures using the Zyppy™ Plasmid Miniprep Kit. This kit was chosen as it provided a fast procedure for high quality, endotoxin-free plasmid DNA by utilising a modified alkaline lysis method that removed the need for culture centrifugation and resuspension steps. The kit stated that the purity of DNA obtained would be suitable for sequencing and stated a typical A_{260}/A_{280} of 1.8 and plasmid DNA yields of up to 25 μg. Initially, it was very difficult to obtain concentrations greater than 150 ng/μL (0.15 μg). This was considerably less than what was stated in the kit protocol. Therefore, the method was optimised using the troubleshooting guide provided with the kit.

4.3.2.1 Low DNA Yield

Growth culture conditions were optimised in order to increase the yield of DNA for each sample. LB was the culture medium recommended by the manufacturer and was used to grow all cultures in. Initially, 2 mL of LB^+ media was inoculated for growth of *E. coli* containing the cloning vector with PCR insert. In order to increase DNA yield, colonies were later inoculated in an increased volume of 10 mL LB^+ media. To enhance aeration, these cultures were split into two tubes to allow a 1:4 culture volume to air volume ratio and shaken overnight at 200 RPM. The increased volume did lead in an increase in DNA yield (156 - 185 ng/μL), however the DNA concentrations did not exceed a total of 0.2 μg. Pre-warming of

the lysis buffer and elution buffer was recommended in the troubleshooting guide, however this did not improve the DNA yield. Therefore, we recommend trialling a different miniprep extraction kit for any future work or upgrading to a midi-prep kit from the same supplier to increase plasmid DNA yield.

4.4 Sequenced PCR Products

The difficulty in optimising DNA extraction protocols led to a focus on sequencing the reference genes, *β2m* and *Gapdh*, and the target genes that had displayed altered gene expression during qPCR, *Arc* and *Bdnf*. The resulting *β2m* and *Bdnf* sequences showed good base-calling with clearly defined peaks and the target sequence was easily extracted and aligned 100% with the reference sequences (section 3.5.6).

4.4.1 Poor Quality DNA

The cloning vector containing the *Gapdh* insert continuously produced no signal during the sequencing reaction, resulting in failure to produce any chromatogram. Failed DNA sequencing reactions are commonly the result of poor quality DNA, especially when sequencing plasmid miniprep templates [94]. A final ethanol precipitation step on the kit-purified plasmid DNA has been recommended to improve the quality of the plasmid DNA template [94].

4.4.2 False Positive

The vector containing the *Arc* insert tested positive during colony PCR and growth subsequently occurred in LB+ media. However, the *Arc* target sequence was not present in the resulting nucleotide sequence. It is therefore likely that a

false positive occurred and a self-ligated cloning vector without the *Arc* insert may have been present in the plasmid DNA. Therefore, it is important to perform a restriction digest to confirm the PCR data. However, in these circumstances, the yield of DNA was not sufficient for this experimental analysis.

4.4.3 Other Sequencing Issues

Some initial plasmid DNA that was sequenced resulted in short reads of poorly resolved trace chromatogram peaks where separate peaks were unable to be defined. This is often the result of capillary overload, where samples with large amounts of other DNA, salts or proteins interfere with the sequencing reaction [94]. Additionally, some reads had weak signal traces with misshapen or secondary reads. This can result from a partially failed sequencing reaction or too little DNA template [94]. In conclusion, increasing the plasmid DNA yield and quality is crucial for obtaining quality sequencing data from remaining PCR fragments; *Arc, CaMKIIα, Gapdh, Gjd2* and *Grin1*. Currently, the laboratory are investigating the use of alternative commerical kits for plasmid DNA extraction.

4.5 Quantitative PCR Analysis

Quantitative PCR was carried out to measure the expression of *Arc, Bdnf, CaMKIIα, Gjd2* and *Grin1* mRNA transcripts that had been extracted from the cortical brain tissue of mice. The qPCR assay was performed using a Rotor-Gene® 6000 analyser and the corresponding software provided amplification data including amplification plots and melting curves.

4.5.1 Optimisation of Quantitative PCR Assay

Several issues arose during initial qPCR testing, including little to no amplification with some samples and contamination of the NTC controls. To overcome these issues, cDNA samples were diluted 1:20 in mQH_20 to prevent potential template inhibition. Additionally, the annealing temperature was raised from 60°C to 65°C to prevent non-specific amplification. Although these methods did produce good results, some experiments still indicated contamination of the NTC. Therefore, the stock solutions of mQH_20, TE buffer and all PCR tubes were autoclaved, all tips were replaced with new ones and primers were re-suspended in the new TE buffer. Following these actions qPCR contamination was eliminated, indicated by the failure of NTCs to amplify past baseline levels.

4.5.1 Internal Normalisation

A crucial part of qPCR analysis is the normalisation of results to an internal standard, such as reference genes [72,92]. Recently published MIQE guidelines have indicated that interpretation of qPCR results strongly relies on the normalisation of reference genes that are stably expressed in both normal and pathophysiological conditions [75,95]. These requirements may not always be met under all experimental conditions; therefore a standard procedure is to test a set of reference genes to determine which are most stable under specific experimental conditions [72,92]. Initially, *Actβ, β2m*, *Gapdh* and *HPRT1* were all tested for use as reference genes to normalise qPCR results.

4.5.1.1 Testing of *Actβ* for Internal Normalisation

The *Actβ* primer set used in this research had been previously validated by Wang et al. (2012) to show stable expression in mouse brain tissue. Although *Actβ*

showed good amplification in standard PCR, there were also a number of issues with amplification in NTC controls. This may have occurred due to contamination of primers or diluent solutions such as mQH_20, carryover contamination during set up of the qPCR assay or leakage of PCR product across wells during gel electrophoresis. Measures to eliminate contamination included replacing primer stock and diluent solutions with new, autoclaved solutions, using new tips and gloves, separating PCR tubes during set up and leaving blank wells between PCR products in the agarose gels. However, the contamination issues persisted and other primer sets were investigated.

4.5.1.2 Testing of *β2m* for Internal Normalisation

The *β2m* primer set had been previously validated by Rijn et al. (2014), who reported *β2m* to be among the most stable reference genes for qPCR. They demonstrated a reaction efficiency of 103.2% and an optimal T_m of 64°C. Gradient PCR with temperatures ranging from 55°C to 62°C was carried out to confirm amplification efficiency with the cDNA template and identify an optimal annealing temperature, which was important to ensure efficiency and reproducibility in qPCR assays. *β2m* amplified at all temperatures tested with no amplification observed in the negative controls.

4.5.1.3 Testing of *Gapdh* and *HPRT1* for Internal Normalisation

Gilsbach et al. (2006) demonstrated that the *Gapdh* and *HPRT1* primer sets showed stable expression in multiple areas of the mouse brain, including the cortex, making them ideal candidates for reference genes in this research. The *Gapdh* primer set produced good amplification during qPCR. *HPRT1* was not

tested in qPCR due to the difficulty gaining amplification in standard PCR. Further optimisation of the PCR conditions and testing with other cDNA templates is required to validate the *HPRT1* primers if they are to be used in further research.

4.5.2 Quantitative PCR Assay Conditions

The qPCR conditions (Table 16) used for all qPCR assays had been previously validated by Keiran Oxton (UoW, NZ; 2013). An additional final melt cycle at 80°C for ten seconds was added to melt out any primer dimers that may have formed during qPCR. Primer dimers can inhibit amplification of the cDNA template and can therefore interfere with accurate quantification [73,92]. Some primer dimerisation did occur during qPCR, which was confirmed using agarose gel electrophoresis (section 3.6.2). Further optimisation of primer design may be required to prevent primer dimerisation.

4.5.3 Melting Temperatures for Target Sequences

Amplification and product analysis are individual procedures that can occur simultaneously during qPCR with the addition of fluorescent dyes that are monitored after each cycle. Following quantitative amplification, it is important to verify that a single, specific PCR product was amplified for each set of primers. This has traditionally been carried out by loading PCR products onto agarose electrophoresis gels to separate the products according to size [96]. Staining with fluorescent dyes, such as EtBr, allows visualization of these products under a UV imager [93]. However, the fluorescent dyes used in qPCR assays, such as EvaGreen®, allow analysis of the oligonucleotide T_m by generating a curve that is obtained by monitoring the fluorescence of dsDNA fragments as they pass

through a product denaturation temperature [42,96]. The T_m value indicated the temperature at which 50% of the oligonucleotide and its complement were in duplex [17,96]. The shape of a melt curve is a function of the GC content, length of product and the sequence itself and can vary greatly between different PCR products [43,96]. The wide range of melting temperatures allows most PCR products to be differentiated by melting curves and also allows identification of nonspecific products, which usually have lower T_m than the expected product [17,96]. Therefore, fluorescence from the intended product can be distinguished from nonspecific amplification with better certainty using melting curves [17,96]. Melt curve analysis in qPCR removes the need for gel electrophoresis, unless certain amplification is in doubt.

4.5.3.1 Melting Temperature Results

The expected T_m for the target sequences of each primer pair was provided by IDT and recorded in Table 20 with the actual T_m observed during qPCR. Although the values were not exactly the same, the actual T_m of each target sequence was consistently 4 – 5 °C higher than the expected T_m. The concentration of components in the EvaGreen® HOT FIREPol master mix may have contributed to a higher T_m than expected from all target sequences.

4.5.4 Melting Curve Profiles from Quantitative PCR Analysis

Melting curves were analysed for each qPCR assay to validate specificity of sequence amplification. Initially, 2 µL of cDNA (diluted 1:20 with mQH_2O) was added to each 20 µL reaction for qPCR. However, the amplification was inconsistent, sometimes very low and some non-specific amplification occurred After decreasing the cDNA dilution concentration from 1:20 to 1:5, amplification

was much more consistent and single, sharp peaks were observed during melting curve analysis (section 3.6.2).

4.5.4.1 Analysis of Multiple Melting Peaks

Specific PCR products and any non-specific or gDNA amplification can be differentiated using melting curve analysis, where the shape of the melting curve is a function of GC content, length and sequence. Ideally, one single peak would be present for each set of primers to indicate amplification of a specific mRNA during qPCR. For all qPCR assays the *B2m, Gapdh, Gjd2* and *Grin1* primer sets amplified a single, specific mRNA sequence. However, the *Arc, Bdnf* and *CaMKIIa* primer sets produced two melting peaks on some occasions (section 3.6.2). However, the temperature at which PCR products melt can vary greatly and two melting peaks are not always indicative of two PCR products being amplified. In this case, gel electrophoresis was required to confirm whether non-specific amplification was occurring.

Agarose gel electrophoresis was carried out to analyse the amplified *Arc*, *Bdnf*, and *CaMKII*α qPCR products. The results indicated that there was no additional product present for *Arc*. The observed melting temperatures were 80°C and 87°C, which were very similar and it is possible that some product melted at a slightly lower temperature than others, consistent with the expected and actual T_m in Table 20. Two amplified products were visualised for *Bdnf*; one at the expected 103 bp and another below the 50 bp molecular marker. The second, smaller product was likely the result of primer dimer formation, which is reflected in the lower melting temperature of 66°C. Primer dimer formation can reduce amplification efficiency and accuracy of the qPCR assay by competing for reaction components during

amplification [97]. Therefore, it may be necessary to further optimise the qPCR assay conditions or investigate other primer sets in order to eliminate primer-dimer formation.

Finally, gel electrophoresis revealed that there were also two products amplified for *CaMKIIα*; one at the expected size of 150 bp and one unexpected band at approximately 1750 bp. Bioinformatic analysis was carried out to determine whether gDNA had been amplified however, the genomic product had an expected size of 5197 bp. Additionally, if gDNA was present the *Arc* primers would have amplified a 349 bp gDNA product. Therefore, further bioinformatic analyses are required to determine what the amplified product of approximately 1750 bp was. This would include gel purification and DNA sequencing of the observed 1750 bp band, which were unable to be carried out in this research die to time constraints.

4.6 Statistical Analysis of Quantitative PCR Results

The GOIs selected for analysis during *t*=2 hour and *t*=4 hour general anaesthetic exposure were *Arc, Bdnf, CaMKIIα, Gjd2* and *Grin1*. They were selected based on previously described roles in various aspects of memory function in order to test our hypothesis that memory-related gene expression would change during a period of general anaesthesia. Gene expression was analysed using real-time qPCR and compared with the expression of *β2m* and *Gapdh* for internal normalisation.

4.6.1 Gene Expression During Anaesthetic Exposure

Group qPCR analysis of the *in vivo* sample sets highlighted that across all time points during exposure to sevoflurane and propofol, levels of *CaMKIIα, Gjd2* and *Grin1* mRNA did not show statistically significant variations in mRNA expression ($p<0.05$). Although our results showed no change in gene expression, it does not rule out the possibility of post-transcriptional or post-translational modifications and further studies would be required to confirm this.

The unchanged expression of *Gjd2* during both sevoflurane and propofol exposure *in vivo* further validated the *in vitro* work previously carried out by Keiran Oxton (UoW, 2013). This study demonstrated that no change in *Gjd2* gene expression occurred during anaesthetic exposure in a mouse brain slice model.

4.6.2 Gene Expression Analysis for Brain-Derived Neurotrophic Factor (*Bdnf*) During Anaesthetic Exposure

During exposure to sevoflurane, significant down-regulation of *Bdnf* was observed at both $t=2$ hours and $t=4$ hours. Furthermore, significant down-regulation of *Bdnf* was also reported at $t=2$ hour during exposure to propofol. Therefore, we can reject H_0 and state with confidence that *Bdnf* was down-regulated during exposure to general anaesthetic within a four hour time frame. *Bdnf* is one of the best studied activity-induced genes and was originally identified as an important factor for the survival of neurons [100]. The expression of *Bdnf* mRNA is modulated by electrical activity in the brain and can be induced by stimuli such as seizures [100]. There is growing evidence to suggest that BDNF is involved in neuronal homeostasis and plasticity-related functions such as learning and memory [54]. Altered *Bdnf* gene expression patterns contribute to several major

pathologies including depression, epilepsy, Alzheimer's, Huntington's and Parkinson's diseases. Homology of transcript variants in human and mouse *Bdnf* ranges from 45% to 95% [54]. All the exons that are expressed in humans are also expressed in mouse and rat, except for exon VIIB and VIII [54]. Aid et al. (2007) demonstrated that transcript variant 1 of mouse *Bdnf* was only expressed in the mouse brain and the thymus, using semi-quantitative RT-PCR [54]. In agreement, our data shows that *Bdnf* transcript variant 1 was expressed in mouse cortex.

The BDNF protein exerts its effect by binding to TrkB and p75 and promoting survival of neurons through inactivation of cell-death machinery and activation of pro-survival genes [100]. In addition to having a pro-survival function, BDNF also modulates synaptic activity [100]. Neuronal *Bdnf* expression is altered by various stimuli such as GABA and glutamatergic neurotransmission and calcium-mediated membrane depolarisation [54]. Differential expression of *Bdnf* can also occur in depression, stress, exercise and learning [54].

Some studies have also demonstrated that a wide range of anti-depressant drugs, such as 5-HT re-uptake inhibitors, tricyclic monoamine oxidase inhibitors and atypical antidepressants, can initiate significant increases in *Bdnf* mRNA levels in cortical and hippocampal brain regions [99]. Coppell et al. (2003) reported down-regulation of *Bdnf* mRNA four hours after inhibition of the 5-HT transporter or monoamine oxidase (TCP) in the rat brain. After 24 hours, *Bdnf* mRNA expression was increased in the hippocampus, demonstrating a bi-phasic effect of 5-HT and TCP inhibition on *Bdnf* expression [92,97]. They hypothesised that excitatory 5-HT receptors on GABAergic interneurons in the hippocampus increased the release of GABA, resulting in inhibition of glutamatergic neurons

and a decrease in *Bdnf* gene expression [97]. Additionally, microdialysis studies have shown that administration of TCP or 5-HT uptake inhibitors resulted in an increase in extracellular 5-HT levels in the rat hippocampus [92,97]. Therefore, general anaesthetics may possibly initiate an increase in extracellular 5-HT, leading to excitation of 5-HT receptors in GABAergic neurons, inhibition of glutamatergic neurons and a decrease in *Bdnf* expression. As one of the main mechanisms of action of anaesthetic agents is direct GABA enhancement, this could be the main pathway in which *Bdnf* is down-regulated. However, further research is required to confirm this hypothesis.

4.6.3 Gene Expression Analysis of Activity-Regulated Cytoskeletal Associated Protein (*Arc*) during Anaesthetic Exposure

Following t=4 hour exposure to sevoflurane and t=2 hour exposure to both sevoflurane and propofol, there was no change in the expression of *Arc* mRNA. However, up-regulation of *Arc* following t=4 hour exposure to propofol was observed. The administration of propofol was not as reliable as sevoflurane and the required dose differed between treatment animals, as did the length of time anaesthesia remained induced. Issues with propofol administration may be a reason for limited animal studies. Administration of propofol during the first two hours was managed well, however considerable variation was observed between the two and four hour time points. Anaesthesia between two and four hours began to last for less time following top-up doses, with some periods as short as five minutes. Many of these top-ups were accompanied by short awakenings. Furthermore, some animals required more doses than others in order to remain anaesthetised. Constant monitoring of the animals was required to ensure they were administered a top-up dose as soon as the anaesthesia started to wear off.

Therefore, the variation observed in the animal response may have caused other stress- or activity- related changes in gene expression, including the up-regulation of *Arc* that was observed.

The activity-regulated cytoskeletal-associated *(Arc)* gene is an IEG that has been previously implicated in memory consolidation for its role in altering synaptic strength [31]. The expression of IEGs is tightly linked to patterns of synaptic activity, making IEGs interesting candidates in the initiation of synaptic plasticity that underlies long-term memory storage and retrieval [17]. The transcription of *Arc* mRNA can be increased several-fold in cortical neurons and is one of the most dynamically regulated IEGs [43]. The *Arc* gene also lacks homology with any other gene and does not belong to any major gene family, indicating a highly specific function [17]. Although expression occurs in the nucleus, *Arc* mRNA rapidly accumulates at sites of synaptic activity and is produced following induction of LTP [15]. Therefore, it is possible that the inconsistent anaesthesia observed during propofol exposure may have triggered a different gene expression response that involved up-regulation of *Arc* in the cortex. This is further supported by the finding that the propofol and sevoflurane results were comparable at the two hour time point. The up-regulation of *Arc* mRNA that was observed after a four-hour exposure to propofol may have been caused by the awakening of mice, leading to increased synaptic activity and accumulation of newly synthesised *Arc* in cortical neurons. In support of this theory, a previous study published results that indicated a bi-phasic increase in *Arc* mRNA expression post-training in mice [101]. The increase in *Arc* mRNA expression was detected specifically in the learning group and provided the first evidence that *Arc* expression is induced by a learning task, suggesting a role of *Arc* in the mechanisms underlying long-term memory

formation. Furthermore, the increase in *Arc* expression in the mouse brain (including cortical regions) was higher 15 minutes after the training task than at 4.5 hours post-training [101]. Therefore, the increase in *Arc* expression we reported after a four hour exposure to propofol may have been the result of frequent awakening of the animals in the last thirty minutes of propofol exposure. Frequent disruption to anaesthesia may have initiated a response from the mice similar to that seen following a learning task, leading to an increase in *Arc* expression in the cortex. In order to further validate these results, an optimised method for more reliable administration of IP anaesthetic to mice must be produced.

4.6.4 Gene Expression Analysis of *CaMKIIα, Gjd2* and *Grin1*

Our results demonstrated no change in the expression of *CaMKIIα, Gjd* or *Grin1* in cerebrocortical brain tissue of mice during sevoflurane or propofol anaesthesia (*t*=2 hours and *t*=4 hours). Previous research demonstrated that propofol caused inhibition of Ca^{2+}/CaMKIIα signalling, however this was reported for the hippocampal region and was not evident in our cerebrocortical research [38]. Furthermore, a reduction in the expression of *Grin1* has been reported six hours after a brief exposure (15 minutes) to isoflurane [6]. These results were obtained from the basolateral amygdala of rats and were also not evident in our investigation of the cerebrocortical tissue of mice.

Chapter Five

Conclusion

The aims of this research were to investigate and select GOIs for gene expression analysis during two and four hour exposures to three commonly used general anaesthetics; isoflurane, sevoflurane and propofol. Gene expression changes in the cortex were analysed using a mouse model. A total of 36 mice were used in this research. Each anaesthetic treatment contained four time points with three replicates of each time point.

In conclusion, the data presented within this thesis demonstrated that no change in gene expression of *CaMKII*α*, Gjd2* or *Grin1* occurred in response to either sevoflurane or propofol. However, *Bdnf* displayed down-regulation after *t*=4 hour exposure to sevoflurane and *t*=2 hour exposure to both sevoflurane and propofol. Up-regulation of *Arc* following a *t*=4 hour exposure to propofol was also observed. A review of literature showed that both *Bdnf* and *Arc* have differing but essential roles in memory consolidation and synaptic plasticity. Furthermore, our research identified the cortex as a region of the mouse brain that was affected at the gene expression level by anaesthetic amnesia. The cortex should be further studied in parallel with the hippocampus in order to fully understand the mechanisms involved. Due to time constraints, the isoflurane exposure and aged mice trials were not carried out.

Chapter Six

Future Recommendations

This chapter will address five future recommendations for the elucidation of a molecular mechanism of action for general anaesthetics in the brain.

6.1 Anaesthetics

Sevoflurane, isoflurane and propofol were the general anaesthetics used in this research as they are commonly used in a clinical setting, however general anaesthetics are seldom administered on their own. Propofol is often administered via an intravenous route for the induction of anaesthesia in humans and a combination of desflurane, sevoflurane and/or isoflurane is used for the maintenance of anaesthesia. For applicability of our results to human health, this research would benefit from imitating the clinical setting more closely. An initial dose of propofol is easily caluculated based on 100 mg/kg of body weight and could be followed by "top-up" doses of a combination of sevoflurane and desflurane or isoflurane. This method would also eliminate the need to further optimise propofol administration.

6.2 Real-Time PCR

6.2.1 Gene Expression for the Control Samples at Differing Time Points

Comparison of gene expression between the *t*=0 hour and *t*=4 hour controls should be carried out in qPCR to ensure there is no change in gene expression

occurring. Any changes between these controls could indicate an environmental influence or stress-related response that would affect the overall results.

6.2.2 Investigation into the Nine *Bdnf* Transcript Variants

The *Bdnf* gene produces nine transcript variants via alternate splicing. The scope of this research only included analysis of transcript variant 1, which displayed down-regulation after exposure to both sevoflurane and propofol. Aid et al. (2007) showed all nine transcript variants were expressed in the cortex and hippocampus and transcript variant 2 was only expressed in the brain. Homology between the human and rodent *Bdnf* is 95% for transcript variant 1, and 93% for transcript variant 2. Therefore, comparative analyses should be carried out for at least transcript variant 2, if not all transcript variants, of mouse *Bdnf*.

6.2.3 Gene Expression Levels 24 hours Post Drug Exposure

This research included analysis of gene expression in response to t=2 hour and t=4 hour expsoure to general anaesthetics. Coppell et al. (2003) similarly reported down-regulation of *Bdnf* after four hours in response to antideppressant agents. However up-regulation of *Bdnf* was observed 24 hours post drug exposure, indicating a bi-phasic effect on *Bdnf* expression [99]. Conversely, Aid et al. (2007) demonstrated up-regulation of *Bdnf* transcript variants 1, 4, 5, 7 and 8 at three and six hours post exposure to kainic acid. Interestingly, the expression levels returned to basal levels at 24 hr posttreatment [54]. Therefore, *Bdnf* gene expression should be analysed 24 hr after exposure to general anaesthetic in order to investigate a potential bi-phasic effect.

6.2.4 *In vitro* Validation using a Brain Slice Model

Further analyses should be carried out *in vitro* to validate the findings reported in this research. A brain slice model can be used to expose *in vitro* tissue to anaesthetic agents before extracting RNA from the region(s) of interest for future qPCR analysis. The advantages of using a brain slice model include ease of anaesthetic administration, simple dosage requirements and no monitoring of animals. Anaesthetic agents can be applied directly to the artificial cerebrospinal fluid that the brain slice is bathed in and easily maintained throughout the anaesthetic exposure period. Following anaesthetic exposure, the region(s) of interest can be quickly isolated and subject to RNA extraction. Thus, an *in vitro* approach would also provide an effective method for analysis of multiple brain regions, such as the cortex and hippocampus. Furthermore, electrophysiological field potential recording can be carried out and an analysis of brain activity during anaesthesia can also be made.

6.3 Transcriptomics

Five GOIs were selected for analysis in this research based on their known roles in various aspects of memory formation and consolidation. The mRNA transcripts of these genes was analysed using qPCR following t=2 and t=4 hour exposures to anaesthetic. Transcriptomics is the study of the whole transcriptome, including the complete set of RNA transcripts produced by the genome [102]. High-throughput methods, such as microarray analysis, can be used to produce an expression profile that represents the complete set of RNAs expressed under specific circumstances. The resulting data sets can be catagorised to display genes that are up- or down- regulated post-anaesthesia, giving a richer snapshot of what is

occuring on the molecular level during anaesthesia. Understanding the transcriptome is essential for interpreting functional elements of a genome, therefore a whole transcriptome approach could allow the molecular networks involved in anaesthesia to be identified [102]. Transcriptomics would be a superior approach to gain a broader understanding of gene expression patterns in the cerebral cortex following anaesthetic exposure. This is especially important as memory impairment induced by anaesthetics may result from changes in the expression of multiple genes. We recommend a whole transcriptome approach in future research in order to produce a more complete picture of gene expression changes in the cerebral cortex during anaesthesia.

6.4 Investigation into Protein Abundance During Anaesthetic Exposure

Although our research reported gene expression changes for *Arc* and *Bdnf*, there may be other post-transcriptional or post-translational changes occuring during anaesthesia. Thus, an analysis of protein abundance post-anaesthetic exposure using immunohistochemistry (IHC) techniques or western blot analysis should be carried out for a deeper insight into the cellular response. Immunohistochemistry methods can be used to understand the distribution or localisation of protein by forming an interaction between the protein and a antibody tagged to a fluorophore that can be visualised via microscopy or an imager [103]. The use of an immunofluoroescent antibody should be investigated for targeting of BDNF protein in a mouse brain slice, allowing detection of the translated BDNF protein before, during and after anaesthetic exposure. Alternatively, the BDNF protein could be quantified using western blot methodologies. Western blot analysis is

widely used for quantification of protein in a complex sample such as tissue homogenates [104]. Using gel electrophoresis, BDNF, or other target protein, can be seperated according to 3-D structure or length of the polypeptide (if denatured). The BDNF protein can then be transferred to a membrane where it is stained with specific antibodies and the relative immunofluoroesnce can be measured [104].

6.5 Further Animal Research

6.5.1 Alternative Target Tissue

Although the cortex was the region of interest to this research, the hippocampus is also a highly important region in terms of memory and learning processes. A joint focus on both the cortex and hippocampal region should be considered for future projects, using a comparison between gene expression changes in both regions.

6.5.2 Aged Animals

Although aged mice (*n*=6) were subject to sevoflurane exposure and subsequent RNA extraction in this research, time constraints prevented further analysis of this work. We recommend that this RNA is analysed for comparison of gene expression changes between the aged and young adult mice. Wang et al. (2011) have previously shown that isoflurane-sensitive memory deficits became more pronounced with age. Furthermore, an age-related decline of the eight transcript variants of *Grin1* has been reported in the brain. Therefore, *Arc, Bdnf* and *Grin1* gene expression should be further analysed in the aged animals.

6.5.3 Genetically Modified Mice

In order to validate memory-related functions of BDNF during anaesthesia, a *Bdnf*-Knockout (KO) mouse model could be used. Inactivating the *Bdnf* gene by disrupting or replacing it with an artifical piece of DNA would produce mice with no *Bdnf* expression, allowing observation of its function after exposure to anaesthetic. Homozygous *Bdnf*-KO mice ($Bdnf^{-/-}$) may produce developmental defects that are embyonic lethal, therefore breeding of heterozygous *Bdnf*-KO mice ($Bdnf^{+/-}$) may be required for this research. Additionally, mice can be bred with induced *Bdnf* mutations for comparative protein and gene expression analysis in wildtype mice, using transcriptomics and IHC methods. Whole transcriptome sequencing of mutant *Bdnf* mice exposed to anaesthetic would provide a means of identifying networks that may be affected by altered *Bdnf* gene expression. Patterson et al. (1996) found that basal synaptic transmission was reduced in BDNF mutant mice, with the mutants presenting fewer presynaptic neurons firing action potentials suggesting that the presynaptic neurons were releasing less neurotransmitter or the postsynapic neurons were less capable of responding. This research demonstrated that BDNF plays a direct role in activity-dependent synaptic plasticity in the hippocampus by treating brain slices from BDNF-KO mice with recombinant BDNF that was able to rescue deficits in basal synatpic transmission and completely reverse deficits in LTP. Therefore, an important role of BDNF during LTP has been previously established and should be further investigated in the cortex.

6.5.4 Behavioural Studies

Behavioural tests such as the Morris water maze and fear conditioning could be used to identify potential alterations to long-term memory in response to clinical doses of anaesthetic. Wang et al. (2011) demonstrated that memory blockade using fear conditioning to tone was blocked by isoflurane at the Effective Dose (ED_{50}) = 0.47 Minimum Alveolar Concentration (MAC). Fear conditioning is a technique that uses a fearful experience to establish a fearful memory that can result in long-term behavourial changes, which can then be analysed [105]. Mice are usually conditioned by pairing a tone with foot shock and fear can be evualated through imobility or freezing behaviour. The Morris water maze is an apparatus where mice learn to escape from water by swimiming to a platform that is hidden just below the surface of the water. Control animals learn this task very quickly (within a few days) and those with memory-impairment will take much longer. The Morris water maze is a more advantageous test to use as it does not require food or water deprivation or painful stimuli [105]. Animal behavioural experiments could be carried out in both wildtype (control) and mutant *Bdnf* mice before and after anaesthetic exposure for evaluation of potential memory-impairments induced by the lack of *Bdnf* expression. For further comparative analyses, the latter tests should be carried out at more than one interval post-anaesthesia; one or two days and fourteen days. This would indicate whether memory-impairment was a prolonged side effect of the anaesthetic exposure in mice.

References

1. Hudetz AG. (2012). General anesthesia and human brain connectivity. *Brain Connectivity 2*(6): 291–302.

2. Jungwirth B, Zieglgänsberger W, Kochs E, Rammes G. (2009). Anesthesia and postoperative cognitive dysfunction (POCD). *Mini-Reviews in Medicinal Chemistry 9*(14): 1568–79.

3. Veselis RA. (2007). Memory: a guide for anaesthetists. *Best Practice & Research Clinical Anaesthesiology 21*(3): 297–312.

4. Jevtovic-Todorovic V, Absalom AR, Blomgren K, Brambrink A, Crosby G, Culley DJ, et al. (2013). Anaesthetic neurotoxicity and neuroplasticity: an expert group report and statement based on the BJA Salzburg Seminar. *British Journal of Anaesthesia 111*(2): 143-151.

5. Zhang F, Zhu Q, Xue Q, Luo Y, Yu B. (2013). Extra-cellular signal-regulated kinase (ERK) is inactivated associating hippocampal ARC protein up-regulation in sevoflurane induced bidirectional regulation of memory. *Neurochemistry Research 38*(7): 1341–7.

6. Rampil IJ, Moller DH, Bell AH. (2006). Isoflurane modulates genomic expression in rat amygdala. *Anesthesia & Analgesia 102*(5): 1431–8.

7. Pan Z, Lu X-F, Shao C, Zhang C, Yang J, Ma T, et al. (2011). The effects of sevoflurane anesthesia on rat hippocampus: a genomic expression analysis. *Brain Research 24*(1381): 124–33.

8. Kobayashi K, Takemori K, Sakamoto A. (2007). Circadian gene expression is suppressed during sevoflurane anesthesia and the suppression persists after awakening. *Brain Research 14*(1185): 1–7.

9. Orser BA, Mazer CD, Baker AJ. (2008). Awareness during anesthesia. *Canadian Medical Association Journal 178*(2): 185–8.

10. Squire LR, Alvarez P. (1995). Retrograde amnesia and memory consolidation: a neurobiological perspective. *Current Opinion in Neurobiology 5*(2): 169–77.

11. Wang D-S, Orser BA. (2011). Inhibition of learning and memory by general anesthetics. *Canadian Journal of Anaesthesia 58*(2): 167–77.

12. Goldman-Rakic PS. (1995). Cellular basis of working memory. *Neuron 14*(3): 477–85.

13. Sackel DJ. (2006). Anesthesia awareness: an analysis of its incidence, the risk factors involved, and prevention. *Journal of Clinical Anesthesia 18*(7): 483–5.

14. Fidalgo AR, Cibelli M, White JPM, Nagy I, Wan Y, Ma D. (2012). Isoflurane causes neocortical but not hippocampal-dependent memory impairment in mice. *Acta Anaesthesiologica Scandinavica 56*(8): 1052–7.

15. Bramham CR, Alme MN, Bittins M, Kuipers SD, Nair RR, Pai B, et al. (2010). The Arc of synaptic memory. *Experimental Brain Research 200*(2): 125–40.

16. Yamauchi T. (2005). Neuronal Ca2+/calmodulin-dependent protein kinase II--discovery, progress in a quarter of a century, and perspective: implication for learning and memory. *Biological & Pharmaceutical Bulletin 28*(8): 1342–54.

17. Miyashita T, Kubik S, Lewandowski G, Guzowski JF. (2008). Networks of neurons, networks of genes: an integrated view of memory consolidation. *Neurobiology of Learning and Memory 89*(3): 269–84.

18. Plath N, Ohana O, Dammermann B, Errington ML, Schmitz D, Gross C, et al. (2006). Arc/Arg3.1 is essential for the consolidation of synaptic plasticity and memories. *Neuron 52*(3): 437–44.

19. Andrade, J. (2007). Unconscious memory formation during anaesthesia. *Best Practice & Research Clinical Anaesthesiology 21*(3): 385-401

20. Sakata K, Martinowich K, Woo NH, Schloesser RJ, Jimenez DV, Ji Y, et al. (2013). Role of activity-dependent BDNF expression in hippocampal-prefrontal cortical regulation of behavioral perseverance. *Proceedings of the National Academy of Sciences 10;110*(37): 15103–8.

21. Lee H-K, Takamiya K, Han J-S, Man H, Kim C-H, Rumbaugh G, et al. (2003). Phosphorylation of the AMPA receptor GluR1 subunit is required for synaptic plasticity and retention of spatial memory. *Cell 112*(5): 631–43.

22. Holt CE, Schuman EM. (2013). The central dogma decentralized: new perspectives on RNA function and local translation in neurons. *Neuron 80*(3): 648–57.

23. Campagna J, Miller K, Forman S. (2003). Mechanisms of Actions of Inhaled Anesthetics. *The New England Journal of Medicine 348*(21): 2110-24.

24. Cammarota M, Bernabeu R, Levi De Stein M, Izquierdo I, Medina JH. (1998). Learning-specific, time-dependent increases in hippocampal Ca2+/calmodulin-dependent protein kinase II activity and AMPA GluR1 subunit immunoreactivity. *European Journal of Neuroscience 10*(8): 2669–76.

25. Ebert DH, Greenberg ME. (2013). Activity-dependent neuronal signalling and autism spectrum disorder. *Nature 493*(7432): 327–37.

26. Das SR, Magnusson KR. (2011). Changes in expression of splice cassettes of NMDA receptor GluN1 subunits within the frontal lobe and memory in mice during aging. *Behavioural Brain Research 222*(1): 122–33.

27. Hasan MT, lez SHAN-GA, Dogbevia G, o MTN, Bertocchi I, Gruart AES, et al. (2012). Role of motor cortex NMDA receptorsin learning-dependent synaptic plasticityof behaving mice. *Nature Communications. Nature Publishing Group 4*(2258): 1–9.

28. Cryan JF, Holmes A. (2005). The ascent of mouse: advances in modelling human depression and anxiety. *Nature Reviews Drug Discovery 4*(9): 775–90.

29. Xie H, Liu Y, Zhu Y, Ding X, Yang Y, Guan J-S. (2014). In vivo imaging of immediate early gene expression reveals layer-specific memory traces in the mammalian brain. *Proceedings of the National Academy of Sciences, Feb 18;111*(7): 2788–93.

30. Hentschke H, Schwarz C, Antkowiak B. (2005). Neocortex is the major target of sedative concentrations of volatile anaesthetics: strong depression of firing rates and increase of GABAA receptor-mediated inhibition. *European Journal of Neuroscience 21*(1): 93–102.

31. Alkire MT, Guzowski JF. (2008). Hypothesis: suppression of memory protein formation underlies anesthetic-induced amnesia. *Anesthesiology 109*(5): 768–70.

32. Sakai EM, Connolly LA, Klauck JA. (2005). Inhalation anesthesiology and volatile liquid anesthetics: focus on isoflurane, desflurane, and sevoflurane. *Pharmacotherapy 25*(12): 1773–88.

33. Franks NP. (2009). Molecular targets underlying general anaesthesia. *British Journal of Pharmacology 147*(S1): S72–S81.

34. Dilger JP. (2002). The effects of general anaesthetics on ligand- gated ion channels. *British Journal of Anaesthesiology 89*(1): 41-51.

35. Ghadami Yazdi A, Ayatollahi V, Hashemi A, Behdad S, Ghadami Yazdi E. (2013). Effect of two different concentrations of propofol and ketamine combinations (ketofol) in pediatric patients under lumbar puncture or bone marrow aspiration. *Iranian Journal of Pediatric Hematology and Oncology 3*(1): 187–92.

36. Sethi S, Wadhwa V, Thaker A, Chuttani R, Pleskow DK, Barnett SR, et al. (2013). Propofol versus traditional sedative agents for advanced endoscopic procedures: A meta-analysis. *Journal of Digestive Endoscopy 26*(4): 515-524.

37. Mikstacki A, Skrzypczak-Zielinska M, Tamowicz B, Zakerska-Banaszak O, Szalata M, Slomski R. (2013). The impact of genetic factors on response to anaesthetics. *Advances in Medical Sciences 58*(1): 9-14.

38. Zhang H, Zhang S-B, Zhang Q-Q, Liu M, He X-Y, Zou Z, et al. (2013). Rescue of cAMP response element-binding protein signaling reversed spatial memory retention impairments induced by subanesthetic dose of propofol. *CNS Neuroscience and Therapeutics 19*(7): 484–93.

39. Isken O, Maquat LE. (2007). Quality control of eukaryotic mRNA: safeguarding cells from abnormal mRNA function. *Genes & Development 21*(15): 1833–56.

40. Amaral PP, Dinger ME, Mercer TR, Mattick JS. (2008). The eukaryotic genome as an RNA machine. *Science 319*(5871): 1787–9.

41. Lockhart DJ, Winzeler EA. (2000). Genomics, gene expression and DNA arrays. *Nature 405*(6788): 827–36.

42. Ginty DD. (1997). Calcium regulation of gene expression: isn't that spatial? *Neuron 18*(2): 183–6.

43. Guzowski JF, Lyford GL, Stevenson GD, Houston FP, McGaugh JL, Worley PF, et al. (2000). Inhibition of activity-dependent arc protein expression in the rat hippocampus impairs the maintenance of long-term potentiation and the consolidation of long-term memory. *The Journal of Neuroscience 20*(11): 3993-4001.

44. Shepherd JD, Huganir RL. (2007). The cell biology of synaptic plasticity: AMPA receptor trafficking. *Annual Review of Cell Developmental Biology 23*: 613–43.

45. Soule J, Alme M, Myrum C, Schubert M, Kanhema T, Bramham CR. (2012). Balancing Arc synthesis, mRNA decay, and proteasomal degradation: maximal protein expression triggered by rapid eye movement sleep-like bursts of muscarinic cholinergic receptor stimulation. *Journal of Biological Chemistry 287*(26): 22354–66.

46. McReynolds JR, Holloway-Erickson CM, Parmar TU, McIntyre CK. (2014). Corticosterone-induced enhancement of memory and synaptic Arc protein in the medial prefrontal cortex. *Neurobiology of Learning & Memory 112*(2014): 148-157.

47. Lyford GL, Yamagata K, Kaufmann WE, Barnes CA, Sanders LK, Copeland NG, et al. (1995). Arc, a growth factor and activity-regulated gene, encodes a novel cytoskeleton-associated protein that is enriched in neuronal dendrites. *Neuron 14*(2): 433–45.

48. Waung MW, Pfeiffer BE, Nosyreva ED, Ronesi JA, Huber KM. (2008). Rapid translation of Arc/Arg3.1 selectively mediates mGluR-dependent LTD through persistent increases in AMPAR endocytosis rate. *Neuron 59*(1): 84–97.

49. Yin Y, Edelman GM, Vanderklish PW. (2002). The brain-derived neurotrophic factor enhances synthesis of Arc in synaptoneurosomes. *PNAS 99*(4): 2368-2373.

50. Lu LX, Yon J-H, Carter LB, Jevtovic-Todorovic V. (2006). General anesthesia activates BDNF-dependent neuroapoptosis in the developing rat brain. *Apoptosis 11*(9): 1603–15.

51. Leal G, Comprido D, Duarte CB. (2014). BDNF-induced local protein synthesis and synaptic plasticity. *Neuropharmacology 76*(PtC):639–56.

52. Alder J, Thakker-Varia S, Bangasser DA, Kuroiwa M, Plummer MR, Shors TJ, et al. (2003). Brain-Derived Neurotrophic Factor-Induced Gene Expression Reveals Novel Actions of VGF in Hippocampal Synaptic Plasticity. *The Journal of Neuroscience 23*(34): 10800-10808.

53. Bennett MR, Lagopoulos J. (2014). Stress and trauma: BDNF control of dendritic-spine formation and regression. *Progress in Neurobiology 112*: 80–99.

54. Aid T, Kazantseva A, Piirsoo M, Palm K, Timmusk T. (2007). Mouse and rat BDNF gene structure and expression revisited. *Journal of Neuroscience Research 85*(3): 525–35.

55. Izquierdo I, Medina JH. (1997). Memory formation: the sequence of biochemical events in the hippocampus and its connection to activity in other brain structures. *Neurobiology of Learning & Memory 68*(3): 285–316.

56. Néant-Fery M, Pérès E, Nasrallah C, Kessner M, Gribaudo S, Greer C, et al. (2012). A Role for Dendritic Translation of CaMKIIα mRNA in Olfactory Plasticity. *PLoS ONE 7*(6): e40133.

57. Sanhueza M, Lisman J. (2013). The CaMKII/NMDAR complex as a molecular memory. *Molecular Brain 6*(10): 1-8

58. Barria A, Malinow R. (2005). NMDA receptor subunit composition controls synaptic plasticity by regulating binding to CaMKII. *Neuron 48*(2): 289–301.

59. Malenka RC, Nicoll RA. (1999). Long-term potentiation - a decade of progress? *Science 285*(5435): 1870–4.

60. Oyamada M, Takebe K, Oyamada Y. (2013). Regulation of connexin expression by transcription factors and epigenetic mechanisms. *Biochimica et Biophysica Acta 1828*(1): 118–33.

61. Lynn BD, Li X, Nagy JI. (2012). Under construction: building the macromolecular superstructure and signaling components of an electrical synapse. *Journal of Membrane Biology 245*(5-6): 303–17.

62. Cicirata F, Parenti R, Spinella F, Giglio S, Tuorto F, Zuffardi O, et al. (2000). Genomic organization and chromosomal localization of the mouse Connexin36 (mCx36) gene. *Gene 251*(2): 123–30.

63. Bloomfield SA, Völgyi B. (2009). The diverse functional roles and regulation of neuronal gap junctions in the retina. *Nature Reviews Neuroscience 10*(7): 495–506.

64. Wang Y, Belousov AB. (2011). Deletion of neuronal gap junction protein connexin 36 impairs hippocampal LTP. *Neuroscience Letters 502*(1): 30–2.

65. Leonard AS, Davare MA, Horne MC, Garner CC, Hell JW. (1998), SAP97 is associated with the alpha-amino-3-hydroxy-5-methylisoxazole-4-propionic acid receptor GluR1 subunit. *Journal of Biological Chemistry 273*(31): 19518–24.

66. Stephenson FA. (2006). Structure and trafficking of NMDA and GABAA receptors. *Biochemical Society Transactions 34*(Pt 5): 877–81.

67. Aman TK, Maki BA, Ruffino TJ, Kasperek EM, Popescu GK. (2014). Separate intramolecular targets for protein kinase: A control of N-methyl-D-aspartate receptor gating and Ca2+ permeability. *Journal of Biological Chemistry 289*: 18805-18817.

68. Dityatev A, Schachner M, Sonderegger P. (2010). The dual role of the extracellular matrix in synaptic plasticity and homeostasis. *Nature Reviews Neuroscience 11*(11): 735–46.

69. Kozera B, Rapacz M. (2013). Reference genes in real-time PCR. *Journal of Applied Genetics 54*(4): 391–406.

70. Ishmael FT, Stellato C. (2008). Principles and applications of polymerase chain reaction: basic science for the practicing physician. *Annals of Allergy, Asthma & Immunology 101*(4): 437–43.

71. Livak KJ, Schmittgen TD. (2001). Analysis of relative gene expression data using real-time quantitative PCR and the 2(-Delta Delta C(T)) Method. *Methods 25*(4): 402–8.

72. Gilsbach R, Kouta M, Bönisch H, Brüss M. (2006). Comparison of in vitro and in vivo reference genes for internal standardization of real-time PCR data. *BioTechniques 40*(2): 173–7.

73. Nolan T, Hands RE, Bustin SA. (2006). Quantification of mRNA using real-time RT-PCR. *Nature Protocols 1*(3): 1559–82.

74. VanGuilder HD, Vrana KE, Freeman WM. (2008). Twenty-five years of quantitative PCR for gene expression analysis. *BioTechniques 44*(5): 619–26.

75. van Rijn SJ, Riemers FM, van den Heuvel D, Wolfswinkel J, Hofland L, Meij BP, et al. (2014). Expression stability of reference genes for quantitative RT-PCR of healthy and diseased pituitary tissue samples varies between humans, mice, and dogs. *Molecular Neurobiology 49*(2): 893–9.

76. Mouse Genome Sequencing Consortium, Waterston RH, Lindblad-Toh K, Birney E, Rogers J, Abril JF, et al. (2002). Initial sequencing and comparative analysis of the mouse genome. *Nature 420*(6915): 520–62.

77. Ezkurdia I, Juan D, Rodriguez JM, Frankish A, Diekhans M, Harrow J, et al. (2014). Multiple evidence strands suggest that there may be as few as 19,000 human protein-coding genes. *Human Molecular Genetics 23*(22): 5866–78.

78. Bustin SA, Benes V, Garson JA, Hellemans J, Huggett J, Kubista M, et al. (2009). The MIQE Guidelines: Minimum Information for Publication of Quantitative Real-Time PCR Experiments. *Clinical Chemistry 55*(4): 611–22.

79. Nanodrop.com. (2014, November 19). NanoDrop spectrophotometers nucleic acid purity ratios [Internet]. Retrieved from: http://www.nanodrop.com/Library/T042-NanoDrop-Spectrophotometers-Nucleic-Acid-Purity-Ratios.pdf

80. Xia L, Delomenie C, David I, Rainer Q, Marouard M, Delacroix H, David D, Gardier A, Guilloux J. (2012). Ventral hippocampal molecular pathways and impaired neurogenesis associated with 5-HT1A and 5-HT1B receptors disruption in mice. *Neuroscience Letters 521*(1): 20-25.

81. Wang Y, Song J-H, Denisova JV, Park W-M, Fontes JD, Belousov AB. (2012). Neuronal gap junction coupling is regulated by glutamate and plays critical role in cell death during neuronal injury. *Journal of Neuroscience 32*(2): 713–25.

82. Zhang J-H, Wang F, Wang T-Y. (2011). A simple and effective SuperBuffer for DNA agarose electrophoresis. *Gene 487*(1): 72–4.

83. Lifetechnologies.com. (2015, Feb 10). Genotypes of Invitrogen™ competent cells [Internet]. Retrieved from: http://www.lifetechnologies.com/nz/en/home/life-science/cloning/competent-cells-for-transformation/chemically-competent/dh5alpha-genotypes.html

84. Sciencegateway.com. (2015, Feb 10). Bacteria Transformation Efficiency Calculator [Internet]. Retrieved from: http://www.sciencegateway.org/tools/transform.htm

85. Crossan HC. (2014). Characterisation of VMO1 in human tissues (Masters thesis, University of Waikato, Hamilton, New Zealand. Retrieved from http://researchcommons.waikato.ac.nz/handle/10289/8792

86. Pfaffl MW, Horgan GW, Dempfle L. (2002). Relative expression

software tool (REST©) for group-wise comparison and statistical analysis of relative expression results in real-time PCR. *Nucleic Acids Research 30*(9) e36.

87. Addgene.com. (2015, Feb 10). Protocol - How to conduct a restriction digest [Internet]. Retrieved from: https://www.addgene.org/plasmid-protocols/restriction-digest/

88. Gene-Quantitfication.com. (2014, Nov 12). [Internet]. Retrieved from: http://www.gene-quantification.com

89. Nolan TE, Klein HJ. (2002). Methods in vascular infusion biotechnology in research with rodents. *ILAR Journal 43*(3): 175–82.

90. Alzet.com. (2015, Feb 11). ALZET® osmotic pumps - implantable pumps for research [Internet]. Retrieved from: http://www.alzet.com/

91. Tsung T, Watts S, Davis R. (2011). Drug delivery: enabling technology for drug discovery and development. *Frontiers in Pharmacology 2*(44): 1-13.

92. Aranda PS, LaJoie DM, Jorcyk CL. (2012). Bleach gel: a simple agarose gel for analyzing RNA quality. *ELECTROPHORESIS 33*(2): 366–9.

93. Sambrook J, Russell DW. (2001). Molecular Cloning. CSHL Press; New York, USA.

94. Nucleics.com. (2015, Jan 26). Failed DNA sequencing reactions [Internet]. Retrieved from: http://www.nucleics.com/DNA_sequencing_support/DNA-sequencing-failed-reaction.html

95. Bryant S, Manning DL. (1998). Formaldehyde gel electrophoresis of total RNA. *Methods in Molecular Biology 86*: 69–72.

96. Ririe KM, Rasmussen RP, Wittwer CT. (1997). Product differentiation by analysis of DNA melting curves during the polymerase chain reaction. *Analytical Biochemistry 245*(2): 154–60.

97. Bio-rad.com. (2015, Nov 14). qPCR assay design and optimization: applications & technologies [Internet]. Retrieved from http://www.bio-rad.com/en-nz/applications-technologies/qpcr-real-time-pcr

98. West AE, Chen WG, Dalva MB, Dolmetsch RE, Kornhauser JM, Shaywitz AJ, et al. (2001). Calcium regulation of neuronal gene expression. *PNAS 98*(20): 11024–31.

99. Coppell AL, Pei Q, Zetterström TSC. (2003). Bi-phasic change in BDNF gene expression following antidepressant drug treatment. *Neuropharmacology 44*(7): 903–10.

100. Le Magueresse C, Monyer H. (2013). GABAergic interneurons shape the functional maturation of the cortex. *Neuron 77*(3): 388–405.

101. Montag-Sallaz M, Montag D. (2003). Learning-induced arg 3.1/arc mRNA expression in the mouse brain. *Learning & Memory 10(*2): 99-107.

102. Wang Z, Gerstein M, Snyder M. (2009). RNA-Seq: a revolutionary tool for transcriptomics. *Nature Reviews Genetics 10*(1): 57-63.

103. Ramos-Vara, JA, Miller M.A (2014). When tissue antigens and antibodies get along: revisiting the technical aspects of immunohistochemistry - the red, brown, and blue technique. *Veterinary Pathology 51*(1): 42–87

104. Taylor SC, Posch A. (2014). The design of quantitative western blot experiment. BioMed Research International 2014: e361590.

105. Levin ED, Buccafusco JJ. (2006). Animal models of memory impairment. Boca Ralton, Florida: CRC Press.

Appendices

Appendix 1: Animal Ethics Approval

UNIVERSITY OF WAIKATO ANIMAL ETHICS COMMITTEE

THE UNIVERSITY OF WAIKATO
Te Whare Wānanga o Waikato

Protocol Number: 905

APPLICATIONCOVER SHEET

Project Details
Full Protocol Title: General anaesthetic modulation of memory-related gene expression in the mouse brain **Name of Primary Applicant:** Laura Bell **Faculty/School/Department:** Department of Biological Sciences **Expected start date:** Nov 2013 **Expected completion date:** Nov 2015 **Animals species:** Mouse (common name) **Number to be used:** 50 **Impact Level:**B (See Q 6 Animal Use Statistics Form – Appendix 1):

Type of Application (Can tick more than one box):	√Research √Part of research thesis (Laura Bell) ☐Teaching ☐Other (Specify)
Standard Operating Procedures:	☐ No √ Yes: SOPNumber/ Title: #9 Euthanasia of rodents by CO_2 asphyxiation #5 The Housing and Care of Laboratory Rodents
Other AEC approval:	Has this application been submitted any other AEC for approval √ No ☐ Yes (Specify Committee) Details:
Funding support:	Is this research part of a funding grant either received or pending √ No ☐ Yes (Specify funding source) Details:

OFFICE USE ONLY This proposal is approved for the period:	***Protocol Number:***
From: 1 Nov 2013	**To:** 1 Nov 2015
Signature AEC Chair:	**Date:** 25/10/13

All research involving the use of animals must comply with the *Animal Welfare Act (1999)* and the University of Waikato Code of Ethical Conduct for the Use of Animals in Teaching and Research.

Appendix 2: Waikato Safety Operating Procedure (SOP) 9

UNIVERSITY OF WAIKATO ANIMAL ETHICS COMMITTEE

STANDARD OPERATING PROCEDURE

SOP Number: 9

Title: Euthanasia of Rodents by CO_2 Asphyxiation

Only persons that have received appropriate training and have been approved by the Animal Ethics Committee may perform this euthanasia

General:

This procedure outlines the general procedure for euthanizing rodents using CO_2 gas.

Equipment Required:

Building Animal House (Glasshouse compound) has a purpose built chamber connected to a CO_2 cylinder.

Setup:

Check with the Technician if there are any questions or concerns.

- Put the cage still containing the animal(s) directly in chamber. It is recommended that animals be euthanised in their „home" cages. There has been less stress observed if the animal(s) are with familiar surroundings and smells.
- Ensure that the chamber lid is shut
- It is essential that there is adequate ventilation for the operator.
- Operation (see diagram):
    1. Ensure needle valve is closed
    2. Open cylinder valve one full turn
    3. Turn regulator until low pressure gauge reads "200"
    4. Slowly open needle valve 2 turns

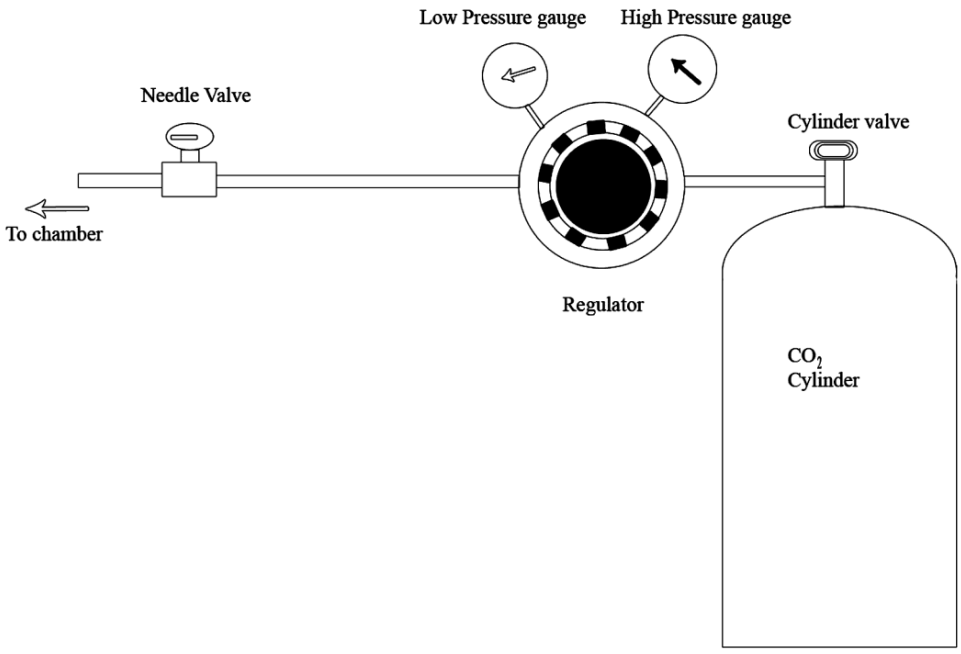

- Once the concentration has caused the animal(s) to stop breathing, the CO_2 may be turned off but the chamber should remain closed for 10 minutes.
    1. Turn off cylinder valve
    2. Wait for pressure to drop
    3. Loosen off the regulator
    4. Close needle valve
- After 10 minutes open the chamber and ensure that the animals are dead. There should be an absence of breathing, no detectable heartbeat and glazed over eyes.

The chamber has a quite large volume and it may take some time for the level of CO_2 to rise up to and into the cage tray.

Alternatives:

Small numbers of animals:

Where there are small numbers of animals involved, an effective method is to place the cage into a plastic bag and insert the gas hose into the bag and seal it off. Single animals maybe euthanised in a clear lidded bucket that has the gas hose inserted. Food wrap or a clear plastic bag over the top works well.

Dealing with large numbers of animals:

The chamber can only fit a limited number of cages at once.

The operator:

1) can rotate the cages through (but chamber must be vented between batches; it is painful for the animals to be dunked straight into high CO2 concentrations (ANZCART, 2006).

2) transfer the animals to as few cages as possible; operator must carefully check that the animals are all dead. Ones at the bottom of the pile may lie in air pockets

3) let all animals run loose in the chamber (without cages). They will be too busy sniffing each other to notice the effects of the gas. The operator will then have to clean up the chamber afterward.

Field work with wild animals:

The chamber in the Animal House is not portable; therefore field euthanasia will have to involve the use of a small CO_2 cylinder, regulator, needle valve and plastic bag or a custom made chamber (or tube). Use a dark bag so not to stress out the animal further. Wild animal respond differently to CO_2 and may take longer to succumb than lab bred animals. DO NOT bring wild animals into Animal House for euthanizing without permission from the technician; wild animals carry diseases/parasites which could transmit to lab animals being housed in Animal House.

Adverse Events and Unexpected Outcomes: Occasionally animals have recovered consciousness and/or exhibited signs of life sometime after the procedure. They were not fully euthanised but the operator did not observe signs of life (wait the full 10 minutes). This possibly is due to the animal(s) being at the bottom of a pile and in a lower (insufficient) concentration of CO_2. The animal(s) must be returned to the chamber (or bucket) without delay to complete the euthanasia.

Occupational Safety and Health Considerations: CO_2 gas is heavier than air. In confined spaces the gas displaces air and could cause asphyxiation to the operator in high concentrations. Ensuring ventilation during these operations is essential (i.e. open the doors and remain away from the chamber when possible, preferably outside). Asphyxiation symptoms may not be apparent and their onset may be quick. Refer to the MSDS for more information.

Reference:

ANZCART, 2006. Report of the International Consensus Meeting on Carbon Dioxide Euthanasia of Laboratory Animals. ANZCART News 19:2 1-7 *summarized* from the final report prepared by Hawkins, P *et al*. Copy available from: (www.nc3rs.org.uk/CO_2ConsensusReport).

Appendix 3: Reagents and Solutions

Agarose (2%) Gel with Superbuffer

To prepare a 2% agarose gel with Superbuffer, add 0.8 g of agarose to 40 mL of 1X Superbuffer and dissolve by heating in a microwave oven. When the solution has cooled to 60°C, add 1 μL of EtBr and gently mix before pouring into the gel tank. Leave for at least 30 minutes to set.

Agarose (1%) Gel with TAE

To prepare a 1% agarose gel with TAE, add 0.4 g of agarose to 40 mL of 1X Superbuffer and dissolve by heating in a microwave oven. When the solution has cooled to 60°C, add 1 μL of EtBr and gently mix before pouring into the gel tank. Leave for at least 30 minutes to set.

Denaturing Formaldehyde Gel with 1% Agarose

To prepare 50 mL of 1% agarose gel containing formaldehyde, add 0.5 g of agarose to 31 mL of sterile H_20 and dissolve in a microwave oven. Cool the solution to 60°C before adding 10 mL of 5X MOPS buffer and 9 mL of de-I formaldehyde in the fume hood and mixing gently. Pour gel into an RNase-free 10 cm x 10 cm mold and allow to set for at least 1 hour at RT.

DEPC H_2O

To prepare 0.1% DEPC H_2O, add 2 mL of DEPC to 2000 mL of sterile mQH_2O in the fume hood. The solution should be mixed with a magnetic stirrer in the fume hood overnight to ensure all DEPC is completely dissolved. It is important to wear gloves and safety glasses and use the fume hood when making this solution, as DEPC is a suspected carcinogen. Once the DEPC has been dissolved overnight, autoclave the solution on a fluids cycle. Store at room temperature.

EDTA (0.5 M)

To prepare EDTA at 0.5 M, add 186.1 g of disodium EDTA-$2H_20$ to 800 mL of mQH20. Stir vigourously using a magnetic stirrer. Adjust pH to desired value with NaOH. Dispense into aliquots and sterilise by autoclaving.

5X Formaldehyde Gel-loading Buffer

To prepare 5X formaldehyde RNA loading buffer, components should be made up to the concentrations listed in the table below. The solution should be stored at -20°C and 2 μL of loading buffer used for every 10 – 20 μL of RNA sample.

Component	**Quantity**
Glycerol	50%
EDTA	10mM
Bromophenol blue	0.25%
Ethidium bromide	10 mg/mL

IPTG (10 mM)

Dissolve 0.238 g of IPTG into 10 mL of water and sterilise by filtration with a 0.22 μM filter. Store at -20°C.

Lysogeny Broth

Dissolve the components listed in the table below in a dedicated 1 L bottle before autoclaving on a media cycle. Allow solution to cool to 55°C before adding 0.2 mL of 50 mg/mL ampicillin to 200 mL of LB if antibiotic is required. Store solution at 4°C in a sterile media fridge.

Component	**Quantity**
Tryptone	10 g
Yeast extract	5 g
NaCl	10 g
Deionised water	Up to 1 L

Lysogeny Broth Agar Plates

Prepare LB medium as above, adding 15 g of agar before autoclaving. After autoclaving, cool to 55°C and add antibiotic if required for LB^+ agar plates. Pour into sterile agar plates and allow to set before inverting and storing at 4°C in the dark. LB^+ agar plates should be kept for no longer than two weeks.

MOPS Buffer (5X) and MOPS Running Buffer (1X)

To prepare 1 L of 5X MOPS buffer (pH 7.0), dissolve 20.9 g of MOPS in 700 mL of sterile DEPC-treated H_20 and adjust to pH 7.0 with NaOH if necessary. Add 20 mL of DEPC-treated sodium acetate (1 M) and 20 mL of EDTA (0.5 M) and make solution up to 1 L with DEPC-treated water. The solution should then be autoclaved and stored at room temperature away from light. Protection from light can be achieved by covering the bottle in tinfoil.

To prepare a 500 mL solution of 1X MOPS running buffer, add 100 mL of 5X MOPS buffer to 400 mL of DEPC-treated H_20 and mix by inversion. This solution should also be stored at room temperature, away from light.

RNA Sample Buffer

Buffer solution to be added to RNA samples can be made with the components listed below. All components should be mixed thoroughly in sterile microfuge tubes. Formamide is a teratogen and formaldehyde is a toxic carcinogen, therefore this solution should be made up in the fume hood with safety glasses, gloves and a lab coat on. After all components have been added to the tube, samples should be incubated at 70°C for 10 minutes before chilling on ice for a further 3 minutes. Centrifuge samples for 5 seconds and store on ice until loaded into the gel.

Component	**Quantity**
RNA (up to 20 μg)	2 μL
5X MOPS buffer	4 μL
Formaldehyde	4 μL
Formamide	10 μL
EtBr (200 μg/mL)	1 μL

Sterile Ampicillin (50 mg/mL)

Weigh out 250 mg of ampicillin into a 15 mL sterile falcon tube. Make solution up to 5 mL with deionized water and sterilise by filtration (0.22 μM filter) into 1 mL aliquots. Store at -20°C.

SuperBuffer (1X)

To prepare a 50X stock solution of sodium borate buffer (SuperBuffer), add 20 g of NaOH to 1 L of mQH_20 and invert to dissolve. To make a 1X working buffer, add 20 mL of the stock solution to 980 mL of mQH_20.

TAE Buffer (1X)

To prepare a 50X stock solution of TAE buffer, add 242 g of Tris and 18.61 g of disodium EDTA to approximately 700 mL mQH_20 and stir until dissolved. Add the acetic acid and adjust volume to 1 L. To make a 1X working buffer, add 20 mL of the stock solution to 980 mL of mQH_20.

Tris-Cl (1M)

To prepare a 1M Tris-Cl solution, dissolve 121.1 g of Tris base in 800 mL of mQH_20. Adjust pH to desired value with HCl.

Tris EDTA (TE) Buffer

To prepare Tris EDTA buffer, add 2 mL of Tris (1 M) and 4 mLs of EDTA (0.5 M) to a sterile bottle. Make up to 200 mL with sterile mQH_2O and mix by gentle inversion. Store at room temperature.

XGal (20 mg/mL)

Dissolve 20 mg of XGal into 1 mL of DMSO in a sterile glass amber vial. Store away from light at -20°C.

Appendix 4: Nanodrop Results for all RNA Samples

RNA Sample	Nucleic Acid Concentration (µg/mL)	A260:A280	A260:A230
I1T2	876.4	1.65	1.99
I1T4	922.7	1.64	1.98
I3T2	1180.6	1.58	1.89
I3T4	962.8	1.69	1.99
I4T2	674.6	0.87	1.97
I4T4	1061.0	1.98	1.99
C1T0	357.4	1.37	1.97
C1T4	640.1	0.89	1.89
C2T0	5234	1.98	2.03
C2T4	138.8	1.75	1.98
C3T2	264.7	1.85	1.99
C3T4	701.7	0.86	1.93
C4T0	916.3	2.01	1.68
C4T4	1129.5	1.93	2.3

RNA Sample	**Nucleic Acid Concentration (µg/mL)**	**A260:A280**	**A260:A230**
S1T2	5194.6	1.94	2.04
S1T4	3375.1	1.96	2.12
S2T2	4259.4	1.97	1.99
S2T4	6280.1	1.88	1.94
S3T2	4028.1	1.96	1.95
S3T4	5823.1	1.9	2.05
S4T2	1022.4	1.99	2.16
S4T4			

RNA Sample	Nucleic Acid Concentration (µg/mL)	A260:A280	A260:A230
P1T0	1192	1.4	2.0
P1T2	2671	1.7	2.0
P1T4C	2788	1.6	2.0
P1T4T	2548	1.4	1.9
P2T0	2351	1.8	2.0
P2T2	2049	1.8	2.0
P2T4C	1939	0.6	1.9
P2T4T	613	0.7	1.8
P3T0	1783	1.4	2
P3T2	2407	1.4	1.9
P3T4C	1319	1.6	1.9
P3T4T	2045	1.7	2.0

RNA Sample	Nucleic Acid Concentration (µg/mL)	A260:A280	A260:A230
A1T0	3430	2.03	2.20
A1T4S	4494.9	1.95	2.01
A1T4C	3079.2	1.97	2.04
A2T0	2264.6	1.98	1.92
A2T4S	1698.3	1.95	1.89
A2T4C	565.4	1.88	1.48

Appendix 5: Map of pLUG-Prime® TA-Cloning Vector.

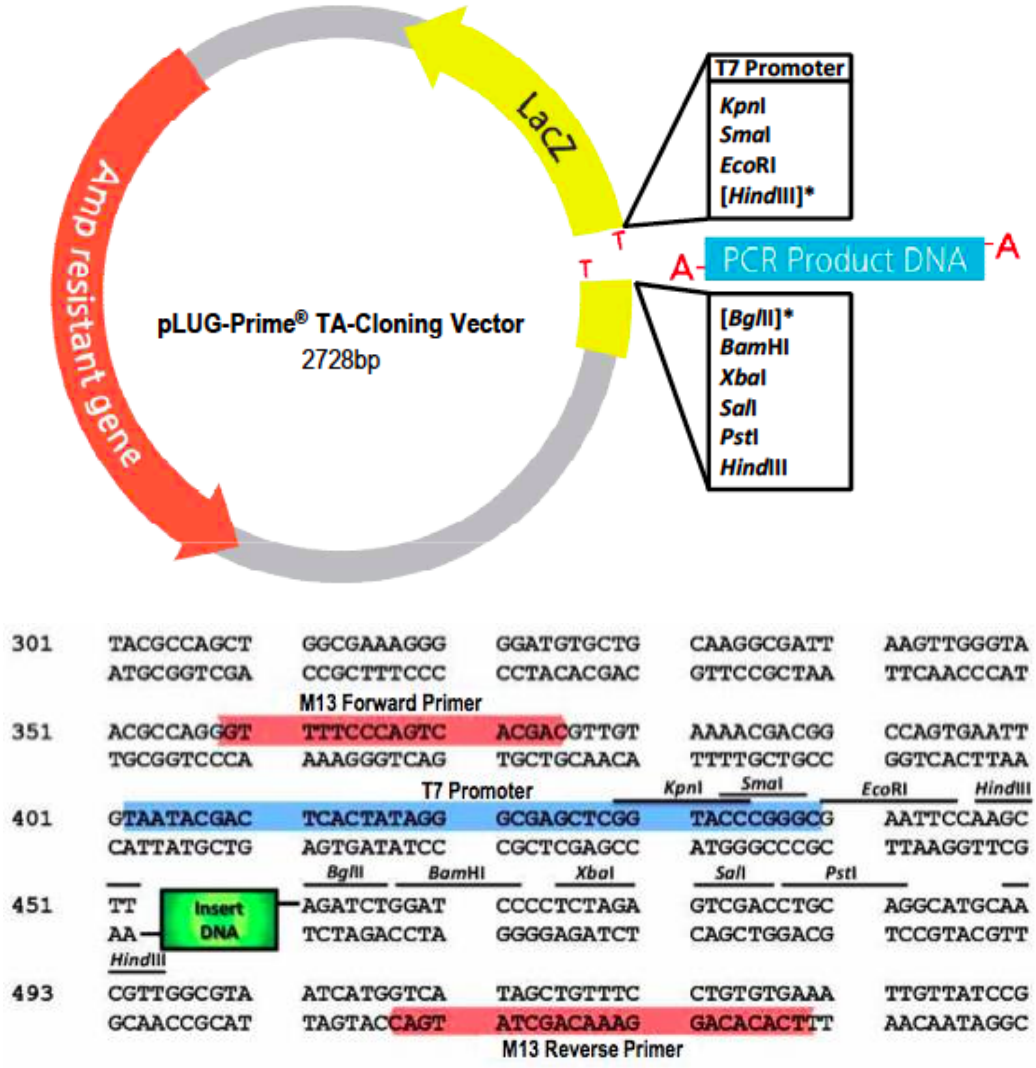

Appendix 6: FASTA mRNA Sequences with Primer Recognition Sites for NCBI Designed Primers

***Mus musculus Arc* mRNA (transcript variant 1) with primer recognition sites**

>GGTGAGCTGAAGCCACAAATGCAGCTGAAGCAGCAGACCTGACATC
CTGGCACCTCCTGGCCCCCAGCAGTGATTCATACCAGTGAAGAAGAGC
AGAGCTCAGC

***Mus musculus Bdnf* mRNA (transcript variant 1) with primer recognition sites**

>TGAGTCTCCAGGACAGCAAAGCCACAATGTTCCACCAGGTGAGAAG
AGTGATGACCATCCTTTTCCTTACTATGGTTATTTCATACTTCGGTTGC
ATGAAGGC

***Mus musculus CaMKIIα* mRNA (transcript variant 1) with primer recognition sites**

>ACAGTCCACTACTCTGCTGCCTGCAAATGCTGCTCTTTCTCACGCTGT
GGGCCCTGGTGCCTTGCCTGGTGTTGCTAACCCTCTACTTTCTCTCCTC
CACAGGAGGGAAGAGCGGAGGAAACAAGAAGAACGATGGTGTGAAG
AAAAGAAAGTCCAG

Mus musculus Grin1 **mRNA (transcript variant 1) with primer recognition sites**

>CAAGTGGGCATCTACAATGGTACCCATGTCATCCCAAATGACAGGAA
GATCATCTGGCCAGGAGGAGAGACAGAGAAGCCTCGAGGATACCAGA
TGTCCACCAGACTAAAGATAGTGACAATCCACCAAGAACCCTTCGTGT
ATGTCA

Mus musculus Gjd2 **mRNA with primer recognition sites**

>CCAGTAAGGAGACAGAACCAGATTGCTTAGAGGTTAAAGAGCTGAC
TCCACATCCATCTGGGCTGCGCACAGCAGCAAGGTCCAAGCTCCGAAG
ACAGGAAGGTATCTCCCGCTTCTACATCATC

Mus musculus Gapdh **mRNA (transcript variant 2) with primer recognition sites**

>TGCACCACCAACTGCTTAGCCCCCCTGGCCAAGGTCATCCATGACAA
CTTTGGCATTGTGGAAGGGCTCATGACCACAGTCCATGCC

Mus musculus ß2m **mRNA with primer recognition sites**

>TTCTGGTGCTTGTCTCACTGACCGGCCTGTATGCTATCCAGAAAACCC
CTCAAATTCAAGTATACTCACGCCACCCACCGGAGAATGGGAAGCCG
AACATACTG

Appendix 7: Gene Abbreviations Description and NCBI Accession Numbers

Gene Abbreviation	**Full gene description**	**Accession Number**
Actβ	Beta-actin	NM_007393.3
Arc	Activity-regulated cytoskeletal-associated protein	NM_018790.3
β2m	Beta-2 microglobulin	NM_009735.3
Bdnf	Brain-derived neurotrophic factor	NM_007540
CaMKIIα	Calcium/calmodulin protein kinase, α subunit	NM_177407
Gapdh	Glyceraldehyde 3-phosphate dehydrogenase	NM_001289726.1
Gjd2	Gap junction delta-2 protein	NM_010290.2
Grin1	Glutamate NMDA receptor subunit zeta-1	NM_008169
HPRT1	Hypoxanthine-quanine phosphoribosyltransferase	NM_013556.2

Appendix 8: *Bdnf* Nucleotide Sequence

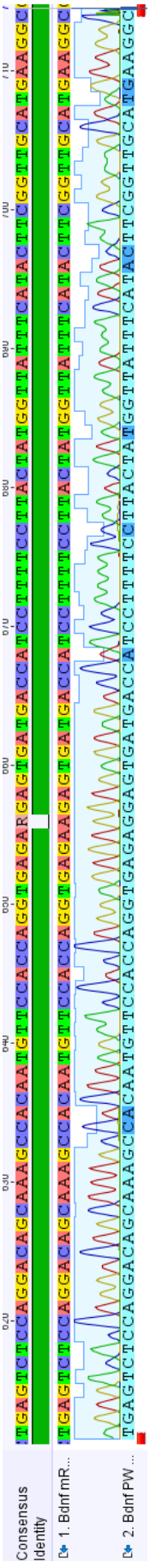

Appendix 9: Raw Expression Data

All raw take-off, amplification and expression ratio data is recorded on the accompanying disc.